2009

# Tactile Sensing System for Lung Tumour Localization during Minimally Invasive Surgery

Melissa Teresa Perri
*Western University*

# Tactile Sensing System for Lung Tumour Localization during Minimally Invasive Surgery

(Spine title: Tactile Sensing System for Lung Tumour Localization)

(Thesis format: Integrated Article)

by

**Melissa Teresa Perri**

Graduate Program in Engineering Science
Department of Electrical and Computer Engineering

A thesis submitted in partial fulfillment
of the requirements for the degree of
Master of Engineering Science

The School of Graduate and Postdoctoral Studies
The University of Western Ontario
London, Ontario, Canada

# Abstract

Video-assisted thoracoscopic surgery (VATS) is becoming a prevalent method for lung cancer treatment. However, VATS suffers from the inability to accurately relay haptic information to the surgeon, often making tumour localization difficult. This limitation was addressed by the design of a tactile sensing system (TSS) consisting of a probe with a tactile sensor and interfacing visualization software. In this thesis, TSS performance was tested to determine the feasibility of implementing the system in VATS. This was accomplished through a series of *ex vivo* experiments in which the tactile sensor was calibrated and the visualization software was modified to provide haptic information visually to the user, and TSS performance was compared using human and robot palpation methods, and conventional VATS instruments. It was concluded that the device offers the possibility of providing to the surgeon the haptic information lost during surgery, thereby mitigating one of the current limitations of VATS.

**Keywords:** minimally invasive surgery (MIS), video-assisted thoracoscopic surgery (VATS), force feedback, haptics, tactile sensor, tumour localization, palpation, sensory substitution

# Co-Authorship

## Chapter 3: Robot-Assisted Tactile Sensing for Minimally Invasive Tumour Localization

This work has been published in the International Journal of Robotic Research, with an author list: A. L. Trejos, J. Jayender, M. T. Perri, M. D. Naish, R. V. Patel, and R. A. Malthaner. I was responsible for designing the experiments, preparation of materials, aided with conducting the experiments, analyzing the results, and editing the manuscript. A. L. Trejos aided with preparation of materials, conducting the experiments, analyzing statistical results, and writing the manuscript. J. Jayender created the hybrid impedance robotic control system used in experiments, operated the robot during the experiments, and edited the manuscript. M. D. Naish and R. V. Patel supervised the research activities, funded the project, and edited the manuscript. R. A. Malthaner funded the project, and edited the manuscript.

# Acknowledgements

First of all I would like to thank my project supervisors, Dr. Patel and Dr. Naish, for their guidance and support of my research and for allowing me the freedom and extensive flexibility to implement my ideas when working on this project. Thank you for always taking the time to lend an ear or provide advice particularly during my frequent unscheduled drop-ins by your offices. I would also like to extend my uttermost gratitude to Dr. Malthaner, for his vision of this project and who provided me the enriching opportunities to present my work abroad. Thank you for your continual motivation and advice, and for always keeping me on track whenever I would digress from my goals.

Special thanks to the CSTAR engineering students and staff who without them, I could never have completed my studies in a 'timely fashion.' I am particularly thankful to Ana Luisa Trejos for her endless guidance since the dawn of the project, her numerous stimulating discussions, and major contributions to this project; Jagadeesan Jayender, Ali Talasaz, and Mahdi Azizian, for unselfishly providing their time and talent required for collaborative projects, and for tolerating my crazy work schedule; David Bottoni, Luc Dubois, and Shiva Jayaraman for their encouragement and for always taking the time from their extremely busy schedules to assist or participate in experiments; Karen Siroen and Sheri VanLingen, for tolerating my seemingly unending request for tissues and, without complaint, stayed hours after workshops to obtain them; and Greig McCreery who, by contributing to the design of the TSI, made the project evolve from a mere idea to a feasible reality.

Most importantly, none of this would have been possible without the support of my family. To my parents and grandparents, thank you for all your love and support, particularly to my mom who is the cornerstone to all of my achievements; to my brother, and brother-in-law, thank you for keeping my head on straight and focused on the light at the end of the tunnel; and *especially* to my sister, for her continuous encouragement and endless support. I could not have accomplished this without all of you.

# Contents

# List of Tables

# List of Figures

# List of Appendices

# List of Abbreviations

| | |
|---|---|
| 2D | Two-Dimensional |
| 3D | Three-Dimensional |
| AHIC | Augmented Hybrid Impedance Controller |
| ANOVA | ANalysis Of VAriance |
| CSTAR | Canadian Surgical Technologies and Advanced Robotics |
| CT | Computed Tomography |
| DOF | Degree Of Freedom |
| EBRT | External Beam Radiation Therapy |
| ICS | InterCostal Space |
| LUT | Look-Up Table |
| MEMS | MicroElectroMechanical Systems |
| MIS | Minimally Invasive Surgery |
| MRI | Magnetic Resonance Imaging |
| NSCLC | Non-Small Cell Lung Cancer |
| PET | Positron Emission Tomography |
| PPS | Pressure Profile Systems |
| SCLC | Small Cell Lung Cancer |
| TSI | Tactile Sensing Instrument |
| TSS | Tactile Sensing System |
| VATS | Video-Assisted Thoracoscopic Surgery |

# Chapter 1

# Introduction

Lung cancer is the leading cause of cancer deaths in North America for both sexes and it is commonly treated using a minimally invasive technique known as video-assisted thoracoscopic surgery (VATS). However, VATS suffers from the inability to accurately provide tactile feedback, thus often making the procedure difficult for surgeons. The motivation of this thesis was to assess the feasibility of a system that was capable of accurately providing tactile sensing to the surgeon during this newly innovative VATS technique that requires small 10 mm incisions. An overview on lung cancer detection and treatments options, surgical techniques for localizing lung nodules, and an introduction to the tactile sensing instrument is presented below.

## 1.1 Lung Anatomy

The lungs are cone-shaped organs, organized in pairs, that are found in the thoracic cavity [1]. Each lung is encased in two layers of serous membrane, known as the

pleural membrane, that allows one lung to remain expanded if the other lung is collapsed (due to trauma or intentionally for medical procedures). Each lung can be divided into lobes via one or two fissures. Both the left and right lungs have an oblique fissure that separates the lungs into the superior (upper/cranial) and inferior (lower/caudal) lobes. For the right lung, the horizontal fissure separates the superior lobe from the middle lobe.

The trachea, a tubular passageway for air, divides into the right bronchus and left bronchus on entering the lungs. Each bronchus branches two more times (secondary and tertiary bronchi) before leading into the bronchioles. At the terminal bronchioles, microscopic air sacks called alveoli are located. The segment that each tertiary bronchus supplies, which are located in the periphery of the lung, can be surgically removed without seriously disrupting the surrounding lung tissue [1].

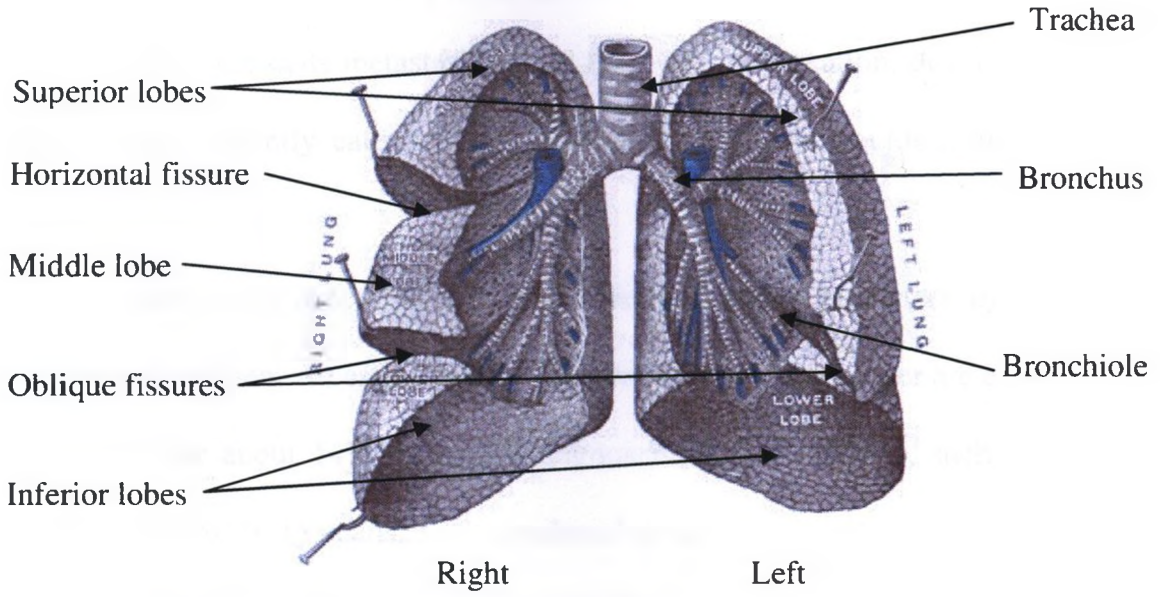


**Figure 1.1:** Basic lung anatomy indicating the lobes, fissures, and internal structures [2].

The primary purpose of the lungs is to allow for the intake of atmospheric oxygen and disposing of carbon dioxide in the blood, through a process termed cellular

respiration. This form of gas exchange, which occurs at the alveoli, is vital for maintaining homeostasis within the body. However, due to the delicate nature of the lungs, they often are involved in infections or injuries. When damage occurs to vast areas of the lungs, these areas can become non-functional. Currently there is no evidence that indicates that lung tissue has regenerative properties [3].

## 1.2 Lung Cancer

### *1.2.1 Overview*

Cancer is a disease classification which is characterized by the uncontrolled growth and spread of abnormal cells. Cancer is caused by both external factors, such as tobacco, chemicals, and radiation, and internal factors, such as inherited mutations, hormones, and immune conditions [4]. If the spread of these cancer cells is not controlled or annihilated before the cells metastasize from their original location, death can result. Worldwide, cancer currently causes more death than AIDS, tuberculosis, and malaria combined [4].

In particular, lung cancer is the overall leading cause of cancer mortality in Canadian men and women. An estimated 23,400 new cases of lung cancer are expected in 2009, accounting for about 14% of cancer diagnoses [5]. Newer tests, such as helical computed tomography (CT) scans, have produced promising results in detecting lung cancer at earlier, more operable stages in patients, but have not yet been shown to reduce lung cancer deaths [6]. An estimated 20,500 deaths due to lung cancer, accounting for about 27% of all cancer deaths in Canada, are expected to occur in 2009 [5].

### *1.2.2 Detection: Pulmonary Imaging*

The primary purpose of imaging the thorax is to confirm or disprove the suspicion of the presence of a pulmonary nodule. There are many diagnostic imaging modalities that can be used to accomplish that purpose. However, the primary modalities used for pulmonary imaging are the chest radiograph and chest computed tomography (CT). Other common imaging modalities can include magnetic resonance imaging (MRI) and positron emission tomography (PET). A brief overview of these imaging modalities for thoracic approaches is presented below.

#### *1.2.2.1 Radiography*

Radiography was the first imaging technique to advance the diagnosis and staging of lung cancer, and its first diagnostic use was recorded in 1896 [7]. Radiography utilizes a form of electromagnetic energy of short wavelength known as X-rays. When acquiring a radiographic image, X-rays, most commonly, are passed posteriorly through the patient and received by a screen film that is located anterior to the patient. An image is produced by the attenuation of those X-rays by material through which they pass, sometimes leading to more blackening of the film. Most lung tumours are detected on conventional chest radiographs. However, difficulties in assessing the images arise when the lesions are less than 3 cm in diameter [8]. Presently, conventional radiography retains a role in evaluating thoracic nodules; however, due to its limits with spatial resolution, CT has become the new cornerstone imaging modality for diagnosing lung cancer.

*1.2.2.2 Computed Tomography (CT)*

Computed tomography is widely accepted as the primary modality for evaluation of the thorax. When compared to standard radiographs, CT can detect more small pulmonary nodules at an earlier stage [8]. Similar to radiography, CT uses radiation energy; however, it is capable of moving both the X-ray tube and detector in unison to produce a series of images. The image produced is a two-dimensional (2D) representation of a cross-sectional slice of the area of interest. In the early 1990s, spherical (helical) CT was introduced which allowed for continuous image acquisition [8]. This continuous scanning allowed for the production of multiplanar reconstruction, as well as three-dimensional (3D) reconstruction of images. Conventional film radiography of the chest is used less frequently now that CT technology is widely available.

*1.2.2.3 Magnetic Resonance Imaging (MRI)*

Magnetic resonance imaging (MRI) is a non-invasive technique that does not use ionizing radiation. This technology relies on the ability of hydrogen protons to emit a radio wave in the presence of a magnetic field to produce high quality images. When performing images of the thorax, MRI has advantages over CT that include improved contrast resolution and the capability to produce images in other planes than axial [8]. However, CT still remains paramount to MRI in pulmonary imaging because of its superior spatial resolution, lower cost, and greater availability [8].

*1.2.2.4 Positron Emission Tomography (PET)*

Positron emission tomography (PET) is the primary imaging technique used in nuclear medicine, and provides functional information rather than anatomical information like with CT [9]. Images produced are tomographical and can be fused to form 3D representations of the area of interest. When available, PET will be performed in conjunction with CT to provide a better anatomic location of lung nodules [9]. Its advantages over CT are that it can play a major role in differentiating benign from malignant pulmonary nodules and has the capability of identifying nodule metastasis [9]. However, due to the low spatial resolution and lack of anatomical landmarks in PET images, its ability to localize pulmonary lesions is severely limited, thus, it is not often used for the purposes of pulmonary imaging.

### *1.2.3 Lung Cancer Treatment Options*

Non-small cell lung cancer (NSCLC) is the number one cause of cancer mortality worldwide, and constitutes about 80% of all lung cancer cases [10]. NSCLC is staged from IA to IV, in order of increasing severity, and indicates the degree of spread of the cancer cells from their original source. Usually NSCLC is diagnosed in the less advanced stages, and only 15% of all NSCLC cases are diagnosed at Stage III [11]. Until the 1990s, platinum-based chemotherapy and radiotherapy were chosen as treatment for unresectable advanced NSCLC [10]. Now with a better understanding of the biology and genetics of tumours, an array of molecular targeted agents are used in combination with

standard chemotherapy to improve the patient's survival rate. Patients with Stages I, II, and III NSCLC can be treated with surgery, chemotherapy, radiation therapy, or a combined modality. Treatment options are determined by the type (small cell or non-small cell) and stage of cancer [6]. In general, small cell lung cancer (SCLC) or Type III NSCLC are treated with radiation therapy and/or chemotherapy, sometimes in combination with surgery. For early stage cancers (Stage I or II disease), surgical resection should always be considered since these tumours usually can be completely resected and are highly curable [8].

*1.2.3.1 Chemotherapy*

Chemotherapy uses chemicals to control or annihilate cancerous cells. However, these chemicals are not biologically specific to cancerous cells, thus they can also attack normal cells to varying degrees, sometimes leading to cell death [12]. Platinum-based chemotherapy was introduced in the 1980s for treatment of patients with NSCLC. A decade later, it became the standard treatment for these patients despite the low median survival rates [10]. Platinum-based chemotherapy is still predominantly used in both clinical practice and clinical trial settings, but is usually used in a combined modality therapy (pre-operatively or post-operatively) or used to treat advanced stages of NSCLC. For example, a retrospective study performed by van Meerbeek *et al.* [13] looked at several trials in which non-surgical therapies (chemotherapy or radiotherapy) were used when surgical resection of Stage III NSCLC was not effective. The study concluded that

the post-operational use of chemotherapy, also known as adjuvant chemotherapy, showed a 17–20% reduction in risk of death and improved the five-year survival rate by 13–15%.

*1.2.3.2 Radiation Therapy*

Similar to chemotherapy, radiation therapy can be used alone, but is most commonly performed in conjunction with surgery. Radiation can be administered as external beams, termed external beam radiation therapy (EBRT), or in surgical implanted radioactive seeds in a procedure called brachytherapy [12]. In a retrospective study by Jeremic *et al.* [14], EBRT was used post-operatively to a complete surgical resection in patients with NSCLC. The results were promising, demonstrating a five-year survival rate of 30% for patients experiencing recurring NSCLC confined to the bronchial stump. However, in most cases of NSCLC, radiation therapy can be used in the cases where patients are not eligible for surgery due to medical conditions or the refusal of surgery [15]. A study by Manz *et al.* [16] presents the case where early stage, medically inoperable NSCLC, was controlled locally, and in some instances was cured, when treated with EBRT and brachytherapy. The patients in the study showed a five-year local disease control rate of 32%. Unfortunately only a small percentage of patients with NSCLC are suitable for radiation therapy [17].

*1.2.3.3 Surgery*

Surgery is the treatment of choice for early stages of NSCLC that have not metastasized upon detection [14]. There are different surgical procedures that can be performed for lung cancer. Listed in increasing severity, these include segmentectomy (removal of a cancerous segment of a particular lobe; also referred to as wedge resection), lobectomy (removal of a lobe), and pneumonectomy (removal of the entire lung) [12]. The procedure chosen for the patient depends on the location of the carcinoma, as well as the patient's health and functional capacity of the lung. A retrospective study performed by Rocco [18] looked at the results of various surgical procedures performed on NSCLC. The study concluded that when completely resected, a thoracotomy remains among the strongest prognosticators of survival. Pneumonectomy was discouraged due to the increase in post-operative morbidity and mortality rates in patients. When identified in its early clinical stages, patients with surgically removed NSCLC have survival rates of 40–85%, and at advanced clinical stages, the five-year survival for patients is 15% [9].

Traditionally, a lobectomy was performed through an open thoracotomy. In this procedure, the lung of interest is collapsed via a double lumen endotracheal tube and the incision is initiated posteriorly, midway between the scapula (shoulder blade) and spine. The incision extends anteriorly in a curvilinear fashion for approximately 12 cm [19]. This large incision allows direct access to the lung and the location of the cancerous nodule can be performed by manual palpation of the organ. When the nodule is located via visual cues and manual palpation, the lobe is resected and removed from the chest

cavity. The excised edge of the remaining lung is stapled with an automatic stapling device. The procedure is completed by closing the chest cavity and surrounding tissue with sutures [20].

## 1.3 Video-Assisted Thoracoscopic Surgery (VATS)

### *1.3.1 Overview*

For localized cancers, lung resection has been the treatment of choice. Traditionally, this procedure was performed through an open thoracotomy (refer to Section 1.2.3.3); however, with the advancement and integration of technology into medicine, minimally invasive surgery (MIS) has become increasingly prevalent over traditional open surgical procedures.

Minimally invasive surgery is a revolutionary technique which began in the early 1980s [21]. When performed specifically on the lung and other thoracic organs, the MIS procedure is referred to as video-assisted thoracoscopic surgery (VATS). VATS is a procedure which involves the use of a thoracoscope, to provide a view of the operational site, and various laparoscopic instruments inserted through ports between 5 and 12 mm in diameter. For this procedure, the patient is anesthetised and placed on their side (in a lateral decubitus position). The involved lung is deflated via a double lumen endotracheal tube or the insertion of a bronchial blocker to permit one-lung ventilation for the procedure. Three 1–2 cm thoracoscopic port incisions are made after verifying the anatomical site of the nodule. The video camera, or thoracoscope, is introduced in the $6^{th}$–$8^{th}$ intercostal space (ICS) in the midaxillary line. This position provides maximal

visualization of the majority of the lung. The other two ports are usually positioned in the $3^{rd}$–$4^{th}$ ICS in the midclavicular line, and the $5^{th}$ ICS near the border of the scapula. Inserted into these ports are other endoscopic instruments, including endoscopic graspers, retractor, scissors, electrocautery, and stapler, which are manipulated by the surgeon [20].

Using pre-operative images via chest X-ray or thoracic CT scan and by visual inspection using the thoracoscope and endoscopic grasper, the surgeon identifies the area of the lung containing the cancerous nodule. When the nodule is found, the surgeon excises a small wedge of lung containing the nodule along with surrounding 1–2 cm margins of normal lung tissue with an endoscopic stapling instrument [20]. The surgical specimen is placed in a retrieval bag and sealed before it is removed through a port incision. This manoeuvre decreases contamination of the trocar site with tumour cells from the specimen and helps to prevent re-infection [22].

### *1.3.2 Benefits and Limitations*

VATS provides many benefits over traditional open surgery. These include:

1) *Decrease in postoperative pain*: Standard thoracotomies and muscle sparing thoracotomies are still associated with significant pain and a lengthy recovery time for patients [21]. In studies performed by Yim [23], Demmy [24], and Giudicelli [25], it was shown that acute postoperative pain in patients undergoing VATS was significantly decreased when compared to a traditional thoracotomy procedure. For their studies, a visual analogue scale was administered and utilized by their patients to score subjective pain after surgery.

2) *Decrease in length of hospital stay*: Patients who undergo VATS procedures have a rapid recovery time and return to normal activity sooner than patients who undergo a thoracotomy [26]. In a study by Demmy [24], VATS patients returned to normal activity within an average of 2.2 months versus 3.6 months when the patients underwent an open thoracotomy.
3) *Preservation of pulmonary function*: Nakuta *et al.* [27] showed preservation of early postoperative pulmonary function in patients who underwent a VATS lobectomy compared to a thoracotomy. Their study concluded that arterial $O_2$ saturation and forced vital capacity (FVC) of the lungs were better in the VATS group by the seventh postoperative day.
4) *Reduced size of incisions*: The incision size for a standard thoracotomy procedure is on average 12 cm [19]. VATS procedures require three incisions that are 5 mm to 12 mm in diameter. Not only do these small incisions reduce the postoperative pain for the patient, but they also improve cosmetic results [28].
5) *Higher survival rates*: Gharagozloo *et al.* [21] presented a study involving a large series of patients undergoing a VATS lobectomy. The postoperative mortality rate was recorded to range from 0% to 2%. After a 36 month follow-up, the survival for patients undergoing VATS lobectomy for Stage I lung cancer ranged from 76% to 94%.

Although VATS presents many benefits over traditional thoracotomy procedures, thoracoscopic techniques have not been readily embraced by the medical community [21]. This may be because the advantages of VATS procedures can often be overshadowed by the major difficulties it creates for the surgeon, particularly since the

accessibility of the organ is limited for manual palpation [29]. Often, the surgeon will experience difficulty in attempting to insert the entire finger through one of the chest incisions or encounter the impossibility of moving the deflated lung parenchyma under the finger [30]. Therefore, surgeons must rely on their prior surgical experiences and the additional use of technologies adopted to locate tumours pre- and intra-operatively. Another current limitation of VATS is that the thoracoscope presents to the surgeon a two-dimensional (2D) view of the operational field which creates a loss of depth perception for the surgeon [21]. The thoracoscope is also supported and manipulated by an assistant and not by the surgeon. Therefore, it is not possible to rapidly adjust the visual field when required [21]. Furthermore, the introduction of long surgical instruments that operate at a fixed point of entry limits the range of motion of the instrument and diminishes and distorts the relay of tactile information from the instrument tip to the surgeon's hand [21]. These effects have increased the technical complexity for surgeons, making what was once considered simple open procedures considerably more difficult as a VATS procedure.

### *1.3.3 Robotic Surgery and Haptics*

In order to overcome some of these obstacles, robotic systems were developed to aid the surgeon in performing MIS procedures. It was not until the early 1990s that it became clear that computer enhanced instrumentation had the potential of solving limitations of conventional VATS techniques [21]. The first computer enhanced surgical instrument was introduced in 1992 and was known as RoboDoc (Integrated Surgical

Systems, Sacramento, CA) [21]. RoboDoc was designed to assist with bone cutting and precise drilling for joint replacement procedures. Two years later, the Automated Endoscopic System for Orthopaedic Surgeons (Computer Motion Inc., Santa Barbara, CA), abbreviated AESOP, was developed to provide a more stable field of vision and control of the thoracoscope [21]. This system could also be directed by the surgeon via voice commands. It was not until the late 1990s that two complete robotic surgical systems were introduced. In 1997 the da Vinci Surgical System (Intuitive Surgical Inc., Sunnyvale, CA) was introduced as a complete robotic surgical system suitable for general minimally invasive surgical procedures and is still currently used. The da Vinci Surgical System consists of a master console where the surgeon has a 3D stereoscopic view of the operating site and performs the surgery using telemanipulator and optical controls. An accompanying surgical arm cart is located adjacent to the patient and translates the movement of the surgeon's hands to two robotic arms which contain the surgical instruments. A third robotic arm which supports the thoracoscope is also controlled by the surgeon [31] and an optional fourth arm to hold an additional instrument can be used by the surgeon to perform additional tasks thereby eliminating the need for a patient-side surgeon [32]. The surgeon can simultaneously control any two of the operating arms via the surgeon's console. The da Vinci Surgical System is shown in Figure 1.2. The second surgical system was introduced a year later, in 1998. The Zeus robotic surgical system (Computer Motion Inc., Santa Barbara, CA) consists of three separate working arms that are independently fixed to the operating table. The surgeon is given a direct external view of the operating room via the Zeus console that provides a computer-simulated 3D view

with the use of special glasses. Although conceptually similar to the da Vinci Surgical System, the Zeus system is no longer available for clinical use [21].

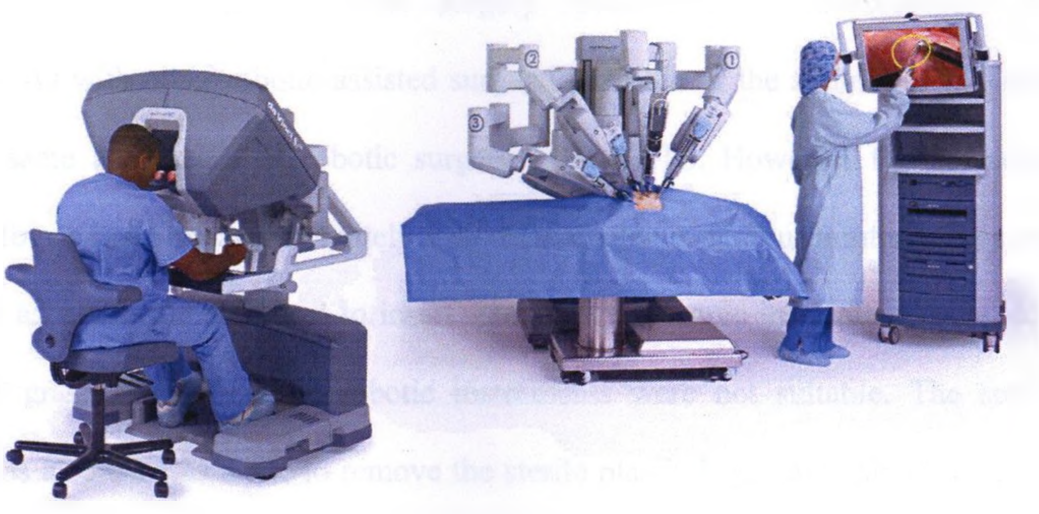

**Figure 1.2:** General clinical setup of the da Vinci Si Surgical System (introduced in 2009). Surgeon is sitting at master console (left) and surgical arm cart is located centrally. Nurse is at vision cart (right) [32].

The da Vinci Surgical System offers improvements to VATS procedures involving pulmonary procedures by providing increased visualization via a 3D stereoscopic view of the operational site, tremor filtration, scaling and indexing, high surgical precision and accuracy, an increase in instrument dexterity at the incision point, and increased instrument wrist manoeuvrability [31]. However, the main limitation of the da Vinci System, common to all commercially available robotic systems, is the inability to relay force and palpable information back to the surgeon [33]. Without the presence of this tactile feedback, the surgeon must rely solely on visual feedback to determine the amount of force being applied to the tissue.

The da Vinci Surgical System gained acceptance in the medical community for selected surgical procedures, however, few reports on the impact of robotics in general thoracic surgery exist. The first documented report on robotic procedures for thoracic diseases is credited to Melfi *et al.* [31] in 2002 who conducted a study that analyzed the advantages and limitations of robotic surgery specifically for thoracoscopic lung procedures. As with other robotic-assisted surgical procedures, the authors of this study found the same advantages of robotic surgery over VATS. However, the procedures required a fourth incision, approximately 3 cm in diameter at the fourth intercostal space, that served as a 'service entrance' to insert standard endoscopic instruments such as an endoscopic grasper or when the robotic instruments were not suitable. The service entrance was also used as a site to remove the sterile plastic bags containing the tumour and specimen at the conclusion of the procedure. Other limitations noted by the authors included considerably increased operative times, the requirement of larger and bulkier instruments for the system, and the difficulties encountered to properly position the trocar in the chest cavity to obtain optimal system performance [31]. Lack of tactile feedback and the reality that surgical instruments currently available for robotic surgical systems are not adequate for thoracoscopic surgery were particularly stressed. A similar report by Bodner *et al.* [28] was conducted two years later that looked at pulmonary resection on clinical Stage I lung cancer. Similar to their predecessor, the authors found that the advantages of robotic systems for thoracoscopic surgery were overshadowed by the need for special devices to be developed and the need for the system to offer tactile feedback. Due to these main constraints, the use of robotic surgical systems is currently discouraged

for thoracoscopic procedures. Modifications are required before the use of robotic-assisted thoracoscopic surgery can be routinely recommended [21].

In view of these limitations, research dedicated to the development of alternative methods for locating tumours intra-operatively has become increasingly active. One such method is the transfer of haptic cues from the contacting tissue surface to the surgeon. Haptic cues can be considered in two distinct modes [34]. The first is kinaesthetic feedback, which relates to motion and bulk forces perceived at the point of contact. The second mode is tactile feedback, which includes the sensation of surface textures. Both modes of haptic feedback have been the focus of active research since, in VATS, the reduction of both tactile and kinaesthetic feedback from the tissue surface can be regarded as a safety concern. Limited tactile information may make intra-operative tumour detection uncertain, and result in a difficult and time-consuming procedure for the surgeon. If the degradation of tactile information prevents a cancerous nodule, identified through pre-operative imaging, from being located during the VATS procedure, this would, on occasion, necessitate the abandonment of the MIS approach and a conversion to an open procedure so that tumour localization can be performed manually [35]. In cases where kinaesthetic feedback is limited or absent while palpating during surgery, complications such as the accidental puncturing of vessels or severe bulk tissue damage when palpating organs are probable, leading to difficulties that could be avoided with the availability of haptic feedback [36].

## 1.4 Minimally Invasive Techniques for Localizing Lung Nodules Intra-operatively

Current clinical technologies adopted for MIS pulmonary tumour localization procedures include pre-operative computed tomography (CT) scans or markers inserted via CT guidance, and the intra-operative use of thoracoscopic ultrasound or endoscopic graspers. Due to the limitations encountered by VATS procedures, specialized surgical instruments are also being developed by researchers to aid in detecting cancerous nodules, and in addition, ensure that the surgeon's sense of touch is not eradicated from the process.

### *1.4.1 Computed Tomography (CT)*

CT is the primary imaging modality used for the diagnosis of lung cancer. The basic description of this technology and its role in diagnosing lung nodules pre-operatively is described in Section 1.2.2.2. Although this technology is widely used to diagnose suspected pulmonary nodules present in the lung, its ability to provide the anatomical location of the nodule during thoracic surgery is limited. Since the lung of interest must be deflated for tumour resection procedures, the anatomical position of the tumour when the lung is inflated pre-operatively and deflated intra-operatively can differ significantly. Due to this tissue shift between the pre-operative CT imaging and the operative procedure, the pre-operative image is often an unreliable resource during surgery [37]. Therefore, there is a need to introduce some method or technology that can

confirm the location of the nodule intra-operatively. This cannot imply using CT technology intra-operatively due to the cost and low availability of CT scanners in the operating room.

### *1.4.2 Pre-operative Placement of Markers*

The pre-operative procedure of inserting a marker, such as a guide wire or methylene blue injection, in the tumour with the assistance of CT guidance prior to surgery has also been adopted. These methods require the pre-operative insertion of a needle percutaneously through the chest wall and into pulmonary parenchyma near the pulmonary nodule. For a guide wire procedure, a 32 cm long hook wire is placed through the needle into or within the proximity of the nodule [38]. For a methylene blue injection procedure, 0.5 ml of the contrast dye is injected into the nodule [39]. Both of these methods, however, are associated with risk of pneumothorax, hemothorax, and pulmonary haemorrhaging [40] and require the use of both the CT facility and operating room simultaneously [41]. Specifically, hook wire procedures can experience dislodgement during transport to the operating room or during the positioning of the patient on the operating table [38]. For methylene blue injection procedures, its effectiveness is proportional to the time elapsed between localization of the nodule and surgery. It was found that with elapsed time, the contrast medium would greatly diffuse in the lung parenchyma making it difficult to identify the exact location of the pulmonary nodule [30]. In a multicare study presented by Santambrogio *et al.* [41], the failure rate of excising pulmonary nodules using the methylene blue injection procedure and hook wire

procedure were 13% and 47%, respectively. In view of these limitations, most clinical centres have avoided the pre-operative use of these markers [30].

### *1.4.3 Intrathoracoscopic Ultrasound*

Diagnostic ultrasound is a non-invasive technique that uses sound waves in the 1–10 MHz frequency range [7]. The reflection of these sound waves from tissue interfaces with different acoustic properties yields information on the size, shape, and internal structure of organs and masses. This technology is favoured due to its non-invasive nature, as well as it portability and ability to present images in real-time. Diagnostic ultrasound is a widely accepted tool for various clinical fields; however, few researchers have reported the beneficial application of ultrasonography when identifying peripheral pulmonary nodules [40]. During VATS procedures, the ultrasound probe is introduced into one of the three trocar ports and isotonic sodium chloride solution is poured into the thoracic cavity [40]. The ultrasound probe is then placed directly on the pulmonary surface where the pulmonary nodule is suspected. The main difficulty encountered by intrathoracoscopic ultrasound is that the ultrasound images of the lung during surgery may be difficult to attain if residual air is present in the lung while imaging. Air present in the alveoli and bronchioles causes significant artifacts in ultrasound images since sound waves are greatly reflected by air–soft tissue interfaces [7]. The resulting poor quality and distorted images limits the use of ultrasound in the chest [42]. Furthermore, ultrasound technologies require specialized personnel, specifically radiologists, to be present in the operating room to interpret the ultrasonic images.

### *1.4.4 Endoscopic Graspers*

The performance of long slender instruments adopted for tissue palpation, such as endoscopic graspers, is affected by forces introduced by the ribs and tissue at the instrument insertion point through the chest wall [35], making it such that they cannot provide reliable force feedback to the surgeon. The length and rigidness of these instruments further reduce the distal dexterity that is available to surgeons since they can only manipulate the instrument through a fixed incision point [29]. Since these long instruments operate at a fixed point of entry at the trocar, creating a fixed fulcrum effect, surgeons experience a limited range of motion, diminished tactile feel, the exaggeration of their natural hand tremor, and a reverse or counter-intuitive response at the instrument tip in relation to the movement in their hand [21]. Furthermore, the long length of the instrument compromises ergonomics, thereby contributing to surgeon fatigue and longer learning curves when compared to conventional open surgery [21].

### *1.4.5 Current Research Development*

Since the early 1990s, there has been a growing interest in implementing microtechnology for miniaturization of sensors for medical devices to enhance their functionality [43]. The combination of electronic and mechanical components miniaturized into one system is known as microelectromechanical systems (MEMS). One application of MEMS in the medical field are intracorporeal devices, devices which operate inside of the body but are not implantable, to provide enhanced features that are

otherwise not available by conventional technology. The most recognized intracorporeal devices are sensor-enhanced surgical instruments to restore to the surgeon tactile feedback during MIS. In the past, prototypes for these specialized devices have failed due to their design complexity and expense [43]. However, with the routine clinical practice of MIS, the desire for tactile sensing in laparoscopic surgery still remains a desirable asset [43]. Therefore, specialized surgical instruments are being developed by researchers to ensure that the surgeon's sense of touch is not eradicated from the MIS process. For the purposes of tumour localization, these hand-held instruments occasionally depend on haptic feedback from the instrument tip to the surgeon's hand and can be based on piezoelectric [44], [45], piezoresistive [46], capacitive [35], [47], or optical fibre [29] technologies. In particular, a new method entitled 'mechanical imaging' has been recently explored by researchers. This technology visually represents the internal structure of soft tissues by sensing mechanical stresses on the surface of organs using a tactile sensor array [48]. Methods involving the use of mechanical imaging are currently being used commercially in technologies designed for mammograms, such as in the Sure Touch Visual Mapping System (Medical Tactile Inc., Los Angeles, CA), and have proved to be an effective palpation method. These instruments for breast tumour localization, however, are not designed for minimally invasive surgery, which allows them to have a large sensing area, and as such, a large tissue area can be palpated at one time. For MIS, the instrument must be restricted to a 1 cm wide area so that it can be inserted through standard trocars. A more thorough literature review on current research development in MEMS and haptic technology can be found in Sections 3.1.1–3.1.2 and Section 4.1.1.

## 1.5 Tactile Sensing Instrument

In previous experiments performed by McCreery *et al.* [49], tests were conducted to determine the sensing force range and resolution required to allow a tumour to be localized via palpation using kinaesthetic sensing methods. The results from these tests informed the design of a device, entitled the tactile sensing instrument (TSI), which meets the sensor performance conditions found in [49].

### *1.5.1 Design and Specifications*

The TSI uses a commercially available pressure pad and was developed by a research team at Canadian Surgical Technologies and Advanced Robotics (CSTAR, London, ON). A custom Industrial TactArray sensor from Pressure Profile Systems (PPS, Los Angeles, CA) was incorporated into a surgical probe suitable for MIS. The TSI is shown in Figure 1.3. The technology used for the Industrial TactArray sensor is capacitive, offering superior sensitivity and repeatability compared to resistive and piezoelectric technologies, while maintaining satisfactory results in resolution (minimum element size), temperature, and design flexibility [50]. The PPS Industrial TactArray on this instrument consists of an array with 15 rows and 4 columns of electrodes that are oriented orthogonally to each other. Each overlapping area created by the row and column electrodes forms a distinct capacitor. Thus, the sensor used in this experiment contains a total of 60 distinct capacitors. A compressible dielectric matrix is used to separate the electrodes, which effectively acts as a spring between the electrodes. This

capacitive array sensor technology is based on the phenomena that when pressure is applied on a capacitor, the decrease in distance between the two capacitor plates generates an increase in the output voltage. Once pressure is no longer applied to the sensor, the spring-like dielectric matrix allows the capacitor plates to return to their resting position. In order to address the biocompatibility issues of the probe, a disposable laparoscopic latex sleeve is placed over both the sensor and the shaft of the probe and can be replaced for each use of the probe. Details of the sensor and probe can be found in Table 1.1.

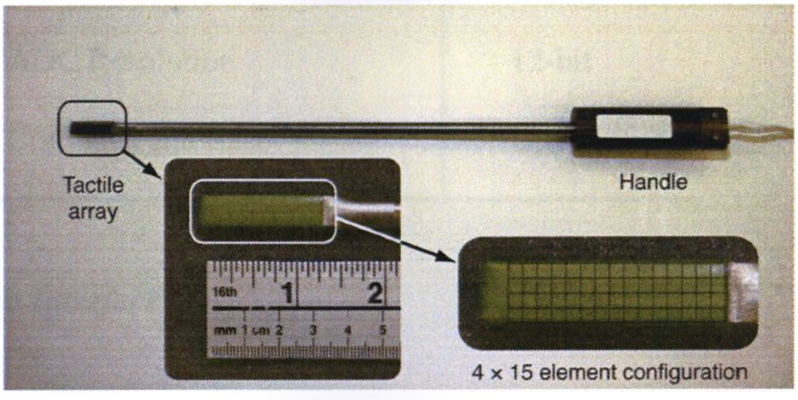


**Figure 1.3:** The TSI emphasizing the 4 × 15 element configuration of the Industrial TactArray sensor.

**Table 1.1:** Details of the tactile sensing instrument.

| | |
|---|---|
| Probe shaft length | 385 mm |
| Probe shaft diameter | 10 mm |
| Number of sensor elements | 60 |
| Resolution | 2 mm |
| Thickness of sensor | 0.3 mm |
| Active area of sensor | 10 mm × 35 mm |
| Pressure range of sensor | 0 – 14,000 kPa<br>(0 – 2,000 psi) |
| Temperature range of sensor | -40° – 200°C |
| Element-to-Element Scan Rate | 10 kHz |
| ADC Resolution | 12-bit |
| Computer Interface | USB |

### *1.5.2 Visualization Interface*

The PPS driver and the Sapphire® Visualization interface are used to display the results from the tactile sensor in a meaningful way. This real-time pressure profiling system converts the measured voltage values from the capacitive sensor to pressure measurements, and displays these results in a colour-contour map of pressure distributions. The visualization software uses the visual colour spectrum to indicate the levels of localized pressure intensity experienced by the probe. Pink areas of the contour map signify areas on the sensor that are experiencing maximal pressures and blue areas of the contour map signify areas that are experiencing small or no contact pressures.

Pressures lying within this dynamic range are linearly represented by the visual colour spectrum, listed in increasing pressure as blue, green, yellow, orange, red, and pink. Therefore, a typical colour-contour map of a tumour would correspond to a region of a localized high pressure represented by pink (due to the stiffer nature of the tumour) surrounded by a region of low pressure indicated by blue (corresponding to softer, healthy tissue), thereby clearly distinguishing a tumour from the surrounding tissue. A sample image of the colour-contour map, indicating the presence of a tumour, is shown in Figure 1.4.

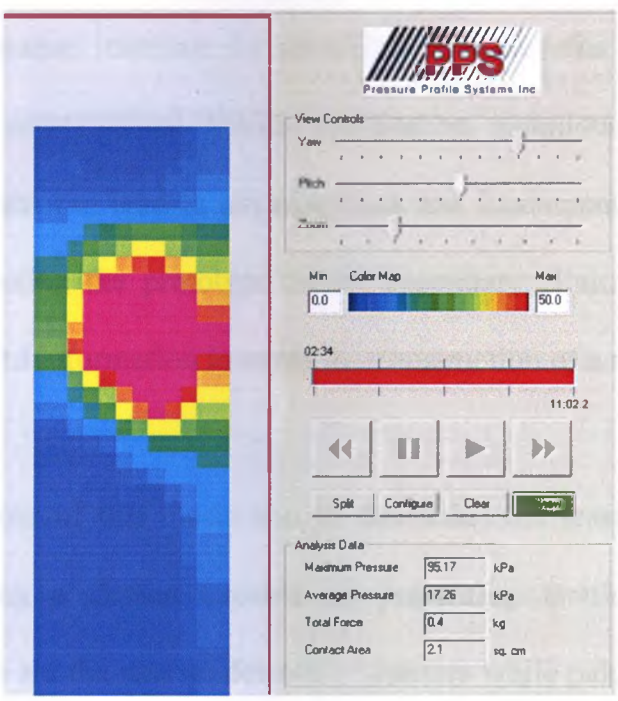


**Figure 1.4:** Screenshot of the PPS Sapphire Visualization interface with presence of a tumour indicated by a concentrated pink area (shown on left).

For the purposes of this research, an interpolated two-dimensional (2D) display of the visualization software was utilized since this display was found to be the most intuitive to interpret when using the probe for tumour localization. However, the visualization interface is capable of providing a three-dimensional (3D), isometric, or

other views of the interpolated display by adjusting the yaw, pitch, and zoom controls on the user interface. When insufficient forces are applied on the pad, or the sensitivity of the display is high, artifacts in the image make it difficult to distinguish tumour location. A special feature in the software allows the user to set the sensitivity of the colour-contour pressure map for the active display window.

## 1.6 Purpose and Objectives

The motivation of this thesis was to thoroughly test and improve the performance of the TSI and visualization interface by identifying its benefits and limitations in comparison with other conventional VATS localization techniques. The exhaustive testing of the entire system can lead to advantageous and fundamental modifications to the system, either promoting the prototype to the secondary clinical stage of *in vivo* testing, or providing useful information towards the construction of a second prototype of the system.

The overall purpose of this thesis was to determine the feasibility and possible benefits of implementing a device capable of presenting tactile and kinaesthetic information for VATS to aid the user in detecting tumours while palpating *ex vivo* lung. The project was divided into four objectives. The first was to test the performance of the TSI in a preliminary study to determine if it was at minimum comparable to the current VATS method of using an endoscopic grasper. The second objective was to determine the effects on device performance when palpating tissue in a linear fashion (i.e., robot-assisted palpation) and a non-linear fashion (i.e., manual-assisted palpation). Based on

the results from the second objective, the third objective was to improve the visualization interface so that, in addition to presenting tactile information, it can present applied force (kinaesthetic) information to the user. The last objective was to compare the new system, consisting of the TSI with a new visualization interface capable of providing contact force data instantaneously to the user, to standard clinical instruments currently used to locate tumours intra-operatively during VATS. The chapters of this thesis are divided into the four project objectives and are presented in historical sequence.

## 1.7 Thesis Outline

### *1.7.1 A New Tactile Imaging Device to Aid with Localizing Lung Tumours during Thoracoscopic Surgery (Chapter 2)*

A new tactile sensing instrument (TSI) was created by a research team at Canadian Surgical Technologies and Advanced Robotics (CSTAR) to meet performance specifications that were required for a tumour to be localized via palpation using kinaesthetic sensing methods. A preliminary study was prepared to assess the performance of the TSI by comparing it to a current clinical standard of using an endoscopic grasper to locate lung tumours during thoracoscopic surgery. A series of experiments were conducted using volunteers who had no medical education or clinical experience. The goal of the experiments was to accurately locate 10 mm artificial tumours sutured into *ex vivo* porcine lungs attained from a local abattoir. The experimental setup utilized a MIS training box, which mimics the environmental and anatomical restrictions a surgeon experiences while performing VATS. The instruments

were assessed and compared according to their sensitivity, positive predicted value, task completion time, and localization distance.

### *1.7.2 Robot-Assisted Tactile Sensing for Minimally Invasive Tumour Localization (Chapter 3)*

Based on the limitations of the TSI identified in Chapter 2, a study was designed which compared the stochastic, varying palpation methods of humans and the controlled, systematic palpation method of a robot using the TSI to assess the feasibility of using the TSI under robotic control to reliably locate underlying tumours. It was hypothesized that the robotic method would reduce collateral tissue trauma when palpating underlying tumours (5 mm and 10 mm in diameter) embedded in tissue. Thinly sliced *ex vivo* bovine livers were used as a surrogate for *ex vivo* porcine lung since it was an easier resource to attain in large quantities. An Augmented Hybrid Impedance Control scheme was implemented on a Mitsubishi PA10-7C robot to perform the force/position control used in the trials. The two methods were assessed on maximum applied forces and tumour detection accuracy.

### *1.7.3 Visual Force Feedback Improves the Performance of a Tactile Sensing System during Minimally Invasive Tumour Localization (Chapter 4)*

In the work presented in Chapter 3, it was shown that TSI performance is highly dependent on the amount of force being applied by the user, which requires the

calibration of the TSI. This chapter presents the calibration method and the integration of calibration data with a visualization interface, collectively referred to as the tactile sensing system (TSS). The TSS allows the forces applied to the tissue during palpation to be displayed in real-time to the user. Experiments were conducted to determine whether providing visual force feedback to the user will significantly benefit TSS performance when attempting to locate 10 mm hemispherical agar tumours in *ex vivo* bovine liver. Performance assessment was based on the forces applied to the tissue and the overall performance of the TSS with and without the display of applied forces. The TSS with and without force display were compared using average and maximum applied forces, and detection accuracy.

### *1.7.4 New Tactile Sensing System for Minimally Invasive Surgical Tumour Localization (Chapter 5)*

The work presented in Chapter 4 demonstrated that visual force feedback improves the performance of the tactile sensing system when compared to the same system without visual force feedback. In this chapter, the relative performance of the TSS with force display is compared to that of conventional MIS intra-operative localization methods (i.e., using an endoscopic grasper to directly palpate tissue or using an ultrasound probe), and the current standard of practice (i.e., manual palpation). The experiments were conducted on *ex vivo* tissue using liver as an ideal tissue model. The performance of the TSS was then tested using collapsed lung as a realistic tissue model. All tissues had the possibility of containing 10 mm artificial tumours. All instruments

were assessed in terms of average and maximum palpation force, localization distance, and 'success rate.' These measures were used to attain the statistical results of accuracy, sensitivity, specificity, and likelihood ratios.

## References


[1] G. J. Tortora and B. Derrickson, *Principles of anatomy and physiology*, 11th ed., John Wiley & Sons, Inc., 2006.

[2] H. Gray. (1918). *Anatomy of the human body*. Philadelphia: Lea & Febiger, Fig. 962. [Online]. Available: http://www.bartleby.com/107/.

[3] Encyclopædia Britannica. (2009). "Lung." *Encyclopædia Britannica Online*. [Online]. Available: http://www.search.eb.com.proxy2.lib.uwo.ca:2048/eb/article-9049375

[4] American Cancer Society. (2007). *Global Cancer Facts and Figures 2007*. Atlanta, GA: American Cancer Society Inc. [Online]. Available: http://www.cancer.org/downloads/STT/Global_Facts_and_Figures_2007_rev2.pdf.

[5] Canadian Cancer Society. (2009). *Canadian Cancer Statistics 2009*. Toronto, Ontario: Canadian Cancer Society Inc. [Online]. Available: http://www.cancer.ca.

[6] American Cancer Society. (2009). *Cancer Facts and Figures 2009*. Atlanta, GA: American Cancer Society Inc. [Online]. Available: http://www.cancer.org/downloads/STT/500809web.pdf.

[7] R. H. Daffner, *Clinical radiology: The essentials*. Baltimore, Maryland: Williams & Wilkins, 1993.

[8] J. A. Roth, J. C. Ruckdeschel, and T. H. Weisenburger, *Thoracic oncology*. 2nd ed., Philadelphia, Pennsylvania: W. B. Saunders Company, 1995.

[9] S. R. Desai, T. Franquet, T. E. Hartman, and A. U. Wells, *Pulmonary imaging: Contributions to Key Clinical Questions*. Boca Raton, Florida: Informa UK Ltd., 2007.

[10] D. Mahalingam, A. Mita, M. M. Mita, S. T. Nawrocki, and F. J. Giles, "Targeted therapy for advanced non-small cell lung cancers: historical perspective, current practices, and future development," *Curr. Probl. Cancer*, vol. 33, (2), pp. 65–112, 2009.

[11] A. F. Cardona Zorrilla, L. Reveiz, E. G. Ospina, and A. Yepes, "Palliative endobronchial brachytherapy for non-small cell lung cancer (Review)," in *The Cochrane Library 2009,* iss. 3, John Wiley & Sons, Inc., 2009.

[12] Encyclopædia Britannica. (2009). "Lung cancer." *Encyclopædia Britannica Online.* [Online]. Available: http://www.search.eb.com.proxy2.lib.uwo.ca:2048/eb/article-9049376.

[13] J. P. van Meerbeeck and V. F. M. Surmont, "Stage IIIA-N2 NSCLC: A review of its treatment approaches and future developments," *Lung Cancer*, 2009, article in press, doi:10.1016/j.lungcan.2009.02.007.

[14] B. Jeremic and M. Bamberg, "External beam radiation therapy for bronchial stump recurrence of non-small-cell lung cancer after complete resection," *Radiother. Oncol.*, vol. 64, pp. 251–257, 2002.

[15] P. A. Kupelian, R. Komake, and P. Allen, "Prognostic factors in treatment of mode negative non-small cell lung cancer with radiation therapy alone," *Int. J. Radiat. Oncol. Biol. Phys.*, vol. 36, pp. 607–613, 1996.

[16] C. A. Mantz, D. E. Dosoretz, J. H. Rubenstein, P. H. Blitzer, M. J. Katin, G. R. Garton, B. M. Nakfoor, A. D. Siegel, K. A. Tolep, S. E. Hannan, R. Dosani, A. Feroz, C. Maas, S. Bhat, G. Panjikaran, S. Lalla, K. Belani, and R. H. Ross, "Endobronchial brachytherapy and optimization of local disease control in medically inoperable non-small cell lung carcinoma: a matched-pair analysis," *Brachyther.*, vol. 3, pp. 183–190, 2004.

[17] B. Hilaris and D. A. Mastoras, "Contemporary brachytherapy approaches in non-small-cell lung cancer," *J. Surg. Oncol.*, vol. 69, pp. 258–264, 1998.

[18] G. Rocco, "Results of cutting-edge surgery in stage IIIA-N2 nonsmall cell lung cancer," *Curr. Opin. Oncol.*, vol. 21, (2), pp. 105–109, 2009.

[19] H. Nakamura, "Controversies in thoracoscopic lobectomy for lung cancer: editorial," *Ann. Thorac. Cardiovasc. Surg.*, vol. 13, (4), pp. 225–227, 2007.

[20] R. H. Bell and D. B. Kaufman, *Northwestern handbook of surgical procedures.* Georgetown, Texas: Landes Bioscience, 2005.

[21] R. Gharagozloo and F. Najam, *Robotic Surgery.* China: McGraw-Hill Companies, Inc., 2009.

[22] R. N. Younes, "Video-assisted thoracic surgery for lung cancer," in *Endosurgery for Cancer*, Eubanks *et al.*, Ed. Austin, Texas: Landes Bioscience, 1999, pp. 199–203.

[23] A. P. C. Yim, K. M. Ko, and W. S. Chau, "Video-assisted thoracoscopic anatomic lung resections: The initial Hong Kong experience," *Chest*, vol. 109, p. 13, 1996.

[24] T. L. Demmy and J. J. Curris, "Minimally invasive lobectomy directed toward frail and high-risk patients: A case control study," *Ann. Thorac. Surg.*, vol. 68, p. 194, 1999.

[25] R. Giudicelli, P. Thomas, and T. Lonjon, "Video-assisted minithoracotomy versus muscle-sparing thoracotomy for performing lobectomy," *Ann. Thorac. Surg.*, vol. 58, p. 712, 1994.

[26] A. Lin, A. L. Trejos, R. V. Patel, and R. A. Malthaner, "Robot-assisted minimally invasive brachytherapy for lung cancer," in *Telesurgery*, S. Kumar *et al.*, Ed. Berlin: Springer-Verlag, 2008. pp. 33–52.

[27] M. Nakuta, H. Saeki, and N. Yokoyama, "Pulmonary function after lobectomy: Video-assisted thoracic surgery versus a thoracotomy," *Ann. Thorac. Surg.*, vol. 70, p. 938, 2000.

[28] J. Bodner, H. Wykypiel, G. Wetscher, and T. Schmid, "First experiences with the da Vinci operating robot in thoracic surgery," *Eur. J. Cardiothorac. Surg.*, vol. 25, (5), pp. 844–851, 2004.

[29] H. Liu, D. P. Noonan, K. Althoefer, and L. D. Seneviratne, "Rolling mechanical imaging: a novel approach for soft tissue modeling and identification during minimally invasive surgery," in *Proc. IEEE Int. Conf. Robot. Autom. (ICRA)*, Pasadena, California, 2008, pp. 845–850.

[30] D. Sortini, C. V. Feo, P. Carcoforo, G. Carrella, E. Pozza, A. Liboni, and A. Sortini, "Thoracoscopic Localization Techniques for patients with solitary pulmonary nodule and history of malignancy," *Ann. Thorac. Surg.*, vol. 79, pp. 258–262, 2005.

[31] F. M. A. Melfi, G. F. Menconi, A. M. Mariani, and C. A. Angeletti, "Early experience with robotic technology for thoracoscopic surgery," *Eur. J. Cardiothorac. Surg.*, vol. 21, pp. 864–868, 2002.

[32] Intuitive Surgical. (2009). "da Vinci Si Surgical System." *Intuitive Surgical, Inc.* [Online]. Available: http://www.intuitivesurgical.com.

[33] R. H. Taylor and D. Stoianovici, "Medical robotics in computer integrated surgery," *IEEE Trans. Robot. Autom.*, vol. 19, (5), pp. 765–781, 2003.

[34] G. L. McCreery, A. L. Trejos, R. V. Patel, M. D. Naish, and R. A. Malthaner, "Evaluation of force feedback requirements for minimally invasive lung tumour localization," in *Proc. IEEE Int. Conf. Intell. Robot. Syst. (IROS)*, San Diego, California, 2007, pp. 883–888.

[35] A. P. Miller, W. J. Peine, J. S. Son, and J. T. Hammoud, "Tactile imaging system for localizing lung nodules during video assisted thoracoscopic surgery," in *Proc. IEEE Int. Conf. Robot. Autom. (ICRA)*, Roma, Italy, 2007, pp. 2996–3001.

[36] M. Tavakoli, A. Aziminejad, R. V. Patel, and M. Moallem, "Tool/tissue interaction feedback modalities in robot-assisted lump localization", in *Proc. IEEE EMBS Ann. Int. Conf.*, New York City, New York, 2006, pp. 3854–3858.

[37] M. Kaneko, C. Toya, and M. Okajima, "Active strobe imager for visualizing dynamic behavior of tumours," in *Proc. IEEE Int. Conf. Robot. Autom. (ICRA)*, Roma, Italy, 2007, pp. 3009–3014.

[38] P. Ciriaco, G. Negri, A. Puglisi, R. Nicoletti, A. Del Maschio, and P. Zannini, "Video-assisted thoracoscopic surgery for pulmonary nodules: rationale for preoperative computed tomography-guided hookwire localization," *Eur. J. Cardiothorac. Surg.*, vol. 25, pp. 429–433, 2004.

[39] J. Hu, C. Zhang, and L. Sun, "Localization of small pulmonary nodules for videothoracoscopic surgery," *Anz J. Surg.*, vol. 76, pp. 649–651, 2006.

[40] S. Matsumoto, T. Hirata, E. Ogawa, T. Fukuse, H. Ueda, T. Koyama, T. Nakamura, and H. Wada, "Ultrasonographic evaluation of small nodules in the peripheral lung during video-assisted thoracic surgery (VATS)," *Eur. J. Cardiothorac. Surg.*, vol. 26, pp. 469–473, 2004.

[41] R. Santambrogio, M. Montorsi, P. Bianchi, A. Mantovani, F. Ghelma, and M. Mezzetti, "Intraoperative Ultrasound during thoracoscopic procedures for solitary pulmonary nodules," *Ann. Thorac. Surg.*, vol. 68, pp. 218–222, 1999.

[42] V. D. M. Hornblower, E. Yu, A. Fenster, J. J. Battista, and R. A. Malthaner, "3D thoracoscopic ultrasound volume measurement validation in an ex vivo and in vivo porcine model of lung tumors," *Phys. Med. Biol.*, vol. 52, pp. 91–106, 2007.

[43] R. M. Satava, A. Gaspari, and N. Di Lorenzo, *Emerging technologies in surgery.* Heidelberg, Germany: Springer-Verlag, 2007.

[44] T. Hemsel, R. Stroop, D. Olivia Uribe, and J. Wallaschek, "Resonant vibrating sensors for tactile tissue differentiation," *J. Sound Vib.*, vol. 308, (3–5), pp. 441–446, 2007.

[45] Y. Murayama, M. Haruta, Y. Hatakeyama, T. Shiina, H. Sakuma, S. Takenoshita, S. Omata, and C. E. Constantinou, "Development of new instrument for examination of stiffness in the breast using haptic sensor technology," *Sens. Actuators, A: Phys.*, vol. 143, (2), pp. 430–438, 2008.

[46] N. Kattavenos, B. Lawrenson, T.G. Frank, H.S. Pridham, R.P Keatch, and A. Cuschieri, "Force-sensitive tactile sensor for minimal access surgery", *Minim. Invasive Ther. Allied Technol.*, vol. 13, (1), pp. 42–46, 2004.

[47] M. V. Ottermo, M. Øvstedal, T. Langø, Ø. Stavdahl, Y, Yavuz, T. A. Johansen, and R. Mårvik, "The role of tactile feedback in laparoscopic surgery," *Surg. Laparosc. Endosc. Percutan. Technol.*, vol. 16, (6), pp. 390–400, 2006.

[48] A. Sarvazyan, "Mechanical imaging: a new technology for medical diagnostics," *Int. J. Med. Inf.*, vol. 49, pp. 195–216, 1998.

[49] G. L. McCreery, A. L. Trejos, M. D. Naish, R. V. Patel, and R. A. Malthaner, "Feasibility of locating tumours in lung via kinaesthetic feedback," *Int. J. Med. Robot. Comput. Assist. Surg.*, vol. 4, (1), pp. 58–68, 2008.

[50] Pressure Profile Systems. (2007). "Capacitive sensing." *Pressure Profile Systems, Inc.* [Online]. Available: http://www.pressureprofile.com/technology-capacitive.php

# Chapter 2

# A New Tactile Imaging Device to Aid with Localizing Lung Tumours during Thoracoscopic Surgery[1]

## 2.1 Introduction

In conventional surgery for lung tumour resection, one of the most effective intra-operative means that a surgeon has of identifying the presence of disease or pathology is direct palpation. Qualitative differences in the mechanical properties of the tissue are used to localize underlying tumours [1]. However in minimally invasive surgery (MIS), the surgeon loses direct physical access to the operational site and thus, can no longer locate tumours via manual palpation [2].

Current localization methods include using an endoscopic grasper inserted through a trocar and sliding the tip of the grasper across the lung surface. As with direct palpation, the goal is to detect any tissue abnormalities or hard growths in the soft lung

[1] A version of this chapter has been published in The International Journal of Computer Assisted Radiology and Surgery (Int. J. CARS) with an author list: MT Perri, DA Bottoni, AL Trejos, GL McCreery, MD Naish, RV Patel, and RA Malthaner

tissue, which could indicate the presence of a tumour. With the grasper acting as a surrogate for a finger, many tactile cues are lost. This results in a procedure that is often time consuming and frustrating, and is prone to uncertainties in tumour detection [3]. Ideally, a more precise and accurate method for tumour localization can be made available to surgeons.

To that end, a tactile sensing instrument (TSI) was developed that employs a sterilizable capacitive-based sensor array mounted on a hand-held minimally invasive probe, 10 mm in diameter. A visualization interface was implemented to use the visual colour spectrum to indicate the localized pressure intensity experienced by the probe, with pink indicating the highest pressure intensity and blue indicating the lowest pressure intensity. When the sensor array was in contact with a tumour, the device confirmed its presence by indicating a localized increase in pressure in that area. Details of the sensor design can be found in [4] – [6] and Section 1.5.

## 2.2 Purpose

The motivation behind this study was to conduct a preliminary assessment of the performance of the TSI by comparing it to a current clinical standard of using an endoscopic grasper to locate lung tumours during thoracoscopic surgery. The goal of this study was to test the design of a capacitor-based sensor to determine the location of artificial agar tumours in an *ex vivo* porcine lung. The results are compared to those generated from the current clinical tumour localization method of palpating with an endoscopic grasper. Furthermore, these results will determine if the implementation of

the TSI in surgery has the potential to greatly facilitate the palpation process for the surgeon.

## 2.3 Methods

A series of experiments were conducted to test the performance of the TSI compared to an endoscopic grasper when attempting to locate agar tumours embedded in *ex vivo* porcine lungs.

### *2.3.1 Materials*

A set of three *ex vivo* porcine lungs were attained from a local abattoir and were separated to isolate the left and right lungs. The lungs were embedded with a random number of agar tumours for the validation experiments. The agar tumours were inserted into incisions made in the dorsal side of the lung and sutured inside the lung parenchyma. The tumours were made from Gelrite Gellan Gum (Sigma-Altrich, Inc.) at a concentration of 53.3 g/L and had a diameter of approximately 10 mm, as shown in Figure 2.1. Only the right superior (cranial) lobe, the right middle lobe, and the left superior (cranial) lobe of the lungs were used for experimentation. Each lung lobe had the possibility of containing one to four agar tumours, and the number of tumours to be embedded was a randomized process. To prevent the assumption that the silk sutures used in the experiment were the items being detected by the TSI, a random number of zero to two sham cuts were performed on the lung. A sham cut is an incision made on the

dorsal side of the lung lobe that is then sutured closed with silk sutures, without the insertion an agar tumour.

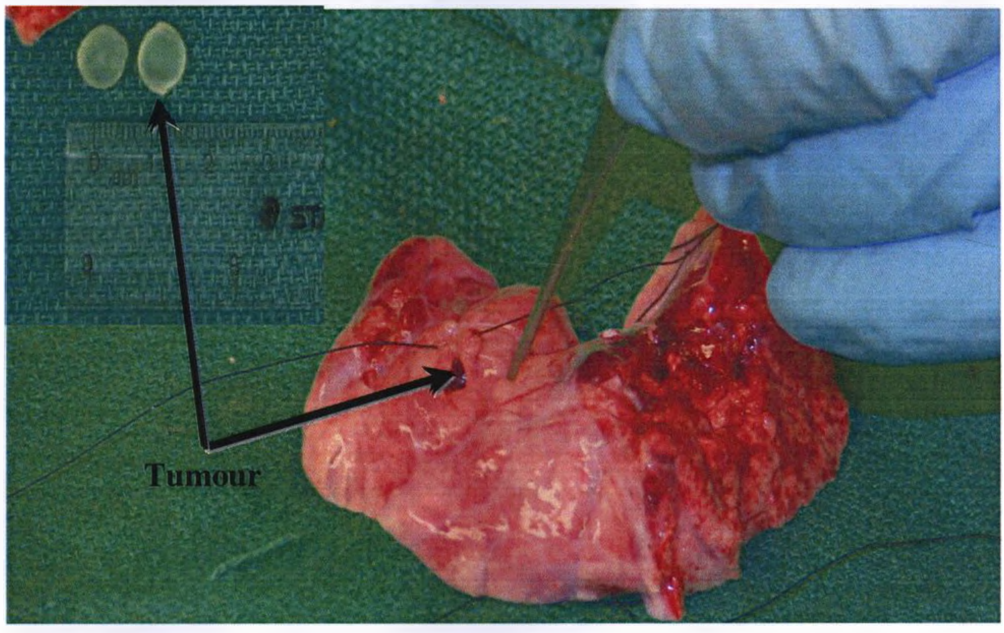


**Figure 2.1: A** 10 mm agar tumour being sutured into lung parenchyma. Left top inset shows the dimensions of the agar tumours.

### *2.3.2 Experimental Setup*

The experimental test-bed consisted of an *ex vivo* porcine lung lobe placed into a MIS training box, which mimicked the environmental and anatomical restrictions a surgeon experiences while performing thoracoscopic surgery. A computer monitor was placed adjacent to the MIS training box and actively displayed the visualization interface to the user when using the TSI. The experimental setup is shown in Figure 2.2.

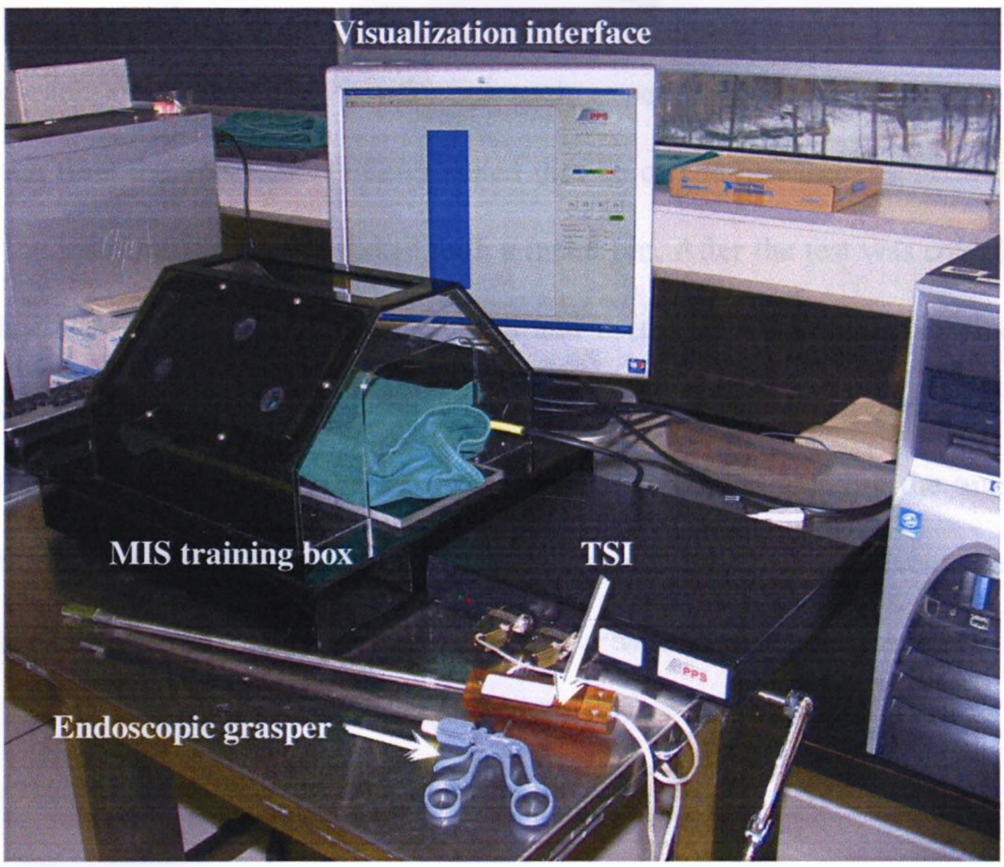


**Figure 2.2:** Experimental setup.

### *2.3.3 Validation Experiments*

Six volunteers with no surgical training were recruited to find the tumours in four randomly-assigned lung phantoms; two lung phantoms using the TSI and two lung phantoms using the endoscopic grasper. To reduce the error attributed to a learning curve, each participant was permitted to practice palpating a 10 mm diameter agar tumour embedded in a superior lobe of an *ex vivo* porcine lung with both the TSI and the endoscopic grasper until he or she felt comfortable with both instruments. The superior lung lobe was prepared especially for the training sessions and was not selected for use during the validation experiments.

All volunteers were blinded to the number of artificial tumours located in the lung phantom. The lung lobe and palpation instrument used in each trial was randomly assigned to each volunteer. The duration of each experiment was restricted to five minutes. Each time the volunteer verbally stated that he or she had found a tumour, the location of the instrument tip was marked with a metal pin. After the test was completed, radiographic images of the lungs were acquired and used to determine the accuracy of tumour localization. The results of the experiment were assessed in terms of task completion time, number of tumours located, and success rate of locating the tumours. The number of false positive results was also measured, which is the event that the volunteer believed that he or she had found a tumour where none were located in that area.

## 2.4 Results

A total of 12 different lung specimens were examined with each localization instrument. Due to randomization, there were 28 hidden agar tumours in the TSI group and 38 in the endoscopic grasper group. The result of the experiments is shown in Table 2.1.

**Table 2.1:** Performance assessment results.

| | **TSI** | **Endoscopic Grasper** |
|---|---|---|
| **Radial distance (mean ± SD)** | 0.24 ± 0.19 cm | 0.33 ± 0.26 cm |
| **Time (mean ± SD)** | 218 ± 109 s | 220 ± 68 s |
| **Sensitivity** | 71% | 61% |
| **Positive predictive value** | 87% | 70% |

The sensitivities of the TSI and endoscopic grasper were 71% and 61% respectively. The endoscopic grasper generated 10 false positive results whereas the TSI generated 3 false positive results. Among accurately identified targets, the TSI localized tumours within a radius of 0.24 ± 0.19 cm (mean ± SD) from the centre of the lesion, while the endoscopic grasper localized tumours within a radius of 0.33 ± 0.26 cm, with a *p*-value of 0.19 using a two-tailed *t*-test. The positive predicted values of the TSI and endoscopic grasper were 87% and 70% respectively. The average time spent evaluating each lung was 218 ± 109 seconds for the TSI, and 220 ± 68 seconds for the endoscopic grasper, with a *p*-value of 0.95 using a two-tailed *t*-test.

## 2.5 Discussion

This study was preliminary in nature, designed to assess the performance of a new tactile device designed by the research team at Canadian Surgical Technologies and Advanced Robotics (CSTAR). The results of this study have determined that the

implementation of the TSI in MIS surgery has the potential to facilitate the lung palpation process for the surgeon as compared to standard clinical practice. However, during this process, the limitations of the TSI also became evident. Volunteers in the validation experiments mentioned the difficulty that they experienced while palpating the lung with the TSI. Most notably was that the volunteers had no indication of the amount of force they were applying to the tissue while palpating. They suspected that if they had a better indication of the applied forces, they could interpret the Visualization interface information from the tactile sensor more accurately. Therefore, there appears to be a need to present to the user the applied forces at the point of contact, in addition to tactile data, to improve the performance of the TSI.

Porcine lungs are a difficult resource to attain for experimental purposes. For this study, only three sets of porcine lungs could be attained from a local abattoir in an adequate time period for the study. Therefore, it is assumed that the results from this study are susceptible to Type II (beta) error since the study's actual sample size of fifteen lung segments was evidently too small to gain statistically significant results. As a result, this created an underpowered study with large, insignificant $p$-values.

A view of the working space was accessible by direct visual contact via the top panel of the MIS training box. This was made possible by removing the top port-placement plate from the box. This allowed the possibility for the volunteers to integrate visual cues with kinaesthetic or tactile information while palpating the tissue. This was an undesirable result since direct visual access of the working area is not possible in traditional minimally invasive surgery. MIS is a procedure involving the use of an endoscope, to provide a visual of the operational site, that is inserted through a port in the

chest approximately 10 mm in diameter. The images displayed by the endoscope, however, typically distort visual cues and the visualization information is usually quite poor [7]. It should be noted that for this study, allowing the volunteers to see the working site directly did not introduce a significant advantage to either instrument since this arrangement was permitted for both instruments during the study. However, a consideration for forthcoming experiments is to introduce an endoscope in the experimental setup to eliminate the possibility of the user receiving direct visual information that is not normally accessible during MIS.

## 2.6 Conclusion

In this study, the TSI demonstrated a 10% absolute increase in sensitivity and a 27% relative increase in localization distance when compared to the endoscopic grasper without the need for additional time. These results indicate that the implementation of the TSI in surgery has the potential to greatly enhance the palpation process for the surgeon compared to using the current palpation method of an endoscopic grasper. Limitations of the design of the study were also identified, including the limited number of available porcine lungs, no method to indicate the applied forces to the user when using the TSI, and the influence of direct visual cues when simulating an MIS environment.

The experimental results suggest that the TSI can offer improvement to the current minimally invasive lung tumour palpation technique by providing to the surgeon some of the tactile information lost during thoracoscopic surgery. This is accomplished via sensory substitution, augmenting tactile sensation with visual stimuli. This addresses

one of the current restricting factors in minimally invasive surgery — limited tactile feedback.

## References

[1] J. Dargahi, S. Payandeh, and M. Parameswaran, "A micromachined piezoelectric teeth-like laparoscopic tactile sensor: theory, fabrication and experiments," in *Proc. IEEE Int. Conf. Robot. Autom. (ICRA)*, Detroit, Michigan, 1999, pp. 299–304.

[2] H. Liu, D. P. Noonan, K. Althoefer, and L. D. Seneviratne, "Rolling mechanical imaging: a novel approach for soft tissue modeling and identification during minimally invasive surgery," in *Proc. IEEE Int. Conf. Robot. Autom. (ICRA)*, Pasadena, California, 2008, pp. 845–850.

[3] A. P. Miller, W. J. Peine, J. S. Son, and J. T. Hammoud, "Tactile imaging system for localizing lung nodules during video assisted thoracoscopic surgery," in *Proc. IEEE Int. Conf. Robot. Autom. (ICRA)*, Roma, Italy, 2007, pp. 2996–3001.

[4] R.S. Fearing, "Tactile sensing mechanisms," *Int. J. Robot. Res.*, vol. 9, (3), pp. 3–23, 1990.

[5] R. D. Howe, W. J. Peine, D. A. Kontarinis, and J. S. Son. "Remote palpation technology," *Eng. Med. Biology Mag.*, vol. 14, (3), pp. 318–323, 1995.

[6] W. J. Peine, J. S. Son, and R.D. Howe, "A palpation system for artery localization in laparoscopic surgery," in *Proc. 1st Int. Symp. Med. Robot. Comput. Assist. Surg.*, Pittsburgh, Pennsylvania, 1994, pp. 22–24.

[7] T. Hemsel, R. Stroop, D. Olivia Uribe, and J. Wallaschek, "Resonant vibrating sensors for tactile tissue differentiation," *J. Sound Vib.*, vol. 308, (3–5), pp. 441–446, 2007.

# Chapter 3

# Robot-Assisted Tactile Sensing for Minimally Invasive Tumour Localization[1]

## 3.1 Introduction

Cancer is the second leading cause of death in North America and Europe [1], [2]. The best way to control the spread of cancer cells to healthy tissue or to other parts of the body is by surgically removing all cancer nodules through a procedure called surgical resection. Intra-operatively, the surgeon relies on direct palpation of the tissue to confirm tumour location or find others that were not detected through imaging. Direct palpation of tissue provides a qualitative assessment of the mechanical properties of the tissue, since malignant tumours are commonly stiffer than the surrounding tissue, allowing them to be easily identified as hard nodules when palpated [3].

Traditional tumour resection surgery involves performing a large incision on the chest or abdomen wall in order to access the diseased tissue, leading to a highly invasive

[1] A version of this chapter has been published in The International Journal of Robotic Research (IJRR) – Special Issue on Medical Robotics with an author list: AL Trejos, J Jayender, MT Perri, MD Naish, RV Patel, and RA Malthaner

procedure. The recent development of novel instruments and techniques has allowed surgical procedures to be performed through 10 mm incisions using long, narrow instruments. These minimally invasive approaches offer the advantages of reduced tissue trauma, decreased risk of infection, faster recovery time, and reduced associated costs. However, the surgeon's ability to use these instruments for force feedback is compromised by the friction and moments introduced by the trocar and the cavity wall, by the length of the instrument, and the fulcrum effect at the incision site.

One such method, which has been the subject of considerable research, is the relay of haptic cues, or the 'sense of touch,' from the tissue–instrument interaction to the surgeon–instrument interface. Haptic information can be considered in two distinct modes: kinaesthetic and tactile [4]. The measurement of tactile information requires a tightly packed array of sensors capable of measuring multiple contact pressures or forces concurrently. For a complete representation of tool–tissue interaction, information related to both the kinaesthetic and tactile modes must be acquired.

### *3.1.1 Passive Measurement*

A variety of instruments have been developed to measure tissue interaction forces when used in a handheld manner. These instruments are dependent on the user for proper operation — the instruments cannot position themselves or control the amount of contact force used during sensing.

A strain gauge sensorized laparoscopic grasper was developed in [5]. The grasping force and grasper position are presented along with a measure of compliance, which

could be used to differentiate between objects of various stiffnesses. Another instrumented grasper, utilizing two thin foil strain gauges, is described in [3]. This system is capable of operating in a wet saline environment due to silicone encapsulation of the electronics, and can determine the location of the applied force along the grasper jaws. The sensitivity can be adjusted by varying the amplifier gain, and the system was reported to be sensitive to a force increase of 'a few grams.' It was also shown through finite element analysis that the system could be used to measure distributed forces, approximating them as a concentrated load. A two dimensional mechanical sensor to measure thrust and pull inside instrument jaws is proposed in [6]. The design of a laparoscopic grasper proposed in [7] uses piezoelectric sensors to detect forces in three degrees of freedom; however, the instrument is quite large for minimally invasive applications. In [8], finite element analysis is used to evaluate the performance of a tooth-like sensor. Miniaturization of this device is still required. In [9], a sensorized grasper was developed incorporating a 6-degrees of freedom (6-DOF) mini sensor (ATI Industrial Automation) and another force sensor on the grasper handle. Other researchers such as [10] and [11] have also tried sensing the forces on the handle of the instrument. In [5] minimally invasive surgical tools were modified by adding two strain gauges onto a sensing module and are used to estimate the properties of the manipulated tissue. [12] proposes the use of a novel high-accuracy 3-DOF miniature force sensor 12.5 mm in diameter and 15 mm long to internally measure tip forces by sensing forces on the shaft of the instrument.

A number of researchers have developed hand-held instruments that incorporate sensors directly onto the instrument gripper. A laparoscopic tactile sensor with a

piezoelectric film is proposed in [13]. Similarly, [14] proposes a tactile sensor that uses image processing to measure the relative motion between a transparent window and the end of an endoscope. An instrumented grasper was used to locate artificial tumours implanted in porcine bowel in [15]. While effective, it was found to be significantly slower than both direct palpation and the use of a standard instrument. Tactile feedback systems have also been proposed for identification and characterization of lesions in the breast [16], [17] and for identifying arteries during robotic surgery [18]. The use of tactile sensors to identify pulmonary lesions using a capacitive array was discussed in [19]. Validation tests using a foam model showed promising results. A review of tactile sensing technologies suitable for MIS is presented in [20].

### *3.1.2 Active and Robotic Measurement*

Some of the difficulties encountered during MIS due to reduced access conditions have been solved by the use of robotic systems. In these master-slave systems, the surgeon remotely and intuitively controls the instruments using the master controls, while a slave robot mimics the surgeon's motions and performs the procedure. Reversal of hand motion, force magnification, and poor dexterity are eliminated, while hand tremors are filtered and the view of the surgical field is magnified. One of the major limitations still present in MIS is the inability to transfer tool–tissue or hand–tissue interaction forces from the instrument tip to the surgeon.

A number of master-slave systems, capable of providing haptic feedback, and suitable for the evaluation of tissue stiffness through palpation have been developed. A

computerized endoscopic surgical Babcock grasper that utilizes existing surgical tools is described in [21], [22]. It performs an automatic palpation consisting of 3 cycles of a 1 Hz sinusoidal displacement of the grasper. Experimental results indicating the tool's ability to distinguish different mechanical properties of tissues appear promising. In [23] tissue interaction is measured using a number of strain gauges and a single-axis load cell integrated into a custom endoscopic instrument. User performance during soft tissue discrimination and lump localization are explored in [24], [25]. A different approach is used in [26], in which tissue stiffness is determined by measuring the amount of current applied to the motor of a motorized grasper.

The system developed in [27] employs a robot to automatically palpate for a patient's arterial pulse at the wrist. The robot is instrumented with an anthropomorphic finger with a tactile sensor array in the fingertip. While not suitable for MIS procedures, this system stands out as the only previous automated system to use tactile sensing for diagnostic purposes.

Research presented in [28] evaluated the effect of using a master-slave robotic system equipped with tactile sensing capabilities to detect the presence of a 19 mm acrylic ball embedded in rubber. The results of using the robotic system were compared to direct manipulation of the tactile sensor. Feedback to the user was provided via a tactile display. The results showed that the performance of the system was greatly dependent on how well the exploration force could be controlled by the user.

Some work in the area of robot-assisted palpation based on kinaesthetic feedback has also been undertaken [29]. A slender probe was attached to a 6-DOF force/torque sensor mounted on a PA10-7C manipulator. By advancing the probe to a constant depth

from the surface of the tissue, underlying tumours may be identified. This work also established the required measurement range and resolution for sensors used to perform palpation tasks.

### *3.1.3 Progress to Date*

Based on the specifications determined in [29], a tactile sensing instrument (TSI) that uses a commercially available pressure pad was developed. Details of the sensor design can be found in [30] – [32]. Other instruments have been developed for breast tumour localization using PPS sensors (www.pressureprofile.com). These instruments are not designed for minimally invasive surgery, which allows them to have a large sensing area, and as such, a large tissue area can be palpated at one time. In contrast, the instrument presented here is restricted to a 1 cm wide area so that it can be inserted through standard trocars. Preliminary tests showing the effectiveness of this hand-held probe, when compared to more traditional tumour localization methods, have been performed with promising results. These tests are detailed in Chapter 2 and [33].

### *3.1.4 Objectives*

The objective of this research is to assess the feasibility of using the TSI under robotic control in order to reduce tissue trauma and improve tumour detection. Furthermore, the research aims to develop an ideal robotic palpation method considering force and position control, magnitude of the palpation force, robot motion across the

palpated tissue, and a proper visualization technique. A section of this work has been presented in [34].

To achieve these objectives, an experimental evaluation has been performed. The experimental design is presented in Sections 3.2 and 3.3, starting with the details of the experimental setups used for the robot and the manual evaluations, and continuing with a thorough description of the experimental methods used. Section 3.4 summarizes the results obtained, which are then discussed in Section 3.5. A short conclusion is presented in Section 3.6.

## 3.2 Experimental Setup

Two experimental setups were used to compare the performance of a human and a robot when using tactile sensing for tumour localization. Both setups incorporated the use of the TSI.

### *3.2.1 Manual Setup*

The layout of the manual setup is shown in Figure 3.1. The TSI was used to palpate tissue resting on a plate that incorporates an ATI Gamma 6-DOF force/torque sensor (Sensor A), (ATI Industrial Automation). To ensure consistency with minimally invasive procedures, the tray and the specimen were shielded by a drape during tissue palpation to ensure that the working field was not physically visible. A 0° scope with a

standard resolution camera (Stryker Endoscopy Inc.) was held in place by the AESOP® endoscope positioner (Computer Motion Inc.).

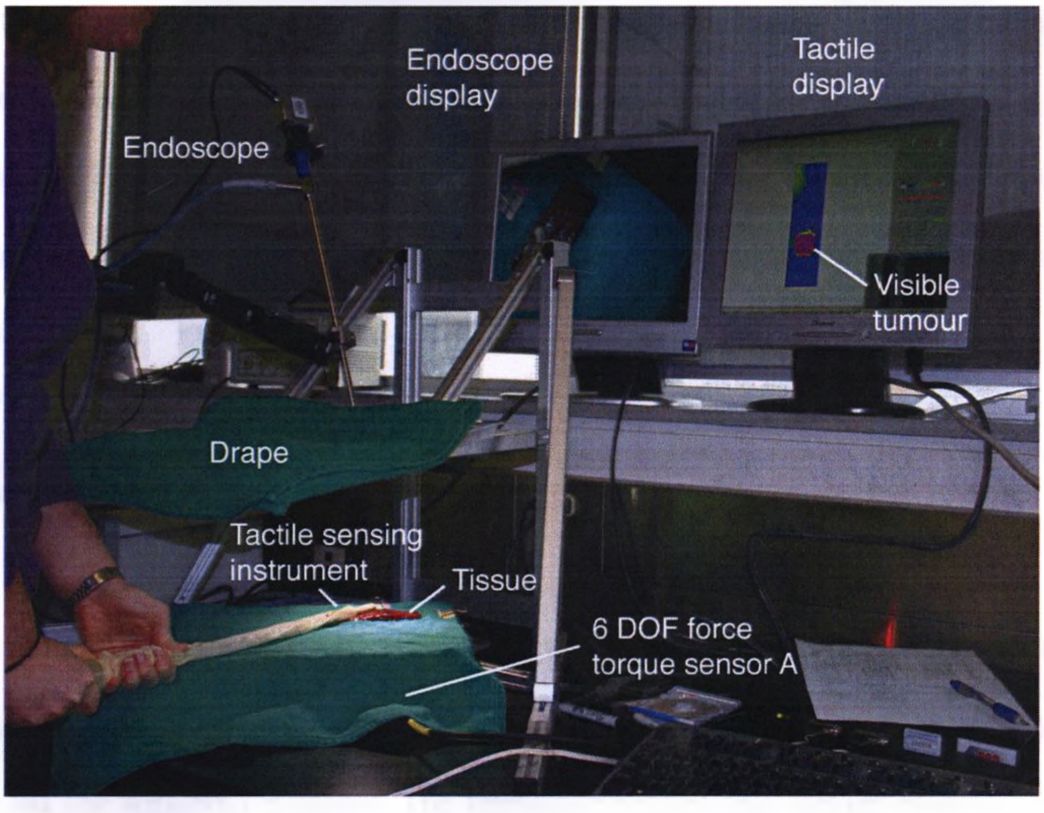


**Figure 3.1:** Layout for the experimental setup for manual testing. The visualization software indicates the presence of a tumour.

The PPS driver and the Sapphire® Visualization software were used to display the results from the tactile sensor in a meaningful way. The visualization software uses the visual colour spectrum to indicate the levels of localized pressure intensity experienced by the probe, with pink indicating the highest pressure intensity and blue indicating the lowest pressure intensity. Therefore, a typical colour-contour map of a tumour would correspond to a region of a localized high pressure represented by pink (due to the stiffer nature of the tumour) surrounded by a region of low pressure indicated by blue

(corresponding to softer tissue), thereby clearly distinguishing a tumour from the surrounding tissue, as shown in Figure 3.1.

For the purposes of this experiment, an interpolated two-dimensional (2D) display of the visualization software was utilized since this display was found to be the most intuitive to interpret when using the probe for tumour localization. When insufficient forces are applied on the pad, or the sensitivity of the display is high, artifacts in the image make it difficult to distinguish tumour location. A special feature in the software allows the user to set the sensitivity of the colour-contour pressure map for the active display window.

### *3.2.2 Robotic Setup*[2]

A 7-DOF Mitsubishi PA10-7C robot was employed to perform robot-assisted force-controlled tissue palpation. In our laboratory, the robot is controlled by a host computer via the ARCNET protocol. The four-layer control architecture consists of the host control computer, motion control card, servo controller, and the robotic arm. The host computer communicates with the PA10-7C arm at a sampling rate of 333 Hz. The complete system used to perform the experiments is shown in Figure 3.2. The host computer (Intel Xeon 3.2 GHz, 3.48 GB RAM running Windows XP) controls the robot and sends data packets via the ARCNET protocol to the servo controller. The ARCNET card (PCI-20U from Contemporary Controls Inc.) has been modified to be compatible

[2] Jagadeesan Jayender, a collaborator on this project, was responsible for the robot setup (Section 3.2.2), and the design and implementation of the robot control strategy (Section 3.2.2.1). These sections briefly outline his approach and are included in this chapter for completeness.

with the Optical Conversion Board (OCB) provided by Mitsubishi Heavy Industries for the PA10-7C robot. An ATI Gamma 6-DOF force/torque sensor (Sensor B) is used as the wrist force sensor on the robot to measure the force exerted by the robot end-effector on the tissue, assuming the instrument to be rigid. A second computer (Pentium IV 2.8 GHz, 1 GB RAM running Windows 2000 Professional) is responsible for data logging and showing the Visualization software interface, when applicable.

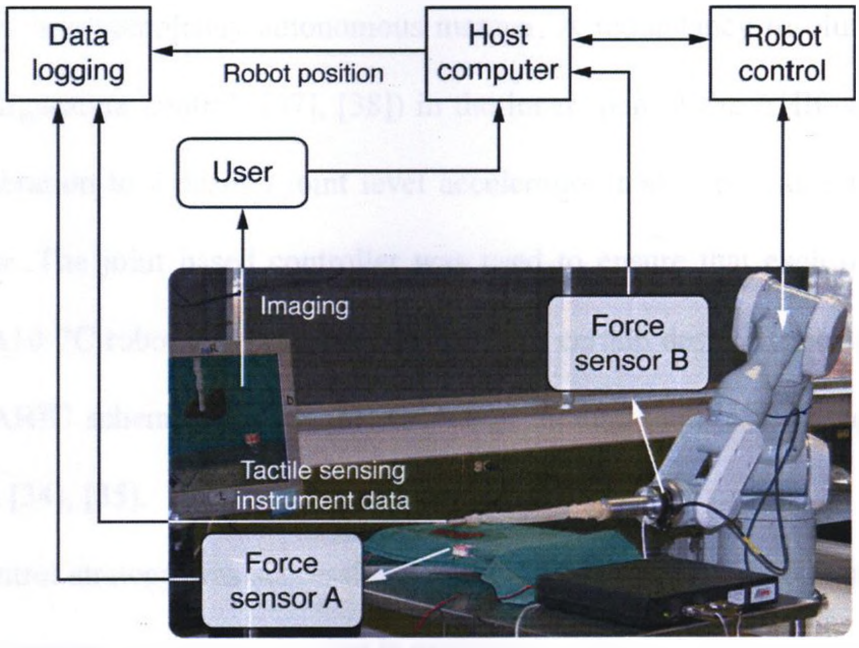


**Figure 3.2:** Configuration of the robotic experimental setup.

To perform force-controlled tissue palpation, the robot must have the ability to control the amount of force exerted on the tissue and must move precisely in Cartesian space to palpate a grid of points on the surface of the tissue.

*3.2.2.1 Robot Control*

An Augmented Hybrid Impedance Control (AHIC) scheme [36] has been implemented on the PA10-7C robot to control the force of palpation and the position of the end-effector in Cartesian space. The task space in the AHIC is divided such that force control is performed in the direction of palpation (in this case the $z$ direction), while the position and orientation of the end-effector are controlled in the orthogonal directions. The area of the tissue palpated is based on the input provided by the user; however, palpation occurs in a completely autonomous manner. A redundancy resolution module (based on 'configuration control' [37], [38]) in the inner loop of the AHIC converts the Cartesian acceleration to a desired joint level acceleration and is provided to the joint-based controller. The joint based controller was used to ensure that each of the seven joints of the PA10-7C robot was controlled to follow a certain desired trajectory. Details regarding the AHIC scheme, redundancy resolution module, and joint based controller can be found in [34], [35].

This control strategy was successfully implemented with the robotic setup shown in Figure 3.3. The experimental evaluation is explained in the following section.

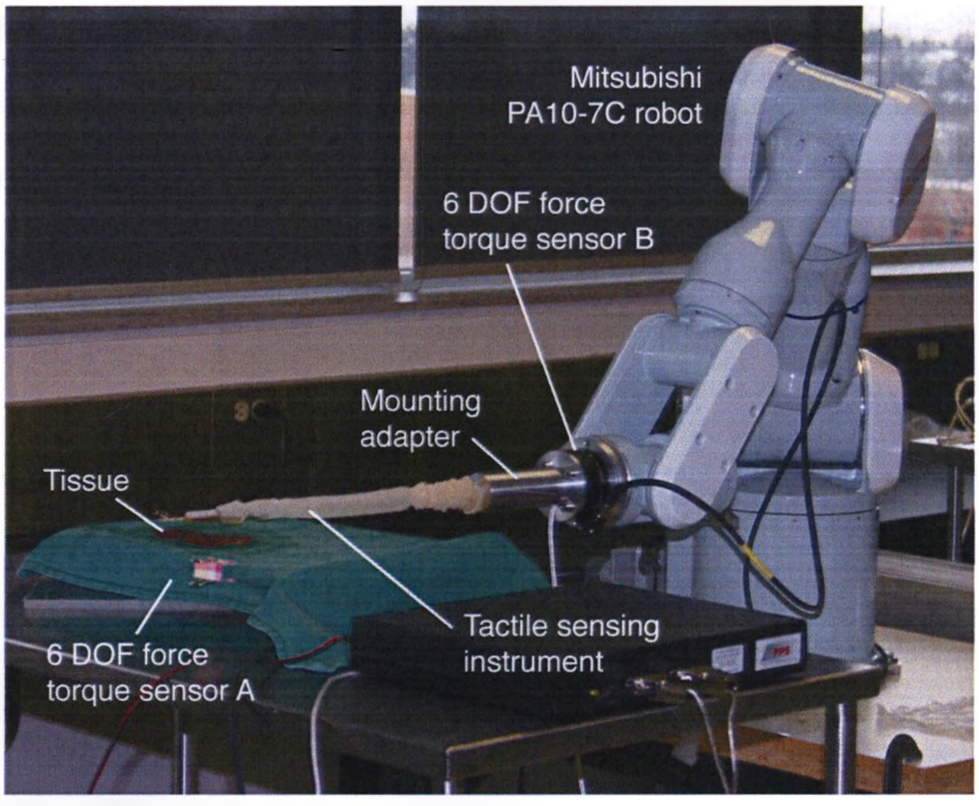


**Figure 3.3:** Robotic setup.

## 3.3 Methods

An experimental evaluation was performed to compare the performance of the Mitsubishi PA10-7C robot to that of a human subject when using tactile sensing for tumour localization. The details of this evaluation are presented below.

### *3.3.1 Tissue Preparation*

The tissue used in these experiments was *ex vivo* bovine liver obtained from a local store. To simulate the presence of tumours, 5 mm diameter spherical objects and 10 mm diameter hemispherical objects (see Figure 3.4) were pressed into the dorsal side of

the liver. These objects were made from thermoplastic adhesive (hot glue) with encased thin metal wires to ensure their visibility on radiographic images, which were later used to assess accuracy.

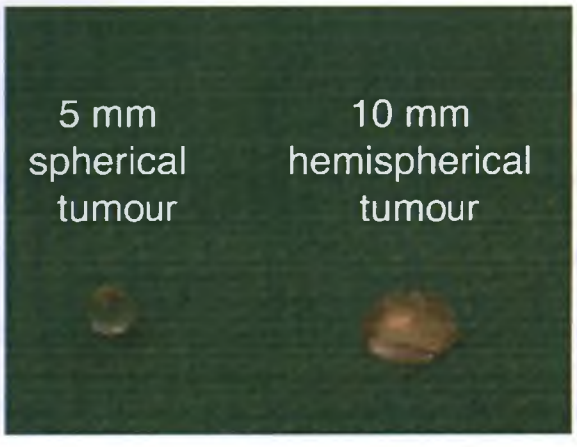


**Figure 3.4:** Simulated tumours.

For each of the palpation methods, nine *ex vivo* livers were prepared with small tumours and nine with large tumours. Each sample had the possibility of containing zero to two tumours, determined *a priori* through a block randomization process. Although in practice a patient will not be scheduled for surgery unless it is certain that a tumour is present in the organ, presenting liver with no embedded tumour is required to determine the statistical results of specificity and negative predicted value. The block randomization process was designed to ensure that an equal number of cases of zero, one, and two tumours embedded in the liver were presented at the end of all trials for each subject. The human subject was blinded to the block randomization process, and allowed to practice using additional liver samples prior to commencing each series of trials.

### *3.3.2 Performance Assessment*

The performance of each of the methods was assessed with different measurables: the success rate of locating tumours, the force exerted by the instrument while palpating, and the task completion time.

The *success rate* of locating tumours aims to determine the ability of the sensing method to correctly identify all of the tumours present in each liver sample. The success rate can be determined using four categories [39]: 1) a *true positive test* occurs when the tumour is correctly identified and found in the liver; 2) a *false positive test* occurs when the user indicates that a tumour is found where none is located in that area; 3) a *false negative test* occurs when the user did not find the tumour located in the liver; and 4) a *true negative test* occurs when the user correctly identifies that there is no tumour located in the liver. These four categories, adapted from [39], can be used to determine measures such as: accuracy (the proportion of tests that were correctly identified as having or not having a tumour); sensitivity (the proportion of tumours present in the samples and test positive); specificity (the proportion of specimens that do not have tumours and test negative); negative predictive value (the proportion of specimens that test negative that do not have tumours); and positive predictive value (the proportion of tumours found that are actually there, indicates the probability of a positive test of actually detecting a tumour).

The *palpation force* exerted while searching for a tumour is an indication of the potential damage to the tissue. In both setups, the maximum palpation force is determined using the ATI force/torque sensor placed below the specimen (Sensor A). The magnitude

of the force vector is computed from the individual forces acting in all three orthogonal directions. For the manual trials, a continuous acquisition of the force data is recorded in Newtons (N) at a sample rate of 50 Hz. If there were any drag or frictional forces acting on the probe, these were included in the measurements. For the robotic trials, the force values are recorded for each palpation point when the instrument is at its lowest position in contact with the tissue, i.e., when the applied force is at its maximum. The external forces acting on the probe (frictional, drag, viscous, etc.) have also been accounted for in the AHIC controller.

Lastly, the *task completion time* is the time required to locate the tumours in the specimen presented during the task. The recorded time begins once the probe has touched the surface of the liver. The task completion time is recorded once the user stops palpating the tissue, signifying the end of the trial.

### *3.3.3 Manual Tests*

Four human subjects participated in this experiment: two of them were experienced in surgical oncology and minimally invasive surgery; the other two had no clinical training. To further reduce the error attributed to a learning curve, the human participants were permitted to practice palpating 5 mm and 10 mm diameter tumours embedded into liver with the TSI until comfortable with its performance. These livers were prepared exclusively for the training sessions and were not selected for use during the trials.

Before the commencement of the trials, the participants were informed that any number of tumours could be located in the presented liver (including no tumours). A total of eighteen trials were completed by each of the four subjects to locate the artificial tumours (nine livers with 10 mm tumours and nine with 5 mm tumours). The livers used in each trial were randomly assigned to the subjects; however, it was ensured that the human subjects would each palpate the same number of tumours as the robot.

During the trials, the task completion time and the palpation force as indicated by force/torque Sensor A were recorded. The location of the tumours found by the participants were marked using a plastic instrument marker and two marking pins, Figure 3.5 (a). The recorded task completion time did not include the time taken to place each marker.

To assess the success rate of the tumour localization method, after palpation, all livers were imaged using a fluoroscopic radiographic machine. Both the tumours and the plastic markers are clearly evident in these images, Figure 3.5 (b). As such, a true positive result is achieved when there is an evident intersection between the area of the tumour and the area of the plastic instrument marker in the radiographic image. It was decided that intersection rather than the entire encapsulation of the tumour with the instrument marker is sufficient to demonstrate proper localization. This mitigates any errors that may have been introduced during marker placement on the tissue. When a tumour was not correctly identified, a false negative result was recorded. A false positive result was recorded when a marker was noted in the radiograph image where there was no tumour present. A true negative test was recorded in cases in which the liver presented to the subject had no tumours and the subject correctly identified it as such.

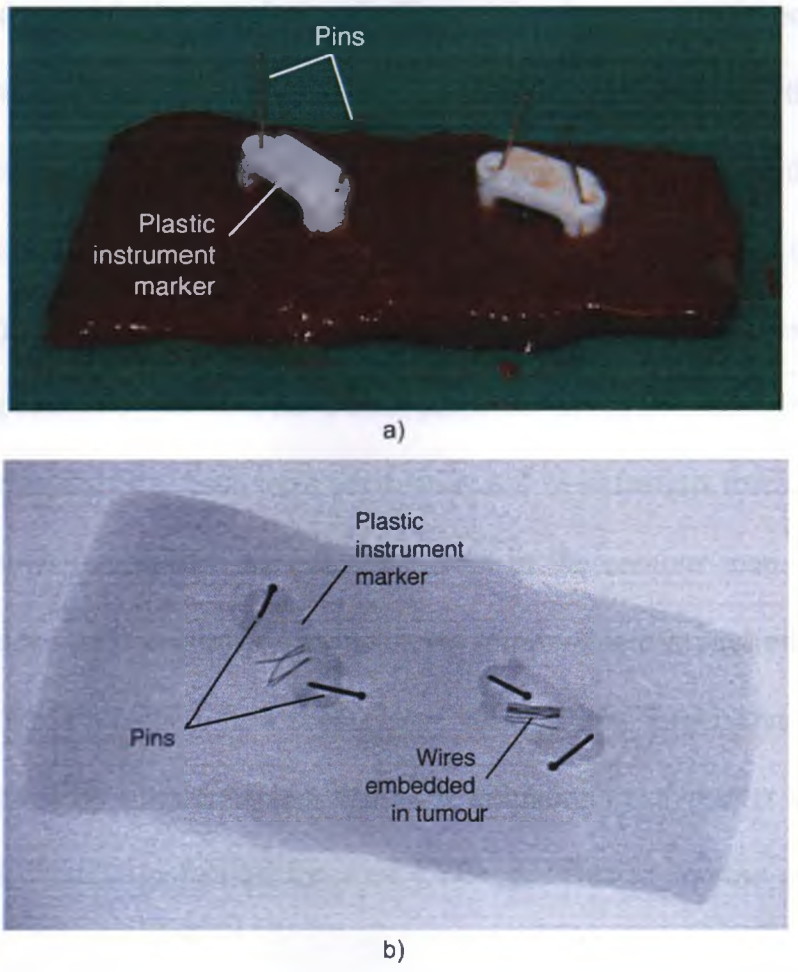


**Figure 3.5:** (a) Manually palpated tissue with each suspected tumour site marked by a plastic instrument marker held in place with two pins. (b) Radiograph of tissue, showing 10 mm tumours with embedded wire and plastic instrument markers.

### *3.3.4 Robotic Tests*

The user interface for the robotic setup allowed the user to input the direction of palpation and the number of points to palpate, while the robot autonomously palpated these points. Two different methods of robotic palpation were implemented: force control and position control.

In the force control setting, the robot approaches the tissue under force control (in the $z$ direction) until the wrist force sensor (Sensor B) registers a desired force. Once the desired force has been reached, the robot end-effector coordinates, corresponding to the tissue surface coordinates, are transmitted to the client. Instantaneously, the readings from the TSI are recorded to register the force profile of the contact made with the tissue. The robot is then commanded to move up ($z$ direction) and sideways ($x$ or $y$ direction) in 3 mm steps through position control to the next point. This process continues until all of the desired points specified by the user have been palpated. In order to choose the desired force of palpation, preliminary tests were done with a 2 N palpation force; these tests showed a poor success rate caused by image artifacts in the contour map. Subsequent tests using a 4 N palpation force showed a significant improvement in preliminary results with no noticeable tissue damage. In a preliminary study it was found that the average maximum force applied by surgeons when manually palpating *ex vivo* liver with 10 mm tumours was 4.4 N. Thus, a palpation force of 4 N was selected for the experimental evaluation.

In the position control setting, the user provides the same commands to the robot as is used in the force control setting. The difference between these settings lies in how deep the instrument palpates the tissue. The position of the end-effector is controlled in all Cartesian directions. The desired trajectory in the $z$ direction was generated such that the robot was commanded to make contact with the surface and move below the surface under position control. However, the readings from Sensor B were constantly polled to detect when contact was made with the tissue and to determine when the force of contact

reached the 4 N threshold. The robot would then move upwards and continue to the next point until the entire area defined by the user was palpated.

For all tests performed by the PA10-7C robot, the palpated livers were assessed using a custom-designed software program that records the position of the robot and the force exerted on the tissue by the robot. During post-processing of the experimental data, a 3D graphical representation of position ($x$ direction, $y$ direction) versus palpation force of the robot was generated. The palpation force consists of the data gathered from the tactile sensor during the trial. The topographical (2D) view of this graph serves to indicate the tumours located by the robot, presented as a colour map with red indicating the highest forces and blue indicating the lowest forces exerted on the TSI. The analysis and assessment of the 2D plot was performed by four human volunteers who were blinded to the number of tumours present and the control method used in each trial. The purpose of having four subjects perform the assessment was to provide an unbiased record of the location and number of tumours that were located by the robot in each of the methods. To ensure that no bias towards either robot method was possible, the images presented to the volunteers were randomized and the file names altered. A similar assessment of success rate was performed and compared to that of the human subject.

The Statistical Package for Social Sciences (SPSS, Chicago, IL) software, version 15.0 for Windows, was used for statistical analysis of the force and time measurements. A one-way analysis of variance (ANOVA) was performed to establish differences among the different methods. Due to the samples having unequal variances, the Dunnett test was then performed to determine significant differences between the individual groups.

Unpaired *t*-tests were used to determine differences between the large and the small tumours within each group.

## 3.4 Results

The experimental results from the force and position control methods were quite similar. The main difference was that the force control method showed marginally better performance for smaller tumours over the position control method. Therefore, only the detailed results from the force control method are shown. The results for position control are summarized in Tables 3.1 and 3.2 for comparison.

Sample graphs showing the pressure maps obtained when the robot palpated the tissue are presented in Figure 3.6. The results of the experimental evaluation are summarized in Tables 3.1 and 3.2. Table 3.1 shows the mean of the maximum force applied in the eighteen trials (nine trials with small tumours and nine with large tumours) with each of the methods, and the associated *p*-values. These results show that there is a significant difference in the forces applied by the human in comparison to the robotic methods, but that there is no significant difference between the forces applied within the robotic methods. It was also found that in the human trials, the application of forces greater than 6 N for extended periods of time caused visible damage to the tissue. An example of a tissue after human palpation, in which a maximum force of 10.6 N was applied, is shown in Figure 3.7. It should be noted that no studies have been found that provide a relationship between palpation forces and tissue damage. A study presented in [40] provides a good evaluation of tissue damage caused by gripping. However, the

pressures found to cause damage in their study (above 100 kPa) are much greater than the forces applied herein (a range of 6 to 11 N corresponds to 20–37 kPa), thus indicating that the methods do not provide an adequate basis for comparison.

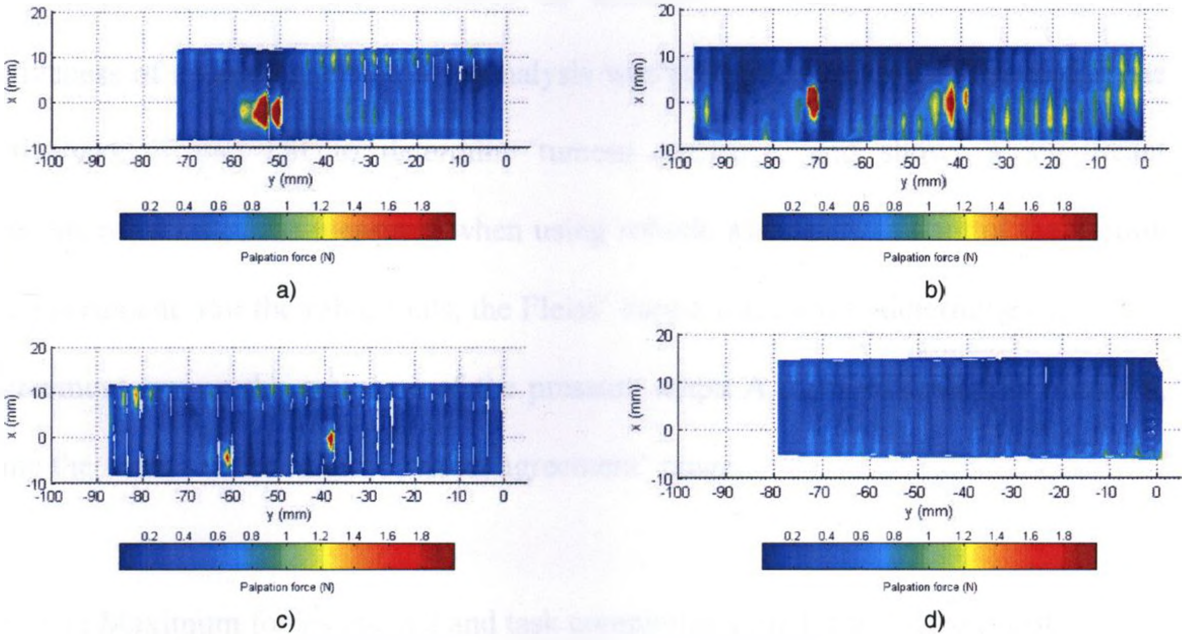


**Figure 3.6:** Sample pressure maps for the robot palpation experiments (a) one large tumour, (b) two large tumours, (c) two small tumours, and (d) no tumours.

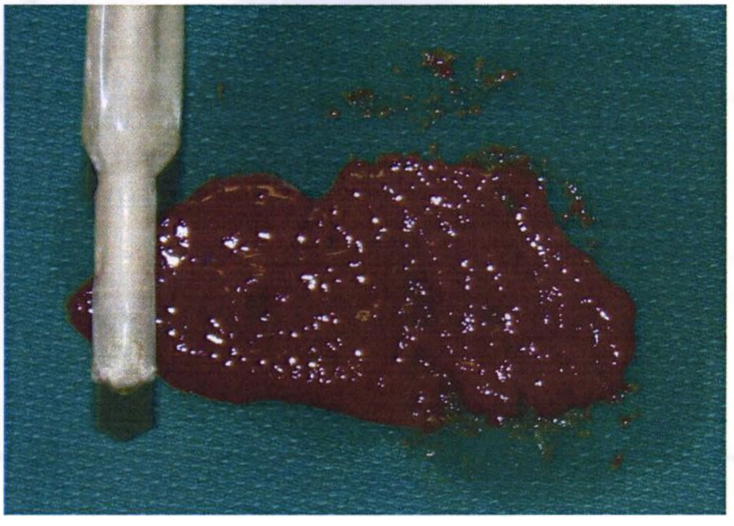

**Figure 3.7:** Damaged tissue due to excessive force applied during manual palpation.

Also shown in Table 3.1 is the average task completion time. The average times for the two robotic methods are significantly different; however, the task completion time for the human and robot trials cannot be compared directly. While the task completion time for the robot includes only the palpation time, the task completion time for the human also included the time it took to assess the information.

Table 3.2 shows the measures of accuracy typically used to assess the effectiveness of a diagnostic test. This analysis was performed as a way of assessing the effectiveness of the TSI to determine tumour presence, and shows a significant improvement in all of the measures when using robotic assistance to control the motion of the instrument. For the robot trials, the Fleiss' kappa was used to determine the degree of agreement among the assessors of the pressure maps. A score of 0.89 was obtained, placing the results in the 'almost perfect agreement' range.

**Table 3.1:** Maximum forces applied and task completion time for the various tests.

| | **Maximum Force (N)** | ***p*-values for Force** | **Avg. Time (s)** | ***p*-values for Time** |
|---|---|---|---|---|
| **A — Human** | | | | |
| Small Tumours | 8.14±2.9 | 0.970 small to large | 217.5±126.2 | 0.173 small |
| Large Tumours | 8.12±3.6 | <0.001 to B and C | 176.8±124.9 | to large |
| Average | 8.13±3.2 | | 197.2±126.4 | |
| **B — Robot Force Control** | | | | |
| Small Tumours | 4.96±0.1 | 0.180 small to | 129.8±25.0 | 0.078 small |
| Large Tumours | 5.38±0.9 | large | 156.0±33.2 | to large |
| Average | 5.17±0.63 | <0.001 to A, | 142.9±31.5 | <0.001 to C |
| | | 0.784 to C | | |
| **C — Robot Position Control** | | | | |
| Small Tumours | 5.10±1.3 | 0.537 small to | 96.2±16.7 | 0.224 small |
| Large Tumours | 5.38±0.3 | large | 105.0±12.3 | to large |
| Average | 5.24±0.9 | <0.001 to A, | 100.6±14.9 | <0.001 to B |
| | | 0.784 to B | | |

**Table 3.2:** Accuracy measures of the tactile sensing instrument as a diagnostic instrument, with and without robotic assistance.

| Trial | Accuracy | Sensitivity | Specificity | Positive Predictive Value | Negative Predictive Value |
|---|---|---|---|---|---|
| **Human** | | | | | |
| Small Tumours | 49% | 67% | 22% | 57% | 29% |
| Large Tumours | 69% | 94% | 30% | 68% | 78% |
| Average | 59% | 81% | 26% | 63% | 46% |
| **Robot Force Control** | | | | | |
| Small Tumours | 87% | 92% | 75% | 89% | 80% |
| Large Tumours | 98% | 97% | 100% | 100% | 92% |
| Average | 92% | 94% | 86% | 94% | 86% |
| **Robot Position Control** | | | | | |
| Small Tumours | 83% | 78% | 100% | 100% | 60% |
| Large Tumours | 96% | 94% | 100% | 100% | 86% |
| Average | 90% | 86% | 100% | 100% | 71% |

## 3.5 Discussion

The results of this study show that using a tactile sensing MIS instrument under robotic control reduces the maximum force applied to the tissue by more than 35% (from 8.13 N to 5.24 N) compared to manual manipulation of the same instrument. Furthermore, detection accuracy is increased by more than 50% (from 59% to at least 90% depending on the robot control method used for palpation).

The primary difference between robot and human tissue palpation is that the robot can apply a consistent amount of force at each step and can move systematically over the entire surface of the tissue, thereby producing a complete, contiguous map of the entire surface. This is equivalent to having one tactile pad that covers the entire specimen and applying an ideal force to the entire surface of the tissue (similar to the tactile sensors that have been developed for breast tumour detection). When a human palpates tissue, he or

she does not know how much force is being applied compared to how much force was applied on another area of the tissue. Therefore, a particular feature might be highlighted only because a higher palpation force is being applied in that area (or the contact angle between the instrument and the tissue becomes more oblique), or a tumour might not be detected only because a lower palpation force is being applied in that area. Although only the subjects with surgical experience have a basis for knowing how much pressure could cause damage, both surgeons and non-surgeons caused very similar tissue damage. It was found that if the subjects observed an increase in pressure on the visual display, the tendency was to focus on that area, applying increased forces to see if the feature observed was in fact a tumour. This led to the significant increase in the applied forces and in the task completion times. This highlights the advantage of using a robot, since humans require a great deal of experience to ensure that excessive force is not being applied to the tissue. Even with experience, subjects cannot always control the amount of force being applied. The advantage of using a robot is that it can restrict the applied force to lie within safe limits.

As mentioned earlier, in order to meet the requirements of MIS, it was necessary to reduce the palpation area to 1 cm in width. In most cases, this area is not enough to fully capture an existing tumour. It is then necessary to compare adjacent pressure maps to identify if a tumour is present. When building a piecewise map, the benefit of applying a consistent palpation force is significant, allowing the narrow instrument to approximate the performance of larger devices designed for non-MIS applications.

When comparing the force and position control robot palpation methods, there is no clear method that performed better than the other. Both methods applied the same

amount of force, while position control reduced task completion time by about 40%. However, force control provides better accuracy and sensitivity measures, which are the most significant indicators that a greater proportion of tumours have been correctly identified.

Preliminary tests performed with the robotic setup showed that the best palpation method was to start at one end of the tissue and move in 3 mm steps towards the other side of the tissue, taking measurements from a single pass over each area that may contain a tumour. Due to the way the data was plotted, if multiple directions of palpation were performed and there was significant overlap between the areas palpated, the visualization software was less capable of detecting the presence of tumours. A force of 4 N was found to be the ideal force required to obtain consistent results when trying to locate 5 mm and 10 mm tumours; however, it should be noted that for different types of tissue and different tumour sizes, the optimal palpation force would be different.

As expected, all the methods performed better when detecting 10 mm tumours than when detecting 5 mm tumours. It should be noted that, the 'large' tumours used in this study are not clinically large. In fact, most diagnostic tests are not capable of detecting tumours that are smaller than 10 mm [41], [42]. The smaller 5 mm tumours were included in this study to properly assess the improvement of one method over another under a worst case scenario.

The measures of accuracy, sensitivity, specificity, and negative and positive predictive values are those commonly used to quantify the effectiveness of diagnostic tests. These measures are based on the number of patients that are successfully or not successfully identified as having or not having the disease in question. In this study, the

calculation of these measures was modified to include the number of tumours present, so that if a specimen contained two tumours, and only one was correctly identified, the measures of accuracy and sensitivity will reflect this outcome. Also, if a specimen contained only one tumour and an additional one was incorrectly found, the measure of specificity was also penalized.

It was determined that the most intuitive way of presenting the information obtained during the robotic experiments to identify tumour location was to plot the data on a 2D map representing the surface (superior view) of the liver, with the information from the tactile sensor overlaid directly on this map. This was accomplished by post-processing the data and assessing the resulting graphs. However, in a clinical setting, it would be ideal if this map were generated in real-time, so that if desired, the surgeon can repeatedly palpate an area of interest with a different force, a different step size, or using a different control method.

An instrument of this type would be especially beneficial for lung tumour resection in which tissue shift is significantly greater due to lung collapse, and where the effectiveness of laparoscopic ultrasound is compromised by air within the lung, making it very difficult to locate tumours that are less than 10 mm in diameter.

It should be noted that the presented system is not at a stage in which it can be used in a clinical setting. First of all, the robotic system used is an industrial robot that is not safe to operate in close proximity to humans. Furthermore, the motion of the instrument is not designed to mimic the remote center of motion required for MIS, where the instrument is inserted through a trocar in order to enter the patient's body. In order to properly palpate tissue through a trocar, the sensing instrument must be designed to have

a flexible or articulating head to ensure that the sensing pad can be placed parallel to the tissue and obtain a proper pressure distribution on the sensor itself. Once the sensing pad can be properly oriented, it would be straightforward to adapt the TSI to currently available surgical robotic systems.

## 3.6 Conclusions

The results of this study show that robotic assistance realizes a relative 55% decrease in the maximum forces applied on tissue, a relative 50% decrease in task completion time and a relative 40% increase in tumour detection accuracy. The use of robotic assistance for tactile sensing during minimally invasive surgery is not only feasible, but results in reduced tissue trauma and increased tumour detection compared to the manual manipulation of a tactile sensing instrument.

## References

[1] American Cancer Society. (2007). *Cancer Facts and Figures 2007*, no. 500807, Atlanta, GA: American Cancer Society Inc. [Online]. Available: www.cancer.org.

[2] American Cancer Society. (2007). *Global Cancer Facts and Figures 2007*, no. 861807, Atlanta, GA: American Cancer Society Inc. [Online]. Available: www.cancer.org.

[3] J. Dargahi, "An integrated force-position tactile sensor for improving diagnostic and therapeutic endoscopic surgery," *Biomed. Mater. Eng.*, vol. 14, (2), pp. 151–166, 2004.

[4] M. V. Ottermo, M. Øvstedal, T. Langø, Ø. Stavdahl, Y. Yavuz, T. A. Johansen, and R. Mårvik, "The role of tactile feedback in laparoscopic surgery," *Surg. Laparosc. Endosc. Percutan. Technol.*, vol. 16, (6), pp. 390–400, 2006.

[5] A. Bicchi, G. Canepa, D. De Rossi, P. Iacconi, and E. Scillingo, "A sensor-based minimally invasive surgery tool for detecting tissue elastic properties," in *Proc. IEEE Int. Conf. Robot. Autom. (ICRA)*, vol. 1, Minneapolis, Minnesotta, 1996, pp. 884–888.

[6] F. Van Meer, D. Esteve, A. Giraud, and A. M. Gué, "Si-micromachined 2D force sensor for a laparoscopic instrument," in *Int. Conf. Comput. Assist. Radiol. Surg. (CARS)*, International Congress Series, vol. 1268, Chicago, Illinois, 2004, p. 1334.

[7] G. Tholey, A. Pillarisetti, W. Green, and J. P. Desai, "Design, development, and testing of an automated laparoscopic grasper with 3-D force measurement capability," in *Int. Conf. Noise Vib. Eng. (ISMA)*, Leuven, Belgium, 2004, pp. 38–48.

[8] H. Singh, R. Sedaghati, and J. Dargahi, "Experimental and finite element analysis of an endoscopic tooth-like tactile sensor," *Sens.*, vol. 1, pp. 259–264, 2003.

[9] J. Rosen and B. Hannaford, "Markov modeling of minimally invasive surgery based on tool/tissue interaction and force/torque signatures for evaluating surgical skills," *IEEE Trans. Biomed. Eng.*, vol. 48, (5), pp. 579–591, 2001.

[10] S. Shimachi, Y. Fujiwara, and Y. Hakozaki, "New sensing method of force acting on instrument for laparoscopic robot surgery," in *Int. Conf. Comput. Assist. Radiol. Surg. (CARS)*, International Congress Series, vol. 1268, Chicago, Illinois, 2004, pp. 775–780.

[11] P. Dubois, "In vivo measurement of surgical gestures," *IEEE Trans. Biomed. Eng.*, vol. 49, (1), pp. 49–54, 2002.

[12] P.J. Berkelman, L. L. Whitcomb, R. H. Taylor, and P. Jensen, "A miniature microsurgical instrument tip force sensor for enhanced force feedback during robot-assisted manipulation," *IEEE Trans. Robot. Autom.*, vol. 19, (5), pp. 917–922, 2003.

[13] J. Dargahi, S. Payandeh, and M. Parameswaran, "A micromachined piezoelectric teeth-like laparoscopic tactile sensor: theory, fabrication and experiments," in *Proc. IEEE Int. Conf. Robot. Autom. (ICRA)*, Detroit, Michigan, 1999, pp. 299–304.

[14] K. Takashima, K. Yoshinaka, T. Okazaki, and K. Ikeuchi, "An endoscopic tactile sensor for low invasive surgery," *Sens. Actuators, A: Phys.*, vol. 119, pp.372–383, 2005.

[15] S. Schostek, C. H. Ho, D. Kalanovic, and M. O. Schurr, "Artificial tactile sensing in minimally invasive surgery—a new technical approach," *Minim. Invasive Ther. Allied Technol.*, vol. 15, (5), pp.296–304, 2006.

[16] P. Wellman and R. D. Howe, "Modeling probe and tissue interaction for tumor feature extraction," presented at the *ASME Summer Bioeng. Conf.*, Sun River, Oregon, 1997.

[17] P.S. Wellman and R. D. Howe, "Extracting features from tactile maps," in *Proc. 2nd Int. Conf. Med. Imag. Comput. and Comput.-Assist. Interv.*, Cambridge, UK, 1999, pp. 1133–1142.

[18] R. A. Beasley and R. D. Howe, "Tactile tracking of arteries in robotic surgery," in *Proc. IEEE Int. Conf. Robot. Autom. (ICRA)*, vol. 4, Washington, DC, 2002, pp. 3801–3806.

[19] A. P. Miller, W. J. Peine, J. S. Son, and Z. T. Hammoud, "Tactile imaging system for localizing lung nodules during video assisted thoracoscopic surgery," in *Proc. IEEE Int. Conf. Robot. Autom. (ICRA),* Rome, Italy, 2007, pp. 2996–3001.

[20] M. E. H. Eltaib and J. R. Hewit, "Tactile sensing technology for minimal access surgery—a review," *Mechatron.*, vol. 13, pp. 1163–1177, 2003.

[21] B. Hannaford, J. Trujillo, M. Sinanan, M. Moreyra, J. Rosen, J. Brown, R. Leuschke, and M. MacFarlane, "Computerized endoscopic surgical grasper," in *Proc. Med. Meets Virtual Real.*, San Diego, California, 1998, pp. 111–117.

[22] J. Rosen and B. Hannaford, "Force controlled and teleoperated endoscopic grasper for minimally invasive surgery – experimental performance evaluation," *IEEE Trans. Biomed. Eng.*, vol. 46, (10), pp. 1212–1221, 1999.

[23] M. Tavakoli, R. V. Patel, and M. Moallem, "Haptic interaction in robot-assisted endoscopic surgery: a sensorized end-effector," *Int. J. Med. Robot. Comput. Assist. Surg.*, vol. 1, (2), pp. 53–63, 2005.

[24] M. Tavakoli, A. Aziminejad, R. V. Patel, and M. Mollaem, "Multi-sensory force/deformation cues for stiffness characterization in soft-tissue palpation," in *Proc. IEEE Int. Conf. Eng. Med. Biol. Soc.*, New York City, New York, 2006, pp. 847–840.

[25] M. Tavakoli, A. Aziminejad, R. V. Patel, and M. Moallem, "Tool/tissue interaction feedback modalities in robot-assisted lump localization," in *Proc. IEEE Int. Conf. Eng. Med. Biol. Soc.*, New York City, New York, 2006, pp. 3854–3857.

[26] G. Tholey, J. P. Desai, and A. E. Castellanos, "Force feedback plays a significant role in minimally invasive surgery: results and analysis," *Ann. Surg.*, vol. 241, (1), pp. 102–109, 2005.

[27] P. Dario and M. Bergamasco, "An advanced robot system for automated diagnostic tasks through palpation," *IEEE Trans. Biomed. Eng.*, vol. 35, (2), pp. 118–126, 1988.

[28] R. L. Feller, C. K. L. Lau, C. R. Wagner, D. P. Perrin, and R. D. Howe, "The effect of force feedback on remote palpation," in *Proc. IEEE Int. Conf. Robot. Autom. (ICRA)*, New Orleans, Los Angeles, 2004, pp. 782–788.

[29] G. L. McCreery, A. L. Trejos, M. D. Naish, R. V. Patel, and R. A. Malthaner, "Feasibility of locating tumors in lung via kinesthetic feedback," *Int. J. Med. Robot. Comput. Assist. Surg.*, published online, DOI: 10.1002/rcs.169, 2008.

[30] R. S. Fearing, "Tactile sensing mechanisms," *Int. J. Robot. Res.*, vol. 9, (3), pp. 3–23, 1990.

[31] R. D. Howe, W. J. Peine, D. A Kontarinis, and J. S. Son, "Remote palpation technology," *Eng. Med. Biol. Mag.*, vol. 14, (3), pp. 318–323, 1995.

[32] W. J. Peine, J. S. Son, and R. D. Howe, "A palpation system for artery localization in laparoscopic surgery," in *Proc. 1st Int. Symp. Med. Robot. Comput. Assist. Surg.*, Pittsburgh, Pennsylvania, 1994, pp. 22–24.

[33] M. T. Perri, D. A. Bottoni, A. L. Trejos, G. L. McCreery, M. D. Naish, R. V. Patel, and R. A. Malthaner, "A new tactile imaging device to aid with localizing lung tumours during thoracoscopic surgery," *Int. J. Comput. Assist. Radiol. Surg. (Int. J. CARS)*, vol. 3, suppl. 1, pp. S257–S258, 2008.

[34] A. L. Trejos, J. Jayender, M. T. Perri, M. D. Naish, R. V. Patel, and R. A. Malthaner, "Experimental evaluation of robot-assisted tactile sensing for minimally invasive surgery," in *Proc. 2nd IEEE RAS/EMBS Int. Conf. Biomed. Robot. Biomechatron. (BioRob),* pp.971–976, 2008.

[35] J. Jayender, "Haptics enabled robot-assisted active catheter insertion," Ph.D. dissertation, Dept. Electrical and Computer Engineering, University of Western Ontario, London, Ontario, Canada, 2007.

[36] R. V. Patel, H. A. Talebi, J. Jayender, and F. Shadpey, "A robust position and force control strategy for 7-DOF redundant manipulators," *IEEE/ASME Trans. Mechatron.*, accepted for publication, 2009.

[37] H. Seraji, M. K. Long, and T. S. Lee, "Motion control of 7-DOF arms: the configuration control approach," *IEEE Trans. Robot. Autom.*, vol. 9, (2), pp. 125–139, 1993.

[38] R. V. Patel and F. Shadpey, "Control of redundant robot manipulators: theory and experiments," *Lecture Notes in Control and Information Sciences*, vol. 315, Springer-Verlag, Heidelberg, Germany, 2005.

[39] M. Davidson, "The interpretation of diagnostic tests: a primer for physiotherapists," *Aust. J. Physiother.*, vol. 48, pp. 227–232, 2002.

[40] S. De, J. Rosen, A. Dagan, P. Swanson, M. Sinanan, and B. Hannaford, "Assessment of tissue damage due to mechanical stress," *Int. J. Robot. Res.*, vol. 26, (11–12), pp. 1159–1171, 2007.

[41] P. Singh, R. A. Erickson, P. Mukhopadhyay, S. Gopal, A. Kiss, A. Khan, and T. Ulf Westblom, "EUS for detection of the hepatocellular carcinoma: results of a prospective study," *Gastrointest. Endo.*, vol. 66, (2), pp. 265–273, 2007.

[42] J. K. LeBlanc, J. DeWitt, and S. Sherman, "Endoscopic ultrasound: how does it aid the surgeon?," *Adv. Surg.*, vol. 41, pp. 17–50, 2007.

# Chapter 4

# Visual Force Feedback Improves the Performance of a Tactile Sensing System during Minimally Invasive Tumour Localization[1]

## 4.1 Introduction

In North America, cancer continues to be the second most common cause of death, preceded only by heart disease [1]. Treatment options for most cancers include chemotherapy, radiation therapy, and surgery [2]. For localized cancers, surgical tissue resection is the treatment of choice. Traditionally, tumour resection is performed through a large incision that permits the localization of tumours by direct manual palpation of the target tissue. The practice of tumour localization via direct finger palpation depends on differential tissue stiffness between the tumour and the surrounding healthy tissue [3]. Although open surgical procedures continue to be performed, minimally invasive surgical

[1] A version of this chapter has been submitted for publication to IEEE Transactions in Biomedical Engineering with an author list: MT Perri, AL Trejos, MD Naish, RV Patel, and RA Malthaner

techniques are becoming more common. Minimally invasive surgery (MIS) provides many benefits over traditional open surgery, including reduction of post-operative pain and a more rapid recovery for the patient due to smaller incisions [4]. For the surgeon, however, the fact that internal tissues are no longer accessible for manual palpation presents a major challenge.

In view of this limitation, research dedicated to the development of alternative methods for locating tumours intra-operatively has become increasingly active. One such method is the transfer of haptic cues from the contacting tissue surface to the surgeon. Haptic cues can be considered in two distinct modes [5]: kinaesthetic and tactile. Both modes of haptic feedback have been the focus of active research since, in MIS, the reduction of both tactile and kinaesthetic feedback from the tissue surface can be regarded as a safety concern. If the degradation of tactile information prevents a cancerous nodule, identified through pre-operative imaging, from being located during the MIS procedure, this would, on occasion, necessitate the abandonment of the MIS approach and a conversion to an open procedure so that tumour localization can be performed manually [6]. In cases where kinaesthetic feedback is limited or absent while palpating during surgery, complications such as the accidental puncturing of vessels or severe bulk tissue damage when palpating organs are probable, leading to difficulties that could be avoided with the availability of haptic feedback [7]. As a solution to the problems caused by a lack of haptic feedback, specialized surgical instruments and accessories are being developed. Most of these instruments are hand-held devices that convey either one or both modes of haptic feedback from the instrument tip to the surgeon's hand. A review of these instruments is presented below.

### *4.1.1 Prior Art*

Piezoelectric and piezoresistive sensor technologies have been incorporated into a variety of devices for tumour localization in organs. Hemsel *et al.* [8] have proposed a device consisting of an ultrasound scaler with a modified contact ball to increase contact surface area and a piezoelectric sensor used as a sensing element which initiates resonant vibration. This technology evaluates the frequency shift and amplitude variation of harmonics output from the sensor to determine the difference between healthy tissue and hard occlusions in gelatine models. The instrument was intended for the purpose of brain tumour resection and did not meet MIS design constraints. Kattavenos *et al.* [9] proposed an instrument prototype using piezoresistive materials on forceps designed for use in MIS. The focus of the research was on the laparoscopic examination of the bowel for tumours, and the current prototype consisted of an 8 × 8 array of resistors (25 mm × 25 mm) that resulted in dimensions slightly too large to be used in traditional MIS. Similarly, Murayama *et al.* [10] proposed a design for a 64-element tactile sensor array using a piezoelectric transducer (PZT) for performing mammograms and locating breast tumours externally. The contact impedance of the sensor was measured using an ultrasonic resonator and phase-shift method.

Devices using capacitance-based technology include a modified conventional laparoscopic grasper, developed by Ottermo *et al.* [11], [12]. A prototype of this instrument, containing a capacitive array sensor with 60 elements, was used in a set of experiments that aimed to determine the hardness and size of rubber balls in water-filled porcine intestine. Miller *et al.* [6] designed a similar technology for the purpose of

locating pulmonary tumours. Their device used a capacitive array sensor designed for video-assisted thoracoscopic surgery (VATS) and was tested on *ex vivo* porcine lungs. The system outputted streaming video images overlaid with colour-contour maps representing the pressure distribution as assessed by the device. The lack of haptic feedback and the method of manually articulating the probe's end-effector were reported in the study to be problematic.

Some researchers have focused on using optical fibre and polymer-based sensor technologies to determine the mechanical properties of, and differences between, soft healthy tissue and diseased tissue. For example, Liu *et al.* [13], [14] designed a force-sensitive wheeled probe, based on optical fiber sensor technology, to generate a 'mechanical image,' defined as the stiffness distribution of tissue represented by a colour-contour image, when the device is rolled across the surface of a solid organ. The force detected by the sensor was used to create the mechanical image and did not provide direct kinaesthetic feedback to the user. Research from Bonomo *et al.* [15] and Dargahi *et al.* [16] were focused on polymer-based sensor technology and were applied to different target organs. A device that used ionic polymer metal composite (IPMC) strips to orient the receiving sensor in a cantilever configuration was presented in [15]. Their goal was to determine the mechanical properties of soft tissue to assist a user during an open brain tumour resection procedure. Research in [16] used a sensor composed of polyvinylidene fluoride (PVDF) to determine and record mechanical properties during a mammogram for a new non-invasive method of localizing tumours in breast tissue.

Other research has focused on using pulsated air jets as a means to locate tumours in an internal organ. Kaneko *et al.* [17] developed a prototype, denoted as the Active

Strobe Imager (ASI), as a non-contact active sensing system composed of a nozzle to supply pulsated air jets to an internal organ, a strobe system for visualizing the dynamic behavior of the tissue, and a camera for capturing strobe images. The prototype was designed for use in VATS, and was tested on *ex vivo* human lungs. The purpose of the device was to visually represent the dynamic behavior of internal organs; however, it does not provide kinaesthetic feedback to the user.

### *4.1.2 Progress to Date*

Results by McCreery *et al.* [18] informed the design of a device that incorporated a capacitive-based pressure sensor, the TactArray sensor, which interfaces with visualization software. The combination of the TSI and the visualization interface is referred to as the Tactile Sensing System (TSS). Further information on this system can be found in [19], [20] and Section 1.5.

The results of preliminary testing on *ex vivo* porcine lung, as detailed in Chapter 2, indicated that the TSS significantly improves the efficiency and accuracy of locating tumours compared to using an endoscopic grasper, which is used as an MIS tumour localization device in standard practice [21]. Further experiments were performed using the TSS that assessed the feasibility of manoeuvring the TSI through robotics-assisted control. As detailed in Chapter 3 and in [20], the study demonstrated that TSS performance is highly dependent on the amount of force that is being applied by the user and that the ability to palpate with a consistent amount of force leads to superior results. Thus, to maximize performance, a handheld TSS must provide information about the

applied force to the user. One approach to providing this information is to calibrate the TactArray sensor at the end of the TSI such that bulk force data can be computed.

### *4.1.3 Purpose*

The purpose of the work presented herein was to determine if TSS performance can be improved by providing a visual display of force information to the user when determining the location of phantom tumours in *ex vivo* bovine liver in an MIS environment. This was achieved by comparing the relative performance of the TSS with and without force display. The hypothesis was that the implementation of visual force feedback in the TSS would greatly facilitate the palpation process for the surgeon.

## 4.2 Calibration

The sensor incorporated into the TSI responds to changes in the relative pressure applied to each sensing element. While this works well for assessing differences in the mechanical stiffness of materials that come into contact with the sensor, it cannot be used to measure the amount of applied force. To address this limitation, the sensor was calibrated to generate a mapping between known forces and the 12-bit binary output from each sensing element. The TSI calibration procedure and validation are described below.

### *4.2.1 Calibration Procedure*

A custom-built platform was constructed and used to ensure that the TSI remained immobile during the calibration procedure. The TSI was fastened to the platform in two places: the handle, and the neck of the shaft just below the TactArray sensor. A Parker Daedal XYZ linear stage was placed adjacent to the TSI platform in such a manner that the stage could access the TSI TactArray sensor. The mounting side of an ATI 6-degree of freedom (6-DOF) Nano 43 force/torque sensor (Sensor A) was attached to a metal bracket held by the linear stage. The tool side of Sensor A was fastened to a customized end-effector, which consisted of a solid cone with a square tip. The dimensions of the cone tip were 2 mm by 2 mm; the same dimensions of one sensor element of the tactile sensor array. The setup for this procedure is shown in Figure 4.1.

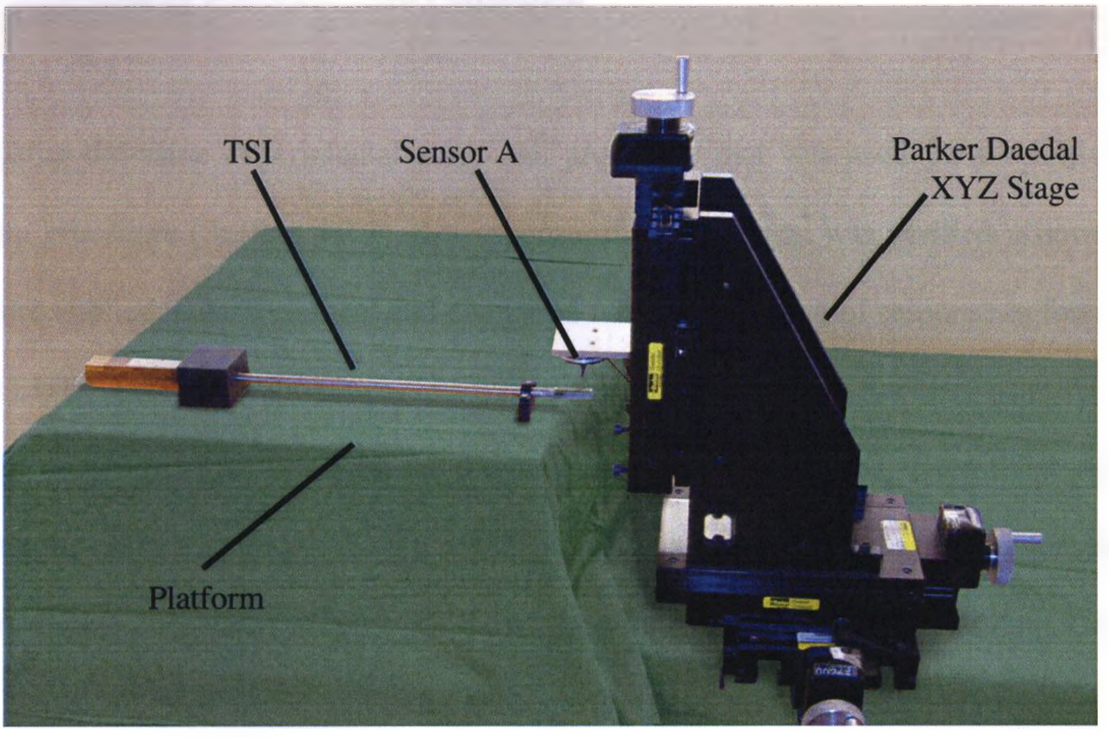


**Figure 4.1:** Experimental setup for calibration of sensing elements.

For each sensor element, the stage containing the customized end-effector was adjusted to administer a uniform force to one sensor element for three seconds. During this time the experimental data, consisting of the force from Sensor A in Newtons and the 12-bit binary output obtained from the TactArray sensor element, was recorded at a rate of 50 Hz. After three seconds of data was recorded, the applied force was incremented by 0.1 N and the process was repeated. The force applied to each sensor element began at 0 N and was linearly incremented until the output of the element saturated. This process was performed on all 60 elements. The experimental data collected was then converted into a look-up table (LUT) for the applied forces on individual elements, with the rows representing the binary output value from the TactArray sensor, and the columns representing the sensor elements 0 to 59 inclusive. The force values recorded in the LUT were then verified by two procedures as presented below.

### *4.2.2 Verification of Element-Based Calibration*

Using the same experimental setup and procedure that was used for the initial calibration procedure (Section 4.2.1), the response of each element was verified. Known forces were applied to each element and compared with the mapping of response to force from the LUT. Three calibration measures were considered:

1) *Accuracy*: The accuracy of the measurement system was determined by comparing the calibrated output from the TSI in Newtons (measured value) to the forces of Sensor A (reference value). Figure 4.2 shows the percent accuracy of each element. On average, the accuracy of an element in the sensor array was 89.4%.

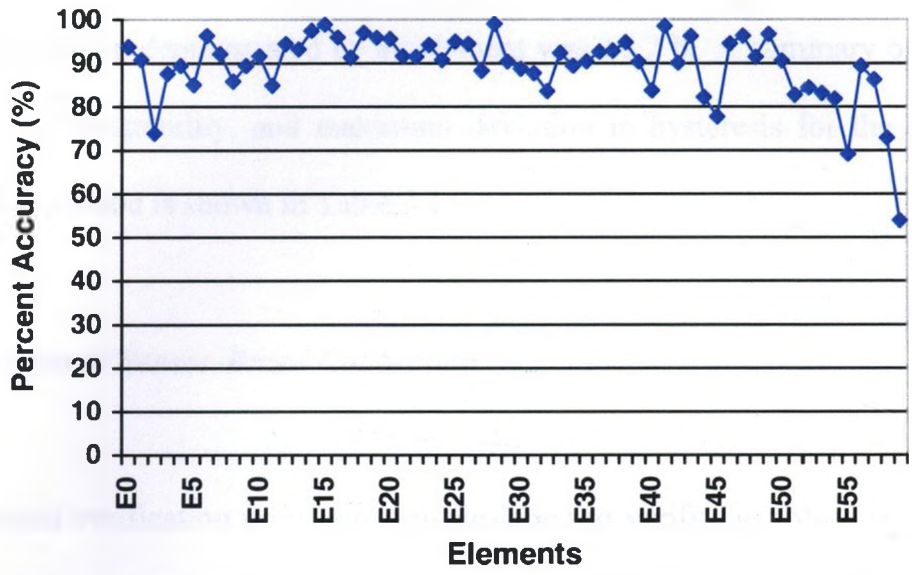


**Figure 4.2:** Graph of percent calibration accuracy of all 60 sensor elements of the TactArray sensor.

2) *Repeatability*: Repeatability was determined by recording data values for each element multiple times while under load with a specific mass. This was accomplished by five repeatable trials performed on a single element for a specified force. Sixteen of the sixty possible sensor elements were randomly selected to assess repeatability. For each selected element, a random force value was chosen within the range of 0.1 N to 3.0 N inclusive. The overall mean percent repeatability of all selected elements was 94.9%.

3) *Hysteresis*: Hysteresis analysis was performed on ten of the sixty possible sensor elements, which were chosen using a block randomization process. For half of the selected elements, hysteresis was assessed starting with no force on the element. The force was then increased until the output of the element saturated, followed by a linear decrease in the force until no force was applied to the sensor. For the other half of the selected elements, an opposite procedure was followed. Data were recorded starting at the

saturation force. The level of hysteresis varied between each element, with some elements showing no signs of hysteresis in their performance. In the worst case scenario, the maximum deviation demonstrated by an element was ±0.2 N. A summary of percent accuracy, percent repeatability, and maximum deviation in hysteresis for the element-based calibration method is shown in Table 4.1.

### *4.2.3 Verification of Sensor-Based Calibration*

The second verification procedure was designed to verify the values recorded in the LUT through the operation of the sensor as a whole. This procedure verified the force output of the TactArray pressure sensor, using the LUT, to that of an ATI 6-DOF Gamma force/torque sensor (Sensor B). The experimental setup is shown in Figure 4.3. The mounting side of Sensor B was fastened to a customized plexiglass ramp, and the tool side of Sensor B was fastened to a tray for holding material samples. This unit, consisting of the ramp and Sensor B, was then placed in an MIS training box. The front of the training box provided an insertion point that enforced a remote centre of motion for the TSI.

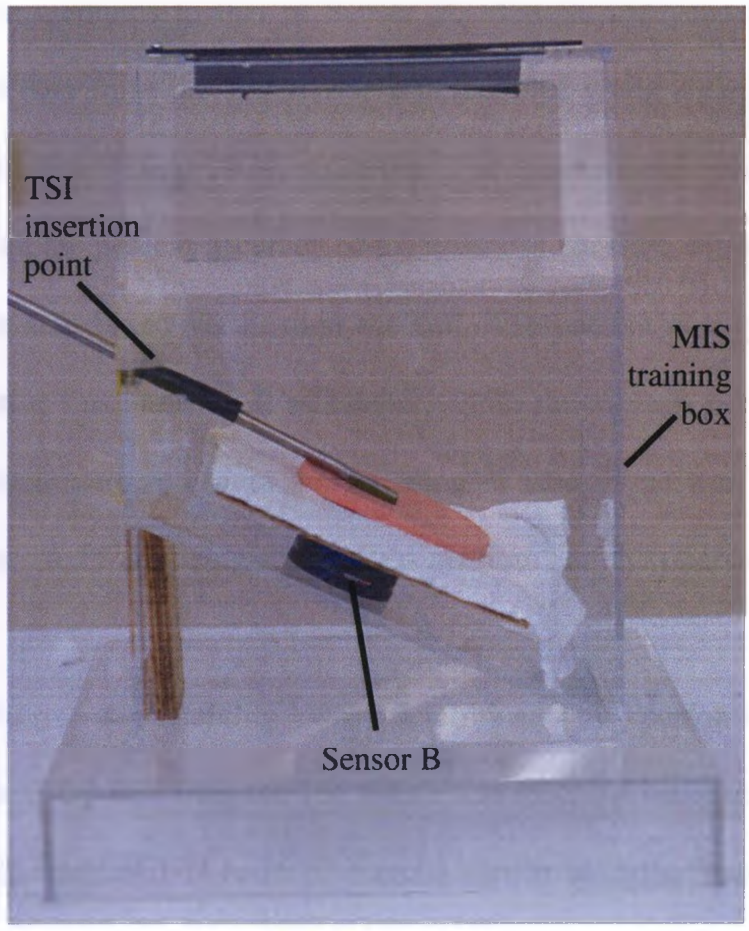


**Figure 4.3:** Experimental setup for validation of sensor calibration. Photo credit: Meg Woodhouse.

The sensor calibration was verified using three mediums as the contact surface: plexiglass, artificial tissue (uterine wall sample from The Chamberlain Group, Great Barrington, MA), and *ex vivo* bovine liver. All contact surfaces were approximately 10 mm in thickness. These mediums were sequentially placed in the training box where the TSI could access them from a single port in the front of the training box. Twenty trials were performed with each medium. The experimental data was recorded at a rate of 50 Hz for three seconds and included the force in Newtons from Sensor B and the TSI calibrated force output in Newtons.

1) *Accuracy*: Accuracy was assessed by comparing the output of the entire sensor on the three different mediums to that of Sensor B. Multiple independent trials were performed where the data from the TSI sensor was recorded while under load with an incremental force between 0 N to 10 N, inclusive. The experimental results, shown in Table 4.1, indicate that the percent accuracy of the sensor is considerably lower than the one found in the element-based verification method. The percent accuracy generated from the artificial tissue medium is still satisfactory, with the average percent accuracy being 83%. The average percent accuracy with using *ex vivo* tissue was 71%, and the percent accuracy generated from using a plexiglass medium had the poorest results, with an average of 57%.

2) *Repeatability*: Repeatability was determined by performing multiple independent trials where the data from the TSI sensor was recorded while under load with a specific force in the range of 1 N to 10 N. Results similar to those for accuracy were observed for percent repeatability. The average percent repeatability observed for plexiglass, artificial tissue, and *ex vivo* tissue were 69%, 85%, and 77%, respectively. Again, the artificial tissue medium showed the best results.

3) *Hysteresis*: Hysteresis analysis was performed by monitoring the output from the TSI sensor beginning with no force on the sensor, then increasing the force until the output of Sensor B reached approximately 11 N, and finally decreasing the force linearly until no force was applied to the sensor. Hysteresis analysis was performed using all three mediums as contact surfaces. Figure 4.4 shows a hysteresis graph when the contact medium was *ex vivo* bovine liver, the tissue medium of greatest interest. A summary of

percent accuracy, percent repeatability, and maximum deviation in hysteresis is shown in Table 4.1.

**Table 4.1:** Percent accuracy, percent repeatability, and maximum deviation in hysteresis.

| | **Percent Accuracy** | **Percent Repeatability** | **Maximum Deviation in Hysteresis Analysis** |
|---|---|---|---|
| **Element-based Calibration (Section 4.2.2)** | 89.4% | 94.9% | ±0.2 N |
| **Sensor-based Calibration (Section 4.2.3)** | | | |
| ***Plexiglass*** | 57.0% | 69.3% | ±0.95 N |
| ***Artificial tissue*** | 82.7% | 84.5% | ±0.12 N |
| ***Ex vivo liver*** | 70.8% | 76.5% | ±0.30 N |

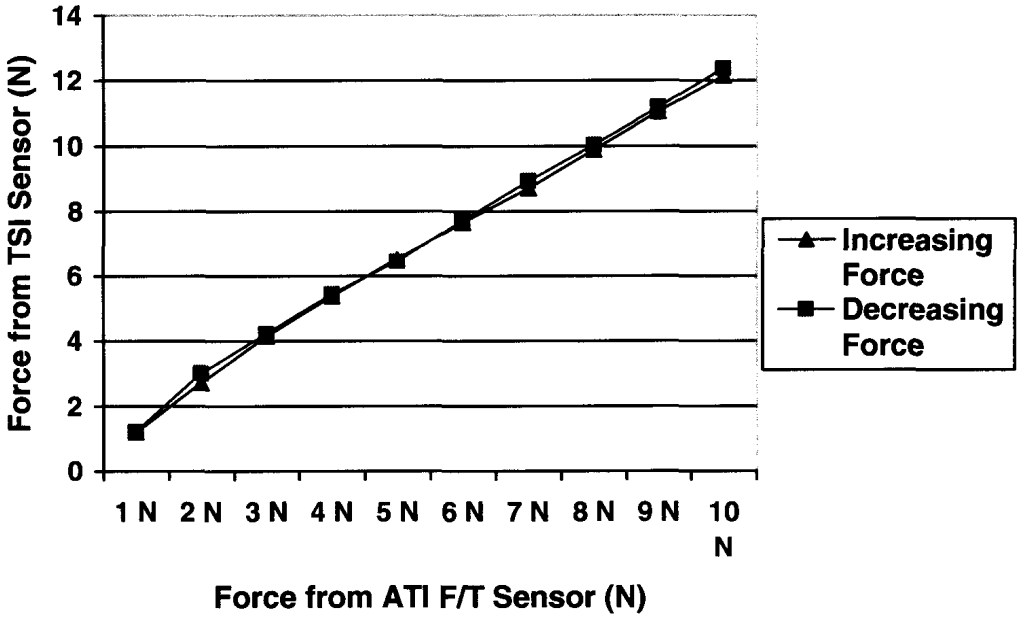


**Figure 4.4:** Observed hysteresis for *ex vivo* (bovine liver) tissue, averaged over 20 trials.

## 4.3 The Implementation of Visual Force Feedback into the TSS

The integration of a visual force display into the TSS visualization interface was motivated by preliminary experiments detailed in Chapter 3 and [20], which compared robotics-assisted palpation methods and manual palpation methods using the TSI. It was noted in the study that a force of 4 N was found to be the ideal force required to obtain consistent results when attempting to locate clinically small (5–10 mm diameter) tumours, and that applied forces greater than 6 N inflicted visible bulk damage to the tissue. At the conclusion of the study, it was hypothesized that if the TSS could display to the user the amount of force applied by the TSI, the performance of manual palpation methods using the TSS would improve.

To test this hypothesis, a new user interface for the TSS was developed. The interface simultaneously displays an active colour-contour map and an adjacent force bar that indicates the total amount of force experienced by the TactArray sensor, computed using the force LUT described in Section 4.2.1. The display of the force bar indicator changes according to four distinct categories indicating the performance of the TSS. The first category represents applied forces that are less than those necessary for optimal performance. For this situation, the colour of the force bar indicator is yellow. For levels in which the applied force is between 3 N and 5 N, the desirable range to receive consistent results from the TSS, the colour of the force bar indicator is green (as shown in Figure 4.5). The third category is represented by a red force bar indicator, and implies that the applied forces are in the range of 5 N to 6 N, which is close to, but not exceeding, the critical force for tissue damage. Lastly, when dangerous force levels are detected at

the end-effector (6 N or greater), the colour-contour map is temporarily disabled and a warning message is displayed to ensure that the user realizes that bulk tissue damage may be occurring.

Although the force bar indicator is the newest feature of the TSS, the central focus of the visualization interface is the colour-contour map. This map displays the pressure distributions on the TactArray sensor in a meaningful way to the user by using the visual colour spectrum to represent the intensity of localized pressure experienced by the probe. An area of low pressure intensity is represented by a blue area on the map, and an area of high pressure intensity is represented by a red area on the map. The other colours of the visual spectrum (orange, yellow, green) are linearly mapped to a corresponding linear increase in pressure intensity. Therefore, in the presence of a tumour, the map will contain a concentrated red area at a specific location indicating the presence of the tumour, surrounded by a blue region, indicating healthy tissue. A colour version of the TSS visualization interface with force display is shown in Figure 4.5.

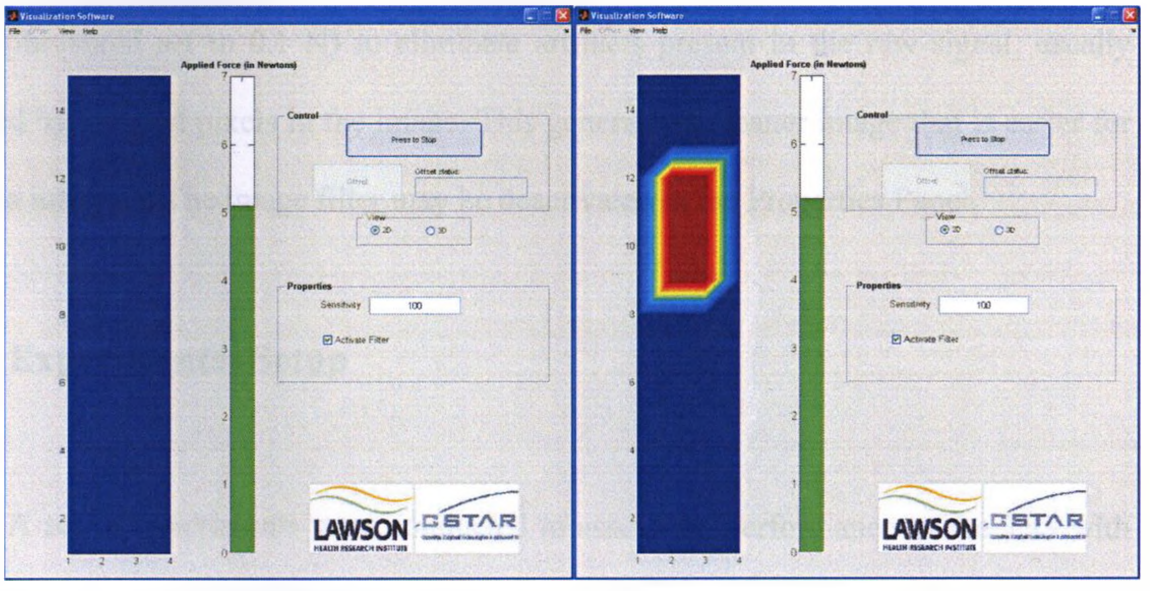


**Figure 4.5:** Left image: TSS visualization interface indicating an area of healthy tissue when applying a force of 5 N. Right image: TSS visualization interface indicating the presence of a tumour when applying a force of 5 N.

The visualization interface includes a Control Panel which provides an 'offset' push-button that, upon activation, removes the DC offset generated by the electronics from the colour-contour map. The View Panel allows the user to control the view of the colour-contour map. The two possible views of the colour-contour map are a topographical (2-dimensional) view, which is set as the default view and is the view selected for Figure 4.5, and an isometric (3-dimensional) view. Other functions are accessible to the user through the Properties Panel. This panel allows control over the sensitivity of the colour-contour pressure map, which is necessary when the system is used in tissues with different mechanical properties, such as tissue stiffness and tissue thickness. The default setting for this feature is 100% sensitivity, implying no amplification in sensitivity. As the sensitivity value is increased above 100%, the signal is amplified, and when the sensitivity value is lowered, the signal is subdued. An additional feature integrated in the user interface is an image filter for the active colour-contour map. The filter is a function found in MATLAB, entitled `bwmorph`, which performs a morphological operation on a binary representation of the colour-contour map image (threshold set to 0.1 N) to eliminate artifacts present in the raw signal, usually signified by isolated pixels in the image. This generates a cleaner image that is easier for a user to interpret. The image filter may be deactivated in the Properties Panel.

## 4.4 Experimental Setup

A set of experiments were conducted to assess the performance of the TSS with and without visual force feedback. The experimental test-bed consisted of an MIS

training box that mimics the conditions present in actual surgery. A 6-DOF Gamma force/torque sensor (ATI Industrial Automation, Inc.) was placed below a tray on which liver samples were placed. Access to the viewing field was made possible by a 0° endoscope with a standard resolution laparoscopic camera (Stryker Endoscopy, Inc.) held over the working field by a portable clamp (WolfCraft, Inc.). The camera output was displayed to the participant via a surgical monitor and an adjacent computer monitor was used to display the TSS visualization interface. The experimental setup is shown in Figure 4.6.

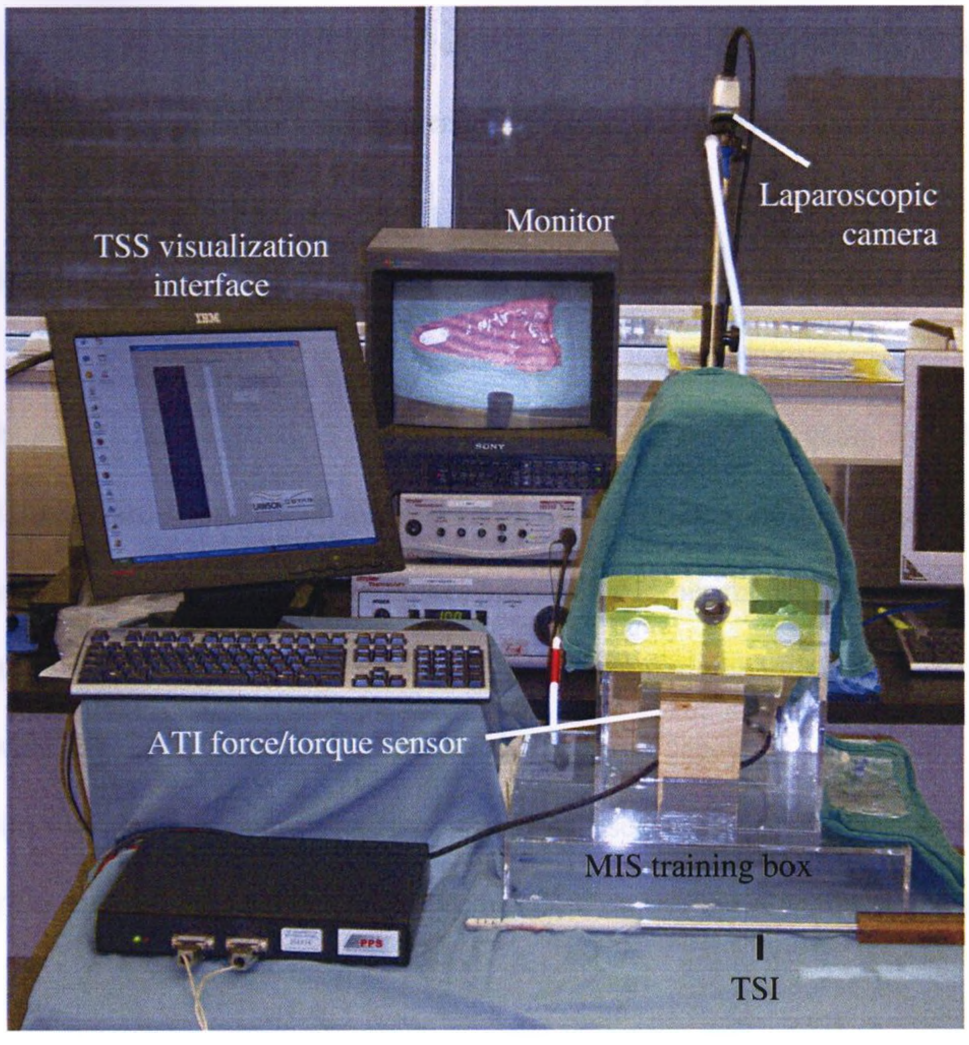


**Figure 4.6:** Experimental setup for evaluation of TSS.

## 4.5 Methods

### *4.5.1 Tissue Preparation*

Seventy-two liver samples were prepared for these experiments. Each sample was sliced to a thickness of approximately 5 mm. To simulate the presence of tumours, 10 mm diameter hemispherical objects made from Gelrite Gellan Gum (Sigma-Altrich, Inc.), with embedded metal wires were inserted into the dorsal side of the liver with the flat side of the object being parallel to the bottom of the tissue. Each *ex vivo* liver sample had the possibility of containing zero to two phantom tumours. The process to determine the number of tumours to be embedded into the liver was performed *a priori* through a block randomization process. It was ensured that an equal number of samples with all possible combinations of embedded tumours were presented at the end of all trials.

### *4.5.2 Procedure*

Four volunteers participated in the experiments: a thoracic surgeon with MIS experience and three third-year general surgery residents with moderate MIS experience. To reduce the error attributed to a learning curve, prior to the experiments the participants practiced palpating 10 mm diameter hemispherical agar tumours embedded in an *ex vivo* bovine liver with the TSS, with and without visual force feedback, until they felt comfortable with their performance. The tissue samples used in the practice trials were prepared solely for the training sessions and were not used during the experimental trials.

For each trial, the participant was presented with one tissue sample. The goal was to locate the phantom tumours, if any, in the *ex vivo* tissue samples. The tissue sample and the use of visual force feedback for each trial was randomly assigned to the subject, however, it was ensured that each subject palpated the same number of tissues and tumours with and without force display at the completion of all trials.

The palpation force as indicated by the Gamma force/torque sensor was recorded for each trial. A proctor, who was blinded to the number and location of tumours in each sample, recorded the location of the tumour found by the participant with a plastic instrument marker and two marking pins. This marking procedure was performed for all tissue samples and radiographic images were taken of the samples using a fluoroscopic radiographic machine so that success rate (outlined in Section 4.5.3) could be determined. An example of a radiographic image is shown in Figure 4.7.

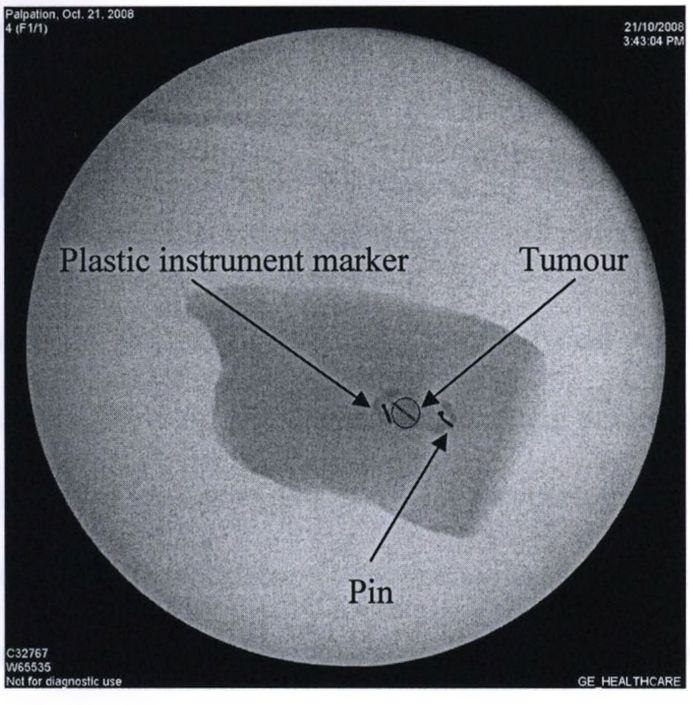


**Figure 4.7:** Radiographic image of liver sample with embedded tumour.

### *4.5.3 Performance Assessment*

The performance of the TSI with and without visual force feedback was assessed by: 1) the palpation force exerted by the instrument, and 2) the success rate for locating tumours.

The *palpation force* exerted while searching for a tumour is an indication of the potential bulk damage that can be inflicted on the tissue during the task. The force values, in Newtons (N), exerted by the TSI on the tissue throughout each trial were acquired from the Gamma force/torque sensor, placed below the tissue samples, at a continuous acquisition rate of 50 Hz. The maximum applied forces were extracted from the recorded force data.

The *success rate* of the trial can be divided into four categories [22]: a true positive result, a false positive result, a false negative result, and a true positive result. Success rate was used to determine the performance of the TSS in terms of accuracy, sensitivity, specificity, positive likelihood ratio (likelihood of tumours when the test is positive), and negative likelihood ratio (likelihood of no tumours when the test is negative).

Statistical analysis was performed using the Statistical Analysis System (SAS, Cary, NC) software, version 9.1 for Windows and significant values were recorded as $p < 0.05$. A one-way analysis of variance (ANOVA) test was performed (95% confidence) to establish if there was a significant difference between groups. The subjects were assumed to be fixed in the analysis since too few volunteers participated in the experiments to be treated as a random factor. The $p$-value for the performance results (accuracy, sensitivity,

and specificity) was established by performing the Fisher's Exact Test (2-sided). An independent statistician from the Biostatistical Support Unit (The University of Western Ontario, London, ON) assisted with the statistical analysis.

## 4.6 Results

The results of the experimental evaluation are summarized in Tables 4.2 and 4.3. Table 4.2 shows the mean and maximum forces applied to the samples with and without visual force feedback, and their associated $p$-values. These results show that the average force decreased by 1.40 N ($p = 0.003$) and the maximum force decreased by 2.14 N ($p = 0.012$) with force display in the visualization interface.

The TSS with visual force feedback demonstrated an improvement in sensitivity of 18% ($p = 0.416$) and a 21% ($p = 0.096$) improvement in accuracy, when compared to the system without force display.

**Table 4.2:** Average and maximum applied forces when using the TSS on *ex vivo* liver.

| | **Average Applied Forces (N ± SD)** | **Maximum Applied Forces (N ± SD)** |
|---|---|---|
| **Without visual force feedback** | 4.28 ± 1.53 | 10.23 ± 3.53 |
| **With visual force feedback** | 2.88 ± 1.01 | 8.09 ± 3.15 |
| | $p = 0.003$ | $p = 0.012$ |

**Table 4.3:** TSS performance results when palpating *ex vivo* liver.

| | Accuracy | Sensitivity | Specificity | Positive Likelihood Ratio | Negative Likelihood Ratio |
|---|---|---|---|---|---|
| **Without visual force feedback** | 40% | 63% | 11% | 0.70 | 3.38 |
| **With visual force feedback** | 61% | 81% | 29% | 1.14 | 0.65 |
| | $p = 0.096$ | $p = 0.416$ | $p = 0.458$ | | |

## 4.7 Discussion

The calibration results of this study show that the mean accuracy, mean repeatability, and maximum deviation in hysteresis of the element-based calibration were 89%, 95%, and ±0.2 N, respectively. Furthermore, the sensor-based calibration using *ex vivo* liver demonstrated accuracy of 71%, repeatability of 77%, and a maximum deviation of ±0.3 N in hysteresis.

As predicted, the calibration results indicate that the percent accuracy of the sensor on an element basis is considerably better than for the aggregate of all elements. This is partly due to the sum of the errors when adding the forces of all sixty elements, which can affect the results. This result was foreseeable since the forces applied to neighbouring elements were ignored when performing element-based calibration. The forces applied to an individual capacitor element could not be determined due to the design of the TactArray sensor, which uses a uniform protective membrane to

encapsulate the entire sensor array. Therefore, the force approximations used during calibration cause the actual sensor force output to be higher than that predicted by the sum of forces experienced by the individual elements. However, it should be realized that the purpose of this study was to determine if TSS performance is improved when force feedback is visually presented to the user. Although approximations of applied forces to sensor elements were used during TSS calibration, the TSS with force display significantly reduced the amount of force applied to the tissue and demonstrated better overall performance than the TSS without force display. Furthermore, the task of attaining applied forces at the end-effector is not limited to the TactArray sensor. Force sensors can be placed at the TSI end-effector to provide more accurate readings of applied force information to the user.

The experimental results of this study show that performing palpation using the TSS with visual force feedback significantly reduces the average and maximum applied forces on the tissue. Specifically, a relative reduction of approximately 33% and 21% were observed when compared to the system without force display. Furthermore, detection accuracy has the potential to relatively increase by 53% when compared to the system without visual force feedback. The TSS with force display also demonstrated that it is a potentially better device to recognize 'diseased' tissues (with tumours) and 'healthy' tissues (without tumours) as indicated by sensitivity and specificity, respectively. Lastly, the largest positive likelihood ratio indicates the best method that will rule in a diseased tissue, and the smallest negative likelihood ratio indicates the best method to rule out a diseased tissue. When compared to the TSS without force feedback, the likelihood ratios for this study indicated that the TSS with force display has the

capability to better determine if the tissue is diseased or healthy. Since the tissues selected for this study are not representative of the prevalence of liver cancer in the human population, likelihood ratios are presented rather than predicted values.

The study is underpowered due to limited resources and a small number of participants. The need to have participants who are experienced with MIS led to a limit in the number of surgeons and surgical residents that were available to participate in this study; therefore, significantly fewer livers were palpated by each instrument than required by sample size calculations. An *a priori* sample size calculation was performed before the commencement of the study. With 80% power and a 5% significance level (2-sided), in order to increase the sensitivity of the TSS by 10% the sample size of *each* group required 196 livers. For this study, only a *total* of 72 livers could be attained from a local abattoir in a reasonable time period. Therefore, it can be assumed that this study is subject to Type II (beta) error. Due to the nature of this study, it would be impractical to suspend it until an adequate number of tissues and participants were attained. Since the development of the TSS is undergoing active development, its validation and refinement are time sensitive. This study was designed as a proof of concept to determine the impact of visual force feedback on the performance of the TSS exclusively.

In this study, *ex vivo* bovine livers were thinly sliced to the same thickness to create an ideal tissue model to test the performance of the TSS with and without visual force feedback. It was decided that an ideal tissue model was needed to control external factors which could substantially influence the results of the study, such as varying tissue thickness or inconsistency of mechanical properties throughout the tissue. With the implementation of an ideal tissue model in this study, the influences of these external

factors are minimized and the experimental results of applied pressure and TSS performance were adequately compared.

The amount of force applied to an organ while palpating for occult tumours during surgery is significant since sustained localized forces can lead to tissue damage. This has been particularly troublesome in MIS since occasionally surgeons must rely on the relay of haptic information from the instrument tip to their hands, which can become distorted or subdued due to friction introduced by the insertion point [5]. The results from this study demonstrated that when users were provided with a visual display of force feedback while attempting to locate tumours in the tissue, the average amount of applied forces that they exerted on the tissue decreased significantly. The study also demonstrated that by providing the force display in the visualization interface, the average forces applied to the tissue were well below the 6 N level that can result in visible tissue damage if exerted for extended periods of time, as reported in [20]. In this case, 17% of the trials using the TSS with no force feedback exceeded an average force level 6 N. There were no trials that on average exceeded 6 N when using the TSS with visual force feedback.

## 4.8 Conclusions

The results of the preliminary study show that the TSI was successfully calibrated to adequately indicate the amount of applied force, in Newtons, between the contact surfaces, demonstrating 70.8% accuracy, 76.5% repeatability, and insignificant hysteresis when tested on *ex vivo* bovine liver. The study further demonstrated that palpating tissue

using the TSS with visual force feedback reduced the average and maximum applied forces on the tissue by 33% and 21%, respectively, and detection accuracy was relatively increased by 53% when compared to using the system without force display. Therefore, it is evident that the implementation of visual force feedback into the TSS had a beneficial effect on the system. In conclusion, the TSS has the potential to improve the efficacy of MIS tumour therapies and techniques, and offers the possibility of restoring haptic information lost during surgery, thus mitigating one of the current limitations of minimally invasive surgery.

## References

[1] American Cancer Society. (2008). *Cancer Facts and Figures 2008*, Atlanta, GA: American Cancer Society Inc. [Online]. Available: http://www.cancer.org/downloads/STT/2008CAFFfinalsecured.pdf.

[2] American Cancer Society. (2007). *Global Cancer Facts and Figures 2007*, Atlanta, GA: American Cancer Society Inc. [Online]. Available: http://www.cancer.org/downloads/STT/Global_Facts_and_Figures_2007_rev2.pdf.

[3] J. Dargahi, S. Payandeh, and M. Parameswaran, "A micromachined piezoelectric teeth-like laparoscopic tactile sensor: theory, fabrication and experiments," in *Proc. IEEE Int. Conf. Robot. Autom. (ICRA)*, Detroit, Michigan, 1999, pp. 299–304.

[4] P. Puangmali, H. Liu, K. Althoefer, and L. D. Seneviratne, "Optical fiber sensor for soft tissue investigation during minimally invasive surgery," in *Proc. IEEE Int. Conf. Robot. Autom. (ICRA)*, Pasadena, California, 2008, pp. 2934–2939.

[5] G. L. McCreery, A. L. Trejos, R. V. Patel, M. D. Naish, and R. A. Malthaner, "Evaluation of force feedback requirements for minimally invasive lung tumour localization," in *Proc. IEEE Int. Conf. Intell. Robot. Syst. (IROS)*, San Diego, California, 2007, pp. 883–888.

[6] A. P. Miller, W. J. Peine, J. S. Son, and J. T. Hammoud, "Tactile imaging system for localizing lung nodules during video assisted thoracoscopic surgery," in *Proc. IEEE Int. Conf. Robot. Autom. (ICRA)*, Roma, Italy, 2007, pp. 2996–3001.

[7] M. Tavakoli, A. Aziminejad, R. V. Patel, and M. Moallem, "Tool/tissue interaction feedback modalities in robot-assisted lump localization", in *Proc. IEEE EMBS Ann. Int. Conf.*, New York City, New York, 2006, pp. 3854–3858.

[8] T. Hemsel, R. Stroop, D. Olivia Uribe, and J. Wallaschek, "Resonant vibrating sensors for tactile tissue differentiation," *J. Sound Vib.*, vol. 308, (3–5), pp. 441–446, 2007.

[9] N. Kattavenos, B. Lawrenson, T.G. Frank, H.S. Pridham, R.P Keatch, and A. Cuschieri, "Force-sensitive tactile sensor for minimal access surgery", *Minim. Invasive Ther. Allied Technol.*, vol. 13, (1), pp. 42–46, 2004.

[10] Y. Murayama, M. Haruta, Y. Hatakeyama, T. Shiina, H. Sakuma, S. Takenoshita, S. Omata, and C. E. Constantinou, "Development of new instrument for examination of stiffness in the breast using haptic sensor technology," *Sens. Actuators, A: Phys.*, vol. 143, (2), pp. 430–438, 2008.

[11] M. V. Ottermo, M. Øvstedal, T. Langø, Ø. Stavdahl, Y, Yavuz, T. A. Johansen, and R. Mårvik, "The role of tactile feedback in laparoscopic surgery," *Surg. Laparosc. Endosc. Percutan. Technol.*, vol. 16, (6), pp. 390–400, 2006.

[12] M. V. Ottermo, Ø. Stabdahl, and T. A. Johansen, "Palpation instrument for augmented minimally invasive surgery," in *Proc. IEEE/RSJ Int. Conf. Intell. Robot. Syst. (IROS)*, vol. 4, Sandal, Japan, 2004, pp. 3960–3964.

[13] H. Liu, D. P. Noonan, K. Althoefer, and L. D. Seneviratne, "Rolling mechanical imaging: a novel approach for soft tissue modeling and identification during minimally invasive surgery," in *Proc. IEEE Int. Conf. Robot. Autom. (ICRA)*, Pasadena, California, 2008, pp. 845–850.

[14] D. P. Noonan, H. Liu, Y. H. Zweiri, K. A. Althoefer, and L. D. Seneviratne, "A dual-function wheeled probe for tissue visoelastic property identification during minimally invasive surgery," in *Proc. IEEE Int. Conf. Robot. Autom. (ICRA)*, Roma, Italy, 2007, pp. 2629–2634.

[15] C. Bonomo, P. Brunetto, L. Fortuna, P. Giannone, S. Graziani, and S. Strazzeri, "A tactile sensor for biomedical applications based on IPMCs," *IEEE Sens. J.*, vol. 8, (8), pp. 1486–1493, 2008.

[16] J. Dargahi, S. Najarian, V. Mirjalili, and B. Liu, "Modeling and testing of a sensor capable of determining the stiffness of biological tissues," *Can. J. Elect. Comput. Eng.*, vol. 32, (1), pp. 45–51, 2007.

[17] M. Kaneko, C. Toya, and M. Okajima, "Active strobe imager for visualizing dynamic behavior of tumours," in *Proc. IEEE Int. Conf. Robot. Autom. (ICRA)*, Roma, Italy, 2007, pp. 3009–3014.

[18] G. L. McCreery, A. L. Trejos, R. V. Patel, M. D. Naish, and R. A. Malthaner, "Feasibility of locating tumours in lung via kinaesthetic feedback," *Int. J. Med. Robot. Comput. Assist. Surg.*, vol. 4, (1), pp. 58–68, 2008.

[19] R. S. Fearing, "Tactile sensing mechanisms," *Int. J. Robot. Res.*, vol. 9, (3), pp. 3–23, 1990.

[20] A. L. Trejos, J. Jayender, M. T. Perri, M. D. Naish, R. V. Patel, and R. A. Malthaner, "Robot-assisted tactile sensing for minimally invasive tumour localization," *Int. J. Robot. Res. — Special Issue on Medical Robotics*, vol. 28, (9), pp. 1118–1133, 2009.

[21] M. T. Perri, D. A. Bottoni, A. L. Trejos, G. L. McCreery, M. D. Naish, R. V. Patel, and R. A. Malthaner, "A new tactile imaging device to aid with localizing lung tumours during thoracoscopic surgery," *Int. J. Comput. Assist. Radiol. Surg. (Int. J. CARS)*, vol. 3, suppl. 1, pp. S257–S258, 2008.

[22] M. Davidson, "The interpretation of diagnostic tests: a primer for physiotherapists," *Aust. J. Physiother.*, vol. 48, (3), pp. 227–232, 2002.

# Chapter 5

# New Tactile Sensing System for Minimally Invasive Surgical Tumour Localization[1]

## 5.1 Introduction

Lung cancer accounts for the most cancer-related deaths in both men and women in North America [1]. Patients diagnosed with lung cancer can survive without remission when the disease is still contained upon detection. Treatment options for lung cancer include surgery, radiation therapy, chemotherapy, and targeted biological therapies [2]. For localized cancers, lung resection has been the treatment of choice. Traditionally, this procedure was performed through an open thoracotomy, which allowed direct access to the lung and location of the cancerous nodule was performed by manual palpation of the organ; however, with the advancement and integration of technology into medicine, minimally invasive surgery (MIS) has become prevalent over traditional open surgical

[1] A version of this chapter has been submitted for publication to The International Journal of Medical Robotics and Computer Assisted Surgery with an author list: MT Perri, AL Trejos, MD Naish, RV Patel, and RA Malthaner

procedures. Although MIS provides many benefits over traditional open surgery, including reduction of post operative pain, decrease in the length of hospital stay, and rapid recovery time for the patient [3], its advantages are often offset by the major difficulties it creates for the surgeon, particularly since the organ is no longer accessible for manual palpation [4]. Therefore, surgeons must rely on their prior surgical experiences and the additional use of technologies adopted to locate tumours pre- and intra-operatively.

Current standard clinical technologies adopted for MIS pulmonary tumour localization procedures include pre-operative computed tomography (CT) scans or inserted guide wires via CT guidance, and the intra-operative use of laparoscopic ultrasound or endoscopic graspers. Although these technologies could be used in the operating room, there are limitations to these methods for lung resection.

In view of these limitations, research has become increasingly active in the field of haptics aiming to find an alternative method for locating tumours intra-operatively [10]. Specialized surgical instruments are being developed by researchers so that the surgeon's sense of touch is not eradicated from the process. For the purposes of tumour localization, these hand-held instruments occasionally depend on haptic feedback from the instrument tip to the surgeon's hand and can be based on piezoelectric [11], [12], piezoresistive [13], capacitive [8], [10], or optical fiber [4] technologies.

### *5.1.1 Progress to Date*

Based on a kinaesthetic analysis of the effect of tumours on reflected force feedback [15], a device, entitled the TSI, was designed by the authors to measure the pressure distribution at the device's end-effector when palpating tissue. Further information on the TSI can be found in [16], [17]. Preliminary testing detailed in Chapter 2 demonstrated superior efficiency and accuracy in locating tumours in *ex vivo* porcine lung using the TSI compared to an endoscopic grasper [18]. Further experiments were conducted where the TSI was manoeuvred using robotic-assisted control [17]. The study, presented in Chapter 3, concluded that the robotic-assisted control methods demonstrated superior performance over manual manipulation of the TSI because TSI performance is dependent on the amount of force being applied by the user during palpation. To improve TSI performance with manual control, the tactile sensor on the TSI was calibrated in order to obtain a relationship between the sensor readings and the amount of applied force on the tactile sensing elements. The results gathered from this calibration procedure, as presented in Chapter 4 and [19], were then incorporated into the visualization interface to provide the contact force data to the user.

### *5.1.2 Purpose*

The purpose of this study is to compare the relative performance of the TSS with force display to that of standard MIS intra-operative localization methods (i.e., using an endoscopic grasper to directly palpate tissue or using an ultrasound probe), and the

current standard of practice (i.e., manual palpation). The experiments were conducted on *ex vivo* tissue using liver as an ideal tissue model. The performance of the TSS was then tested using lung as a realistic tissue model.

## 5.2 Materials and Methods

### *5.2.1 Manufacturing the Lesions*

To simulate tumours, a mould for six spherical tumour phantoms was constructed and filled with a heated mixture consisting of Gelrite Gellan Gum (6% by weight, Sigma-Altrich Inc., St. Louis, MO), barium sulfate (1% by weight, E-Z-EM Canada Inc., Anjou, QC), and water (93% by weight). As shown in Figure 5.1, the diameter of the phantom tumours was approximately 10 mm. Prior to injection of the mixture, the mould was lined with two or three thin metal wires (30-gauge). The warm mixture was then injected into the mould by using a large syringe and allowed to solidify for approximately three minutes. The phantom tumours were immediately removed from the mould and cut in half along the diameter resulting in a hemispherical object with the wires embedded within it. The phantom tumours were then placed in a sealed container to ensure that no moisture could evaporate and change the mixture concentration or the volume of the tumours.

The size of the phantom tumours used for this study was chosen to be 10 mm in diameter since most diagnostic tests are not capable of detecting tumours that are smaller than that size [20], [21]. Therefore, the phantom tumours utilized in this study can be

used to properly assess the performance of all four localization methods under a worst case scenario.

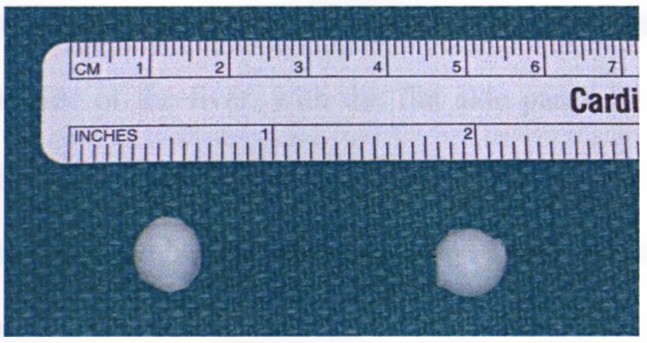


**Figure 5.1:** Phantom tumours.

### *5.2.2 Ex vivo Tissue Selection*

The varying boundary and testing conditions presented by lung tissue, due to its asymmetrical anatomical shape and naturally embedded calcified structures, made it essential to perform tests with ideal biological soft *ex vivo* tissue prior to tests in lung. These preliminary tests served to minimize external influential factors, such as inconsistent tissue depth, naturally embedded structures, and the presence of residual air, that could significantly influence the experimental results. Therefore, for the purposes of this study, the performance of the TSS and other MIS techniques were conducted on thinly sliced, rectangular, bovine liver samples, selected to be consistent in both tissue thickness and mechanical tissue properties, so that the performance of each instrument could be adequately compared. To test the feasibility of implementing the TSS for clinical pulmonary tumour localization purposes, the TSS was then tested using collapsed *ex vivo* porcine lung.

### *5.2.3 Implanting the Lesions into ex vivo Bovine Liver*

Approximately 120 liver samples were acquired from a local grocery store. The liver samples were pre-sliced into 5 mm thick slices. The hemispherical tumours were pressed into the underside of the liver, with the flat side parallel to the bottom of the tissue as shown in Figure 5.2. Each liver sample had the possibility of containing between zero and two tumours. The number of tumours, if any, to be embedded into each liver sample was determined *a priori* through a block randomization process. This ensured that an equal number of samples with all possible combinations of embedded tumours were presented at the end of all trials.

**Figure 5.2:** Phantom tumour pressed into underside of *ex vivo* liver.

### *5.2.4 Implanting the Lesions into Excised Porcine Lung*

To simulate the condition of the lung during a clinical resection procedure, it was necessary to acquire collapsed porcine lung tissue. These were obtained from other experiments occurring in the lab. To alleviate the air within the lung tissue, the bronchus

of the left porcine lung was clamped to prevent ventilation, however, blood circulation was still permitted for the removal of residual oxygen gas within the lung. After the pig was euthanized, the lung was excised. Thirty-two lung samples were segmented from eight *ex vivo* porcine left lung lobes. Prior to experimentation, the lung samples had a number of small incisions made on the dorsal side of the tissue so that the 10 mm hemispherical tumours could be inserted with the flat side of the tumour being parallel to the bottom of the tissue. The incisions were then sutured using 3-0 silk sutures (Ethicon, Markham, Ontario). To ensure that the sutures were not the objects being detected during the trials, a number of sham cuts were made and then sutured closed with no tumour inserted. The number of tumours and sham cuts to be sutured in the lung was determined by the same block randomization process performed on the liver samples.

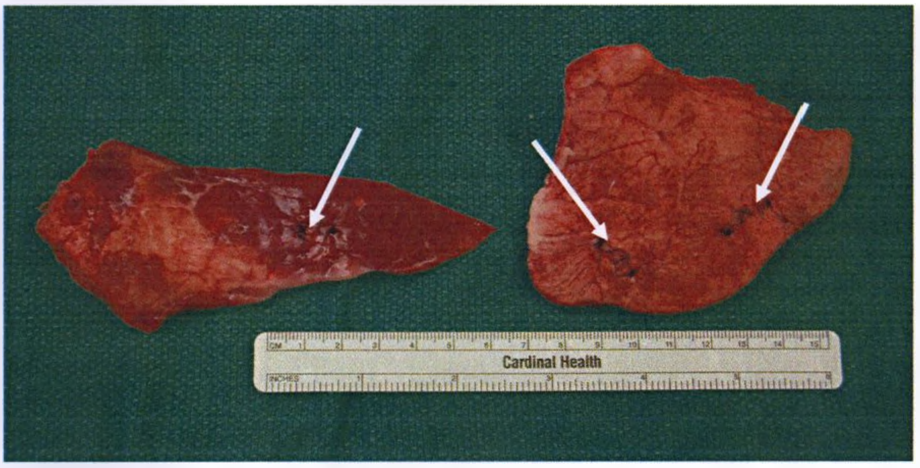


**Figure 5.3:** Incisions were made on underside of lung, phantom tumours were inserted, and then incisions were sutured closed.

## 5.3 Experimental Setup

The experiments were performed inside an MIS training box. A 6-degree of freedom (6-DOF) Gamma force/torque sensor (ATI Industrial Automation, Apex, NC)

was placed inside and fastened to a wooden tray over which the tissue samples were placed. A drape was placed over the MIS training box during the trials (not shown in Figure 5.4). Access to the viewing field was made possible by a 0° scope with a standard resolution laparoscopic camera (Stryker Endoscopy, Inc., San Jose, CA) elevated over the working field with the aid of a portable clamp (WolfCraft, Kempenich Germany). The camera output was displayed on a television monitor. Before commencement of the experiments, it was ensured that the video image showed the entire working field inside the training box, so that no movement of the camera was necessary during the trial. Adjacent to the television monitor was a computer monitor that displayed the TSS visualization interface when applicable. The experimental setup is shown in Figure 5.4.

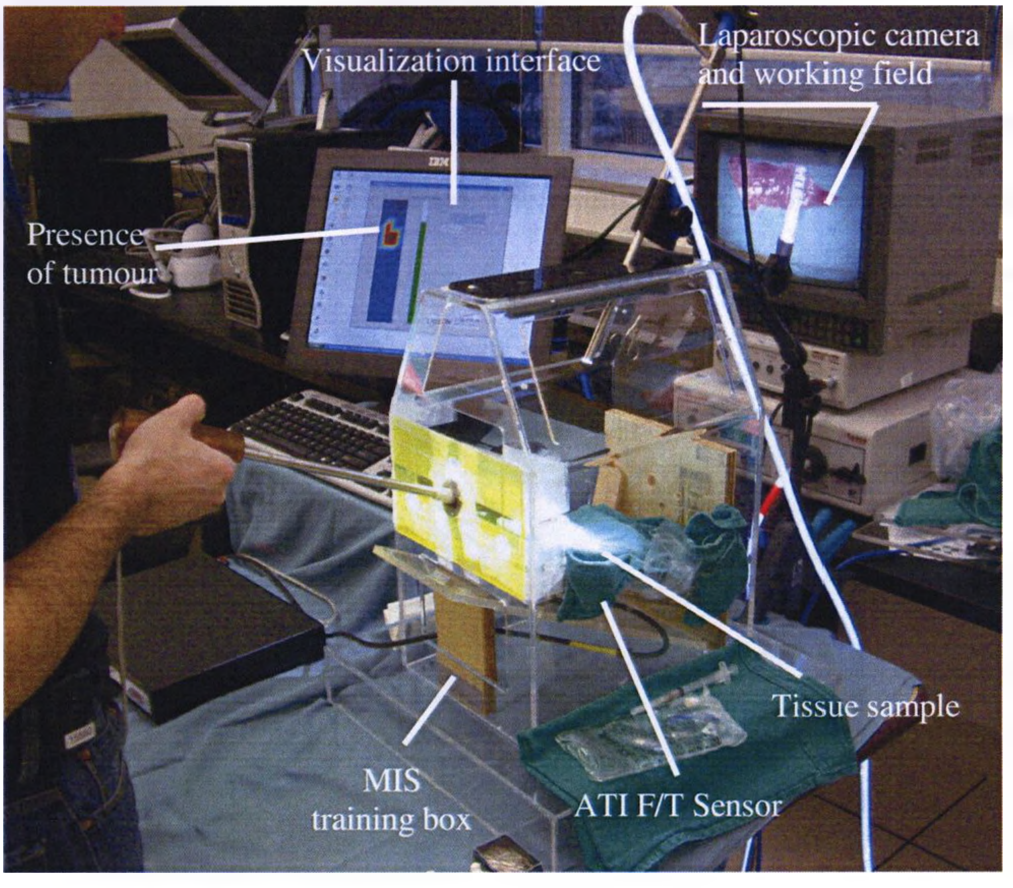


**Figure 5.4:** Experimental setup.

## 5.4 Procedure

Four volunteers participated in the experiments. One of the participants was a thoracic surgeon expert in MIS and the other three were third year general surgery residents with moderate MIS experience. To reduce the error attributed to learning, the participants practiced palpation techniques with all instruments, prior to commencement of the experiments, until they felt comfortable with their performance. The tissue samples used in the practice trials were prepared solely for the training sessions and were not selected for use during the experimental trials.

One tissue sample was presented for each trial and the participants were blinded to the number and location of tumours in all trials. When a participant indicated that he or she found a tumour, the location was recorded with a plastic instrument marker and two marking pins, as shown in Figure 5.5. All samples were imaged using a fluoroscopic radiographic machine (GE OEC 9900 Elite). The resulting radiographic images were then used to assess performance (see Section 5.4.1). Performance was assessed by four blinded volunteers.

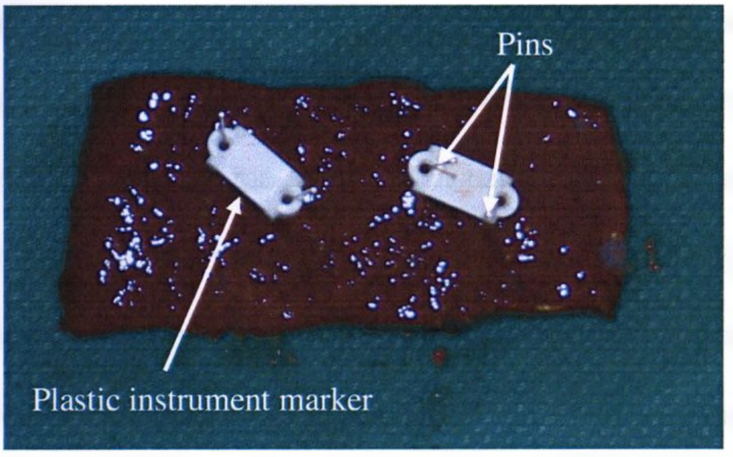


**Figure 5.5:** Tissue marked with plastic instrument marker and pins at tumour locations.

### *5.4.1 Performance Assessment*

The palpation force, localization distance, and the success rate were the three measurables used to assess the performance of each palpation method. They are described as follows:

The *palpation force* was defined as the amount of force exerted by the instrument or hand onto the tissue while palpating. The maximum applied forces were extracted from recorded force data to indicate the potential bulk damage applied to the tissue while searching for a tumour. Due to the varying sizes of the end effectors for the TSI, endoscopic grasper, and ultrasound probe, pressure values were attained by dividing the force values by the corresponding end-effector area during post-processing of the data, so that the different methods could be adequately compared.

The *localization distance* was defined as the average horizontal distance between the centres of the instrument markers and the centres of the corresponding tumour. Location distance was only recorded for tumours that were correctly identified during the trials. ImageJ software (National Institutes of Health, Bethesda, MD) was used to measure the localization distance directly.

The *success rate* of locating the tumours was represented by four measures from the radiographs [22]: a true positive result, a false positive result, a false negative result, and a true negative result. These four measures are visually represented in Figure 5.6. Success rate was recorded in terms of accuracy, sensitivity, and specificity. Likelihood ratios were also calculated since these ratios are independent of the prevalence of the disease in the population. The largest positive likelihood ratio indicates the best test to

use to rule in a disease, and the smallest negative likelihood ratio indicates the best test to rule out a disease.

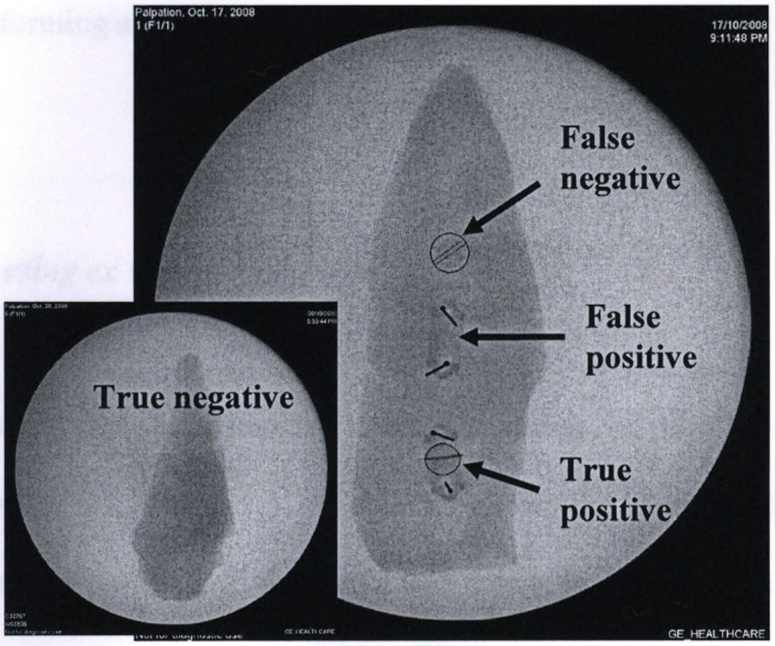


**Figure 5.6:** Fluoroscopic radiographic images of tissue samples. Visual representations of the four success rate measures are indicated.

To attain the *p*-values for the applied pressures, localization distances, and performance results, the Statistical Package for Statistical Analysis System (SAS, Cary, NC) software, version 9.1 for Windows, was utilized. For the experiments involving bovine liver, a repeated measures analysis of variance (ANOVA) test was performed (95% confidence) to establish if there was a significant difference among the different techniques. A post-hoc Tukey-Kramer correction was then performed to establish if there was a significant difference between the individual techniques. For the experiments involving porcine lung, an analysis of variance (ANOVA) test was performed (95% confidence) to establish if there was a significant difference between groups. The subjects

were assumed to be fixed in the analysis since the number of volunteers that participated in the experiments was too few to be treated as a random factor. The $p$-value for the performance results (accuracy, sensitivity, and specificity) using both liver and lung was established by performing a Fisher's Exact Test (2-sided).

## 5.5 Results

### *5.5.1 Palpation using ex vivo Bovine Liver*

The results of the experimental evaluation using *ex vivo* bovine liver are summarized in Tables 5.1, 5.2, and 5.3. Table 5.1 shows the mean maximum pressure applied to the samples, the average localization distance, and their associated $p$-values. These results show that there was a significant difference in the pressures applied by the endoscopic grasper and the TSS on the liver samples with an absolute decrease of 2.76 N ($p = 0.002$) and 5.09 N ($p < 0.001$) in average pressure applied and maximum pressure applied, respectively, when using the TSS as the palpation instrument. There was no significant difference in applied pressure between the ultrasound and TSS palpation methods. For average localization distance, manual palpation produced the best results. The TSI followed manual palpation, however with no significant difference was observed between the remaining MIS techniques.

Tables 5.2 and 5.3 display the performance results of all diagnostic instruments when palpating *ex vivo* liver. As expected, manual palpation exceeded all MIS techniques in performance. However, it should be realized that manual palpation cannot be performed during MIS and should only be used as a control group to which the MIS

techniques can be compared. Excluding specificity, the TSS demonstrated a better performance when compared to the other MIS techniques, however, with no significant difference among the techniques. The TSS demonstrated an absolute increase of 9% ($p$ = 0.247) in accuracy, and 16% ($p$ = 0.318) in sensitivity when compared to ultrasound. Furthermore, there was an absolute increase of 16% in both accuracy ($p$ = 0.627) and sensitivity ($p$ = 0.318) when comparing TSS to the endoscopic grasper. For likelihood ratios, manual palpation was predicted to be the best method to use to both rule in and rule out a disease. The TSS was the next best method in terms of both positive and negative likelihood ratios.

**Table 5.1:** Pressures and localization distances for the various tests on *ex vivo* liver.

| | **Average Pressure** ($N/cm^2 \pm$ SD) | ***p*-values for Average Pressure** | **Maximum Pressure** ($N/cm^2 \pm$ SD) | ***p*-values for Maximum Pressure** | **Average Localization Distance** (mm ± SD) | ***p*-values for Average Localization Distance** |
|---|---|---|---|---|---|---|
| **A. Manual** | – | – | – | – | 3.33±2.02 | 0.752 to B, 0.034 to C, 0.970 to D |
| **B. Endoscopic grasper** | 3.56±1.73 | 0.002 to C, and D | 7.20±2.79 | <0.001 to C and D | 4.68±2.90 | 0.752 to A, 0.163 to C, 0.931 to D |
| **C. Ultrasound** | 0.66±0.31 | 0.002 to B, 0.946 to D | 1.58±0.77 | <0.001 to B, 0.585 to D | 6.85±4.09 | 0.034 to A, 0.163 to B, 0.058 to D |
| **D. TSS** | 0.80±0.29 | 0.002 to B, 0.946 to C | 2.11±0.79 | <0.001 to B, 0.585 to C | 3.93±1.69 | 0.970 to A, 0.931 to B, 0.058 to C |

**Table 5.2:** Performance results of the diagnostic instruments when palpating *ex vivo* liver.

| | Accuracy | *p*-values for Accuracy | Sensitivity | *p*-values for Sensitivity | Specificity | *p*-values for Specificity |
|---|---|---|---|---|---|---|
| **A. Manual** | 88% | 0.001 to B,<br>0.007 to C,<br>0.048 to D | 88% | 0.168 to B,<br>0.168 to C,<br>0.999 to D | 89% | 0.011 to B,<br>0.067 to C,<br>0.024 to D |
| **B. Endoscopic grasper** | 51% | 0.001 to A,<br>0.647 to C,<br>0.247 to D | 67% | 0.168 to A,<br>0.999 to C,<br>0.318 to D | 29% | 0.011 to A,<br>0.694 to C,<br>0.999 to D |
| **C. Ultrasound** | 58% | 0.005 to A,<br>0.647 to B,<br>0.627 to D | 67% | 0.168 to A,<br>0.999 to B,<br>0.318 to D | 42% | 0.067 to A,<br>0.694 to B,<br>0.999 to D |
| **D. TSS** | 67% | 0.048 to A,<br>0.247 to B,<br>0.627 to C | 83% | 0.999 to A,<br>0.318 to B,<br>0.318 to C | 33% | 0.024 to A,<br>0.999 to B,<br>0.999 to C |

**Table 5.3:** Likelihood ratios of the diagnostic instruments when palpating *ex vivo* liver.

| | Positive Likelihood Ratio | Negative Likelihood Ratio |
|---|---|---|
| **Manual** | 7.88 | 0.14 |
| **Endoscopic grasper** | 0.94 | 1.13 |
| **Ultrasound** | 1.14 | 0.80 |
| **TSS** | 1.25 | 0.50 |

### *5.5.2 Palpation using ex vivo Porcine Lung*

TSS performance was also evaluated for palpation of *ex vivo* collapsed porcine lung. These results, as shown in Tables 5.4 and 5.5, demonstrate the TSS performance

when tested on a more realistic tissue model, similar to that encountered during an MIS lung tumour resection procedure. The *p*-value indicates if there was a significant difference in TSS performance when compared to palpation of liver.

The results in Table 5.4 demonstrate that the TSS when palpating lung showed an absolute decrease of 0.08 N ($p = 0.395$) in average pressure and an absolute increase of 0.35 N ($p = 0.260$) in maximum pressure when compared to palpating liver with the same instrument. However, both results show that there was no significant difference when the instrument was palpating both types of tissues. In terms of accuracy, sensitivity, and specificity, again there was no significant difference in performance when the TSS was palpating the ideal tissue model (liver) and the realistic tissue model (lung).

**Table 5.4:** Pressures and localization distances for *ex vivo* lung using the TSS.

| | **Average Pressure** ($N/cm^2 \pm SD$) | | **Maximum Pressure** ($N/cm^2 \pm SD$) | | **Average Localization Distance** (mm ± SD) | |
|---|---|---|---|---|---|---|
| **Lung** | 0.72±0.20 | $p = 0.395$ | 2.46±1.04 | $p = 0.260$ | 6.38±3.86 | $p = 0.082$ |

**Table 5.5:** TSS performance when palpating *ex vivo* lung.

| | **Accuracy** | **Sensitivity** | **Specificity** | **Positive Likelihood Ratio** | **Negative Likelihood Ratio** |
|---|---|---|---|---|---|
| **Lung** | 57% | 66% | 33% | 0.98 | 1.03 |
| | $p = 0.705$ | $p = 0.125$ | $p = 1.000$ | | |

## 5.6 Discussion

The results of this study show that palpation using the TSS significantly reduced the average and maximum pressures applied on the tissue by a relative 78% and 71%, respectively, when compared to the endoscopic grasper. The TSS also has the potential to more accurately locate occult tumours as demonstrated by localization distance. Furthermore, detection accuracy was increased by 31% and 16% relatively when compared to the grasper and ultrasound techniques, respectively.

It is hypothesized that the results for accuracy, sensitivity, and specificity using liver were statistically insignificant due to an underpowered study. An *a priori* sample size calculation was performed before commencement of the study. With 80% power and a 5% significance level (2-sided), in order to increase the sensitivity of the TSS by 10% the required sample size of *each* group was 196. Only a *total* of 120 liver segments could be attained for this study, and due to the delicacy of the tissue slices, each liver segment could only be used once during the experiments. The sample size of the experiment determined *a priori* was not satisfied because of the limited number of tissue resources and the few specialized volunteers that could be recruited for the study. Fulfilling the theoretical sample size would be unfeasible since the development of the TSS is an active endeavour and its validation was time sensitive. Since the sample size was not satisfied for this study, it is assumed that a Type II (beta) error has occurred. Furthermore, this study is not intended to disprove the quality of current MIS techniques or impose that the TSS should replace techniques currently used in MIS, but rather to investigate whether

the implementation of the TSS in the operating room is feasible and determine how it compares to conventional MIS techniques.

The TSS was designed to be a diagnostic test for intra-operative use. Since the focus of this study was on lung resection procedures, the MIS techniques selected for this study, particularly palpation using endoscopic graspers and using ultrasound, were chosen based on their well accepted use in MIS pulmonary tumour resection procedures and their intra-operative performance. Although CT technology and the pre-operative insertion of markers are also widely accepted techniques used in MIS pulmonary tumour resection procedures, they were not selected for inclusion in this study because of their pre-operative nature.

The applied forces as recorded during the trials could not be directly used in this study to compare the performance of all MIS techniques since the dimensions of their end-effectors differed significantly. In order to normalize this measurement, the surface area being palpated was taken into account, thus the maximum mean pressure applied to the tissue by the MIS instruments was used for analysis rather than the maximum mean force as recorded by the Gamma force/torque sensor. The disadvantage of using the maximum mean pressure as a parameter for comparative analysis is that manual palpation could not be analysed due to the different manual techniques performed by the subjects. However, this limitation is not detrimental to the study since manual palpation is not a valid competitor to other clinical MIS techniques and was included in this study as a control for the experiments.

When comparing the ultrasound method to the remaining MIS techniques, it should be realized that the ultrasound technique is not a palpation method, thus its

performance is not dependent on the force applied by the user. Rather, it only requires direct contact between the tissue and transducer to produce an image at that location. Even though the practicality of the TSS is dependent on the applied force to perform tissue palpation, the results showed that it required relatively the same amount of applied pressure as the ultrasound technique.

Manual palpation was included in this study solely as a control group since it is the current standard of practice for the localization of tumours during open surgery. It was expected that manual palpation performance would exceed those of other MIS techniques due to the fidelity of human sensory perception at the fingertips. This phenomenon is attributed to a highly dense array of sensory receptors at the fingertips that can simultaneously provide information about pressure applied on an object and its texture [23]. For researchers it is challenging to provide to the surgeon a diagnostic system that is capable of intra-operative tactile sensation and can also provide at least the same resolution and sensitivity as the surgeons' fingertips. It should be emphasized that manual palpation is not a competitive diagnostic test in this study since manual palpation cannot be used during minimal invasive surgery.

Localization distance demonstrated that the TSS has the potential to better localize occult tumours during surgery. If the surgeon can identify the exact location of the tumour with the TSS, the advantage of preserving more healthy tissue while excising the tumour would be significant, particularly to organs that cannot self-repair, such as the lung.

It should be noted that the performance results demonstrating accuracy, sensitivity, and positive likelihood ratios are most important to this study. Results for

specificity and negative likelihood ratios were included for completeness, and are less significant since in clinical pulmonary tumour localization procedures, the presence of disease is confirmed by pre-operative imaging. Since it is assumed that all patients scheduled for surgery have a nodule present in the lung, it is less vital that the intra-operative instruments can correctly detect healthy patients.

The experiments performed on *ex vivo* porcine lungs demonstrate that the TSS has the potential to perform well in locating occult tumours in collapsed lung. It was foreseeable that the TSS performance when palpating lung would decrease when compared to liver due to the complexity of the lung tissue that contains other calcified structures, such as the bronchus and bronchioles, and the tissue itself is more pliable and elastic when compared to the relatively uniform liver tissue samples.

## 5.7 Conclusion

The results of this study show that that when performing palpation on *ex vivo* bovine liver, the TSS realized an overall increase in performance, specifically a relative 71% reduction in maximum pressure applied on the tissue when compared to the endoscopic grasper, and a 31% and 16% relative increase in detection accuracy when compared to the grasper and ultrasound techniques, respectively. When tested using a realistic tissue model, the TSS was able to maintain its performance in collapsed *ex vivo* porcine lungs. Therefore, the results indicate that the developed TSS has the potential to help surgeons better identify occult tumours with more accuracy during MIS, and offers the possibility of providing to the surgeon the haptic information lost during MIS surgery.

## References


[1] American Cancer Society. (2008). *Cancer Facts and Figures 2008*, Atlanta, GA: American Cancer Society Inc. [Online]. Available: http://www.cancer.org/downloads/STT/2008CAFFfinalsecured.pdf.

[2] American Cancer Society. (2007). *Global Cancer Facts and Figures 2007*, Atlanta, GA: American Cancer Society Inc. [Online]. Available: http://www.cancer.org/downloads/STT/Global_Facts_and_Figures_2007_rev2.pdf.

[3] A. Lin, A. L. Trejos, R. V. Patel, and R. A. Malthaner, "Robot-assisted minimally invasive brachytherapy for lung cancer," in *Telesurg.*, Kumar and Marescaux, Ed. Berlin: Springer-Verlag, pp. 33–52, 2008.

[4] H. Liu, D. P. Noonan, K. Althoefer, and L. D. Seneviratne, "Rolling mechanical imaging: a novel approach for soft tissue modeling and identification during minimally invasive surgery," in *Proc. IEEE Int. Conf. Robot. Autom. (ICRA)*, Pasadena, CA, 2008, pp. 845–850.

[5] M. Kaneko, C. Toya, and M. Okajima, "Active strobe imager for visualizing dynamic behavior of tumours," in *Proc. IEEE Int. Conf. Robot. Autom. (ICRA)*, Roma, Italy, 2007, pp. 3009–3014.

[6] R. Santambrogio, M. Montorsi, P. Bianchi, A. Mantovani, F. Ghelma, and M. Mezzetti, "Intraoperative ultrasound during thoracoscopic procedures for solitary pulmonary nodules," *Ann. Thorac. Surg.*, vol. 68, pp. 218–222, 1999.

[7] V. D. M. Hornblower, E. Yu, A. Fenster, J. J. Battista, and R. A. Malthaner, "3D thoracoscopic ultrasound volume measurement validation in an ex vivo and in vivo porcine model of lung tumors," *Phys. Med. Biol.*, vol. 52, pp. 91–106, 2007.

[8] A. P. Miller, W. J. Peine, J. S. Son, and J. T. Hammoud, "Tactile imaging system for localizing lung nodules during video assisted thoracoscopic surgery," in *Proc. IEEE Int. Conf. Robot. Autom. (ICRA)*, Roma, Italy, 2007, pp. 2996–3001.

[9] R. H. Taylor and D. Stoianovici, "Medical robotics in computer integrated surgery," *IEEE Trans. Robot. Autom.*, vol. 19, (5), pp. 765–781, 2003.

[10] M. V. Ottermo, M. Øvstedal, T. Langø, Ø. Stavdahl, Y, Yavuz, T. A. Johansen, and R. Mårvik, "The role of tactile feedback in laparoscopic surgery," *Surg. Laparosc. Endosc. Percutan. Technol.*, vol. 16, (6), pp. 390–400, 2006.

[11] T. Hemsel, R. Stroop, D. Olivia Uribe, and J. Wallaschek, "Resonant vibrating sensors for tactile tissue differentiation," *J. Sound Vib.*, vol. 308, (3–5), pp. 441–446, 2007.

[12] Y. Murayama, M. Haruta, Y. Hatakeyama, T. Shiina, H. Sakuma, S. Takenoshita, S. Omata, and C. E. Constantinou, "Development of new instrument for examination of stiffness in the breast using haptic sensor technology," *Sens. Actuators, A: Phys.*, vol. 143, (2), pp. 430–438, 2008.

[13] N. Kattavenos, B. Lawrenson, T.G. Frank, H.S. Pridham, R.P Keatch, and A. Cuschieri, "Force-sensitive tactile sensor for minimal access surgery", *Minim. Invasive Ther. Allied Technol.*, vol. 13, (1), pp. 42–46, 2004.

[14] A. Sarvazyan, "Mechanical imaging: a new technology for medical diagnostics," *Int. J. Med. Inf.*, vol. 49, pp. 195–216, 1998.

[15] G. L. McCreery, A. L. Trejos, R. V. Patel, M. D. Naish, and R. A. Malthaner, "Evaluation of force feedback requirements for minimally invasive lung tumor localization," in *Proc. IEEE Int. Conf. Intell. Robot. Syst. (IROS)*, San Diego, California, 2007, p. 883–888.

[16] R. S. Fearing, "Tactile sensing mechanisms," *Int. J. Robot. Res.*, vol. 9, (3), pp. 3–23, 1990.

[17] A. L. Trejos, J. Jayender, M. T. Perri, M. D. Naish, R. V. Patel, and R. A. Malthaner, "Robot-assisted tactile sensing for minimally invasive tumour localization," *Int. J. Robot. Res. — Special Issue on Medical Robotics*, vol. 28, (9), pp. 1118–1133, 2009.

[18] M. T. Perri, D. A. Bottoni, A. L. Trejos, G. L. McCreery, M. D. Naish, R. V. Patel, and R. A. Malthaner, "A new tactile imaging device to aid with localizing lung tumours during thoracoscopic surgery," *Int. J. Comput. Assist. Radiol. Surg. (Int. J. CARS)*, vol. 3, suppl. 1, pp. S257–S258, 2008.

[19] M. T. Perri, A. L. Trejos, M. D. Naish, R. V. Patel, and R. A. Malthaner, "Analysis of the performance of a tactile sensing system when providing visual force feedback during minimally invasive tumour localization," submitted to *IEEE Trans. Biomed. Eng.*, 2009.

[20] J. K LeBlanc, J. DeWitt, and S. Sherman, "Endoscopic ultrasound: how does it aid the surgeon?" *Adv. Surg.*, vol. 41, pp. 17–50, 2007.

[21] P. Singh, R. A. Erickson, P. Mukhopadhyay, S. Gopal, A. Kiss, A. Khan, and T. Ulf Westblom, "EUS for detection of the hepatocellular carcinoma: results of a prospective study," *Gastrointest. Endo.*, vol. 66, (2), pp. 265–273, 2007.

[22] M. Davidson, "The interpretation of diagnostic tests: a primer for physiotherapists," *Aust. J. Physiother.*, vol. 48, (3), pp. 227–232, 2002.

[23] L. R. Bobich, J. P. Warren, J. D. Sweeny, S. I. Helms Tillery, and M. Santello, "Spatial localization of electrotactile stimuli on the fingertips of humans," *Somatosens. Motor Res.*, vol. 24, (4), pp. 179–188, 2007.

# Chapter 6

# Conclusions

## 6.1 Summary

Chapters 2 to 5 chronologically presented published or submitted papers that were used to assess the feasibility of implementing a new tactile sensing system to aid in localizing pulmonary nodules during VATS procedures. A summary of each of these papers and its impact on subsequent papers are presented below.

### *6.1.1 A New Tactile Imaging Device to Aid with Localizing Lung Tumours during Thoracoscopic Surgery (Chapter 2)*

A new tactile sensing instrument (TSI) was created to meet performance specifications that were required for a tumour to be localized via palpation using kinaesthetic sensing methods. A preliminary study was prepared to assess the performance of the TSI by comparing it to a current clinical standard of using an

endoscopic grasper to locate lung tumours during thoracoscopic surgery. The goal of the experiments was to accurately locate 10 mm artificial tumours sutured in *ex vivo* porcine lungs attained from a local abattoir by novice volunteers. At the conclusion of the study, the limitations of the TSI and the design of the experiments became evident. These included the limited number of resources for obtaining porcine lung, the lack of information about the forces applied by the user when using the TSI, and the influence of direct visual cues when simulating an MIS environment. Regardless, experimental results concluded that the implementation of the TSI in MIS surgery has the potential to facilitate the lung palpation process for the surgeon as compared to standard clinical practice. This was made evident by the 10% absolute increase in sensitivity and a 27% relative increase in localization distance of the TSI when compared to the endoscopic grasper without the need for additional time. Therefore, by providing tactile information via sensory substitution, tactile feedback is restored to the surgeon, thus addressing one of the current restricting factors in VATS.

### *6.1.2 Robot-Assisted Tactile Sensing for Minimally Invasive Tumour Localization (Chapter 3)*

The results of preliminary testing detailed in Chapter 2 indicated that the TSS significantly improves the efficiency and accuracy of locating tumours compared to using an endoscopic grasper, which is used as an MIS tumour localization device in standard practice. However, limitations in the design of the experiments were also identified at the conclusion of the study. In order to address some of these limitations, a study was

designed to assess the feasibility of using the TSI under robotic control to reliably locate underlying tumours while reducing collateral tissue trauma. The performance of humans and a robot using the TSI to locate tumour phantoms embedded into *ex vivo* bovine livers was compared. An Augmented Hybrid Impedance Control scheme was implemented on a Mitsubishi PA10-7C robot to perform the force/position control used in the trials. The results show that using the TSI under robotic control realizes an average 35% decrease in the maximum forces applied and a 50% increase in tumour detection accuracy when compared to manual manipulation of the same instrument. This demonstrates that the detection of tumours using tactile sensing is highly dependent on how consistently the forces on the tactile sensing area are applied, and that robotic assistance can be of great benefit when trying to localize tumours in VATS.

### *6.1.3 Visual Force Feedback Improves the Performance of a Tactile Sensing System during Minimally Invasive Tumour Localization (Chapter 4)*

TSI performance is highly dependent on the amount of force that is being applied by the user and that the ability to palpate with a consistent amount of force leads to superior results. This result was established from the study presented in Chapter 3 that indicated that the robotic-assisted methods were feasible and that the localization accuracy for tumours embedded in liver was improved using robotic-assisted control. Therefore, to maximize performance, it was hypothesized that the TSI's visualization interface must provide information to the user about the applied forces experienced by the tip of the TSI. To provide this information, the TactArray sensor at the end of the TSI

was calibrated such that bulk force data can be computed and displayed instantaneously to the user.

This chapter presented the calibration of the TSI and its integration with a visualization interface that allows the forces applied to the tissue during palpation to be displayed. The objective of the study was to determine whether providing visual force feedback to the user will significantly benefit TSS performance when attempting to locate 10 mm hemispherical agar tumours in *ex vivo* bovine liver. The results of the preliminary study show that the TSI was successfully calibrated to adequately indicate the amount of applied force, in Newtons, between the contact surfaces, demonstrating 70.8% accuracy, 76.5% repeatability, and insignificant hysteresis when tested on *ex vivo* bovine liver. The study further demonstrated that palpating tissue using the TSS with visual force feedback reduced the average and maximum applied forces on the tissue by 33% and 21%, respectively, and detection accuracy was relatively increased by 53% when compared to using the system without force display. Therefore, it is evident that the implementation of visual force feedback into the TSS had a beneficial effect on the system.

### *6.1.4 New Tactile Sensing System for Minimally Invasive Surgical Tumour Localization (Chapter 5)*

As detailed in Chapter 4, the TSI was calibrated in order to obtain a relationship between the sensor readings and the amount of applied force on the tactile sensing elements. The results gathered from this calibration procedure were then incorporated into the visualization interface to provide the contact force data to the user, collectively

known as the tactile sensing system (TSS). The results from that study concluded that visual force feedback improves the performance of the tactile sensing system.

In this chapter TSS performance was compared to MIS techniques using an ideal tissue model (thinly sliced *ex vivo* bovine liver). TSS performance was also tested using a realistic tissue model (collapsed *ex vivo* porcine lung). Experiments consisted of palpating tissue samples with 10 mm phantom tumours within an MIS training box using direct manual palpation, an endoscopic grasper, ultrasound, and the TSS. Performance assessment included applied pressure, localization distance, and accuracy. The results of this study show that that when performing palpation on *ex vivo* bovine liver, the TSS realized an overall increase in performance, specifically a relative 71% reduction in maximum pressure applied on the tissue when compared to the endoscopic grasper, and a 31% and 16% relative increase in detection accuracy when compared to the grasper and ultrasound techniques, respectively. There was no significant difference in applied pressure between the ultrasound and TSS palpation methods. For average localization distance, manual palpation produced the best results. The TSI followed manual palpation, however no significant difference was observed between the remaining MIS techniques. When tested using collapsed porcine lung, the TSS showed an absolute decrease of 0.08 N in average pressure and an absolute increase of 0.35 N in maximum pressure when compared to palpating liver with the same instrument. However, both results show that there was no significant difference when the instrument was palpating both types of tissues. Therefore, the TSS may help surgeons identify tumours during surgery by restoring some of the haptic information lost during VATS.

## 6.2 Conclusion

The work in this thesis has demonstrated that a newly developed haptic instrument, entitled the Tactile Sensing System, performed better at localizing carcinomas in *ex vivo* tissue than standard VATS localization instruments. This was achieved via sensory substitution by providing to the user both tactile and kinaesthetic information visually in a graphic user interface. Therefore, the TSS has the potential to improve the efficacy of MIS tumour therapies and techniques, and offers the possibility of restoring haptic information lost during surgery, thus mitigating one of the current limitations of minimally invasive surgery and VATS.

## 6.3 Contributions

My contributions to the work presented herein involved the calibration of the TSI TactArray sensor, the design and implementation of a new visualization interface for the TSI, and the design and implementation of a testing procedure to compare the TSS to conventional VATS instruments in an *ex vivo* environment. The result of these efforts is a complete clinical system that is capable of proving both tactile and kinaesthetic feedback to the surgeon; a valuable asset to surgeons during VATS since the limitation or absence of haptic feedback during surgery can be regarded as a safety concern. In addition, the system is affordable, provides a reliable source of sensing and imaging information visually to the user, and provides information that can be easily interpreted directly by the user, with no need of specialized or trained personnel. There is no existing technology in

the operating room that is identical or similar to the TSS. With respect to existing research technologies that are designed for palpation and localization of nodules in surgery, the TSS differs from those technologies in the following manner:

1) Most of these technologies are designed for open surgery or for external palpation applications (e.g. breast palpation). Their physical dimensions do not meet the constraints for minimally invasive procedures.
2) Systems based on pressure sensor technologies have not been calibrated to provide to the user, quantitatively, the applied force between the end-effector and contact surface.
3) Few of these systems found in the literature consider the effect of elevated applied forces on tissue, specifically, an indication to the user when applied force levels can begin causing damage to the tissue.
4) Few of these systems found in the literature are capable of providing *both* tactile and kinaesthetic information to the user.
5) The technologies are designed solely as hand-held devices. Few of these technologies have been developed or modified to be adapted for robotic or robotic-assisted control.

The results of this work can be used to inform the design of a next generation prototype that will address the limitations of the system identified in this work. Furthermore, the results of this work has shown promise for advancing the system to the second clinical stage of *in vivo* testing, bringing the TSS one step closer to FDA approval and into the operating room. Therefore, the TSS would be of immediate benefit for

VATS procedures because it will help restore to the surgeon a means of haptic sensation, thus improving the efficacy of current tumour therapies and interventions.

## 6.4 Recommendations for Future Work

The following is a list of recommendations for possible future work resulting from research described in this thesis.

### *6.4.1 The TSI*

Through performance evaluations of the TSS in a VATS environment, a feature that was identified to provide additional beneficial functionality to a future TSI prototype was to redesign the sensor end-effector (sensor 'head') to ensure that the TactArray sensor can be placed parallel to the tissue at all orientations. For all experimental procedures presented in this thesis that used a VATS environment, the rigidity of the TSI sensor end-effector was accommodated by modifying the internal structure of the training box to introduce an inclined plane. This modification enabled uniform pressure contact between the TactArray sensor and tissue medium. Without this modification, uniform pressure contact on the sensor is not probable, often leading to artifacts in the image. This can lead to an increase in false positive results or can make it difficult to distinguish tumour locations. Since this modification cannot be performed inside the thoracic cavity, it is recommended that future TSI prototypes have a redesigned end-effector. A solution, presented by Miller *et al.* [1], was the implementation of an active joint in the centre of

the sensor area, that will allow the surgeon to manually adjust the sensor head via a knob or other mechanical mechanism located at the probe handle. Thus, the orientation of the sensor (roll, pitch, yaw leading to translation in $x$, $y$, and $z$ directions) can be accomplished by using pulleys, Hooke or spherical (ball) joints. This will be beneficial since it will give the surgeon complete control over the orientation of the sensor and will increase the number of degrees of freedom available inside of the chest cavity, which proved to be beneficial for endoscopic robotic attachments [2]. However, these benefits can be overshadowed by the difficulty and frustration experienced by the surgeon when attempting to adjust the instrument when palpating, as recorded in [1]. Therefore, to avoid the complexities of adjusting the sensor to be parallel to the tissue surface, it is advised that the end-effector for a future prototype is a mobile gripper. With the TactArray sensor located on the top gripper jaw, the bottom gripper jaw will ensure that the tissue is uniformly distributed along the TactArray sensor, thereby simplifying the palpation process for all tissues, including those with highly irregular geometries. Surgeons will also be comfortable with its operation since they have experience using conventional endoscopic graspers and staplers during VATS.

### *6.4.2 The Visualization Interface*

Some of the advantages of the visualization interface presented in Chapters 4 and 5 are that it can provide to the user, visually, the amount of force being applied to the palpated tissue and it can decrease the number of false positives by incorporating an image filter to eliminate artifacts due to small underlying tissue structures, and tissue

inhomogeneity. To further improve the new interface, the orientation of the TSI should be provided to the user. With the introduction of a position sensors or an electromagnetic tracker (EMT) on the tip or handle of the TSI, the software would have the capability of indicating if the TSI is parallel to the palpating surface and the instrument's orientation within the working space. The position sensor would have the additional benefit of determining the penetration depth of the instrument into the tissue so that in combination with the TactArray force data, it can be ensured that the signals from the TactArray sensor are within the optimal operating range and damaging forces are avoided. This would be especially beneficial since the absence of an accurate indication of applied forces during VATS can be dangerous, sometimes leading to tissue damage or the puncturing of vessels [3].

An additional feature of the software would be to display in real-time a topographical colour-contour force map of the entire tissue as it is being palpated. This could be achieved by processing position information from a position sensor in unison with the kinaesthetic and tactile information gathered from the TSI. Therefore, with the force map of the entire tissue, the surgeon will be able to easily identify tumour locations, and possibly the size of the tumours, effectively and efficiently.

### *6.4.3 Calibration*

Although the calibration results, presented in Chapter 4, are satisfactory, the calibration method can be improved for future prototypes. Error was introduced during calibration because the forces applied to neighbouring elements were ignored when

performing element-based calibration. The sum of these errors when calculating the forces applied to the entire sensor had a direct effect on the accuracy of the system. It was difficult to minimize this error since the TactArray sensor has a uniform protective membrane that encapsulates the entire sensor array. For future calibration procedures with the TactArray sensor, the following should be considered:

- *Motorized XYZ linear stages*: Motorized XYZ linear stages should be used if additional calibration attempts are to be performed on the system. A significant source of error was introduced into the data simply because the stages were operated manually, providing a source of human error in the data.
- *Effect of neighbouring elements*: When calibrating, the binary output values of neighbouring elements (8-neighbour configuration) to the element of interest should be recorded and analyzed for a signature when specific forces are applied. The inclusion of this additional information could improve the accuracy of the system.
- *Calibration using a pressure tank*: Instead of calibrating the sensor by applying a specific force to the sensor elements, the entire probe can be placed into an air-sealed container connected to an air tank that permits a user to control the amount of pressure in the container. This setup ensures that all 60 sensor elements are experiencing the same amount of pressure, thus eliminating the error attained when elements were calibrated individually. Binary output values of all 60 elements could be recorded simultaneously for linear increments of pressure in the tank. The pressure values of the sensor elements can then be converted to applied forces, via the equation Force = Pressure × Area, with 'Area' representing the size of the sensor element (i.e., 4 $mm^2$).

- *Effect of temperature and humidity*: While calibrating, a careful record of the temperature and humidity of the environment was performed. On average, the temperature of the room was 23.4 ± 0.3 °C and the humidity was 59.8 ± 0.5 %. These conditions were ideal since experiments detailed in this thesis were performed *ex vivo*, thus the environment of the sensor was at room temperature (approximately 25°C). However, if the experiments are to progress to *in vivo* stages, the effect of increased temperature and humidity on both the sensor and calibration data should be analyzed. If by increasing the temperature of the environment to that within the body (37°C) the calibration data of the sensor significantly changes, then the calibration procedure should be repeated with the environment matching that which is experienced *in vivo*.

It should be noted that the task of attaining applied forces at the end-effector is not limited to the TactArray pressure sensor. Additional sensors, i.e., force sensors, can be placed on the TSI end-effector to provide more accurate readings of applied force information to the user. For example, this can be accomplished by using KFWS small-sized waterproof strain gauges (Kyowa Electronic Instruments Co., Tokyo, Japan) or similar force sensor technologies.

### *6.4.4 Experimental Models and Procedures*

#### *6.4.4.1 Artificial Tumours*

The tumour phantoms used in this thesis were not modelled to be surrogates for lung carcinomas. Unlike in breast cancer studies, there is no research which has

determined the Young's modulus of lung tumours. Since the tumours used for the project are considered to be clinically small [4], [5], the percent compositions of the tumours were arbitrarily chosen to ensure that the tumours were durable and did not fracture easily when being palpated. This required a relatively high agar to water ratio when manufacturing the tumour phantoms, thereby placing tumour robustness paramount to physical accuracy. To improve the tumour models in future explorations, the following should be investigated:

- Research should be conducted to create practical and realistic tumour phantoms. A study should be performed in which different concentrations of agar tumours are prepared and, based on their experience, surgeons should assign an analogue score to each tumour model based on realism. Results can be compared to a preliminary study conducted by [6] which has begun to use a free standing desk-top instrument to quantify the indentation of target lung tissues and carcinomas. This will aid in determining the Young's modulus of lung tissue and tumours, thereby giving researchers a base to develop a tumour-mimicking platform.
- The tumours used in the experiments described in this thesis were always spherical or hemispherical in shape. Different shaped tumours should be used during experiments to test the limitations of the TSS. This can include tumours which are oval, concave, convex, or cystic (fluid-filled).
- Tumours were manually inserted via incisions and sutured into lung parenchyma. If incisions were made too large, this would sometimes be problematic since the location of the tumours could shift inside of the incision. To avoid this, the method of injecting agar into lung should be investigated. If successful, this approach would not

alter the tissue surrounding the nodule (unlike incisions) and this will limit the movement of the tumour when palpated.

*6.4.4.2 Tissues*

The tissues for experiments were attained from a local abattoir, however to accommodate to the busy schedule of the residents and surgeons, the tissues were often refrigerated and were used up to 7 days after being excised. Before being palpated, the tissues were usually at room temperature. A consideration for future *ex vivo* experiments should be to incubate tissues to body temperature (approximately 37°C) before palpation. This would simulate a more realistic environment of the tissue. If experiments involving liver are being continued, then it is advised to purchase whole livers from the abattoir instead of thinly-sliced livers from a local grocery store. This will test the TSS using a more 'realistic' liver model.

*6.4.4.3 Robot Control System*

If further experiments using a robot control system are pursued, a virtual remote centre of motion should be incorporated into the robot controls in order to assess the ability to robotically locate a tumour when the instrument enters the surgical area through a trocar. With this in place, tests using the VATS training box and a robot capable of remote centre of motion could be pursued. The possibility of integrating the TSI into the

ZEUS Surgical System as a cost-effective and FDA approved alternative, allowing the TSS to be used in the operating room.

An additional modification to the control schemes should include a user selectable and/or adaptive palpation step size in order to increase the number of palpations around a suspicious area. For this purpose, a master-slave interface (that still ensures consistent palpation force and a systematic movement across the surface) should be implemented. The increased control achievable through a master interface could overcome the fear that surgeons may have about the use of robots in surgery.

## References

[1] A. P. Miller, W. J. Peine, J. S. Son, and Z. T. Hammoud, "Tactile imaging system for localizing lung nodules during video assisted thoracoscopic surgery," in *Proc. IEEE Int. Conf. Robot. Autom. (ICRA),* Rome, Italy, 2007, pp. 2996–3001.

[2] R. Gharagozloo, and F. Najam, *Robotic Surgery.* China: McGraw-Hill Companies, Inc., 2009.

[3] M. Tavakoli, A. Aziminejad, R. V. Patel, and M. Moallem, "Tool/tissue interaction feedback modalities in robot-assisted lump localization", in *Proc. IEEE EMBS Ann. Int. Conf.*, New York City, New York, 2006, pp. 3854–3858.

[4] P. Singh, R. A. Erickson, P. Mukhopadhyay, S. Gopal, A. Kiss, A. Khan, and T. Ulf Westblom, "EUS for detection of the hepatocellular carcinoma: results of a prospective study," *Gastrointest. Endo.*, vol. 66, (2), pp. 265–273, 2007.

[5] J. K. LeBlanc, J. DeWitt, and S. Sherman, "Endoscopic ultrasound: how does it aid the surgeon?," *Adv. Surg.*, vol. 41, pp. 17–50, 2007.

[6] D. Bottoni, G. Campbell, and R. A. Malthaner, "Development and validation of a novel instrument for the quantification of pulmonary tissue mechanics," Conference presentation at the *2008 CAGS Resident Research Retreat*, Halifax, Nova Scotia, September 9–10, 2008, p. 28.

21 August 2009

Dear Melissa,

**A. L. Trejos, J. Jayender, M. T. Perri, M. D. Naish, R. V. Patel, and R. A. Malthaner "Robot-Assisted Tactile Sensing for Minimally Invasive Tumour Localization" International Journal of Robotics Research, OnlineFirst, May 19, 2009 - doi:10.1177/0278364909101136**

Thank you for requesting permission to include the above material in your forthcoming Master of Engineering Science (M.E.Sc.) thesis at the University of Western Ontario (London, Ontario, Canada).

Permission is granted by Sage Ltd (as the rightsholder) for use of the above article, for **non-exclusive world rights in print and electronic media in the English language only.**

Proper acknowledgement of the original place of publication (such as 'Reprinted by permission of Sage Publications Ltd from Author, Title, Copyright (© Owner, Year)) is to be made.

**Thank you for contacting us for permission.**

**With very best wishes for your thesis,**

Marta Granatowska
Rights Executive
Sage Publications
email: **permissions@sagpub.co.uk**

SAGE Publications Ltd
1 Oliver's Yard
55 City Road
London EC1Y 1SP
Phone +44 (0)20 7324 8500
Fax +44 (0)20 7324 8600
sagepublications.com
Reg. England No 1017514
Los Angeles London New Delhi Singapore